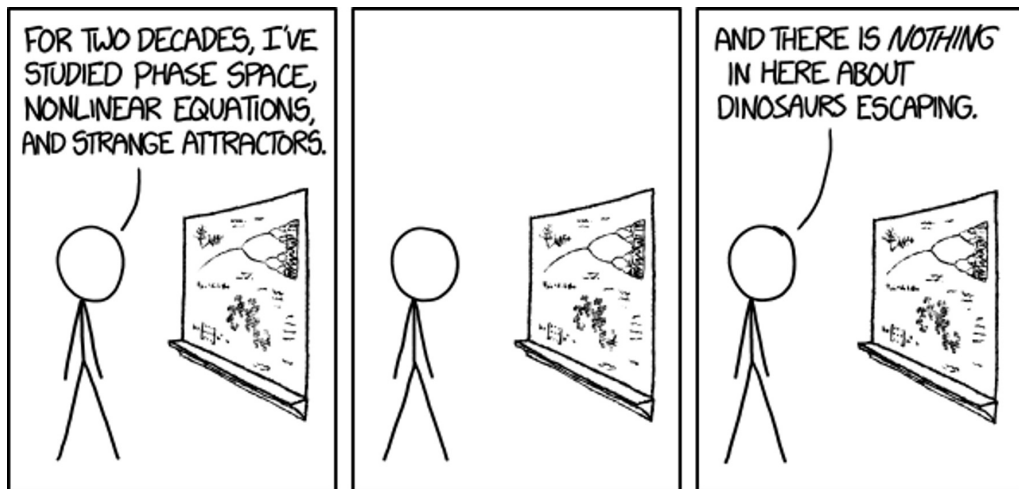


PHYS2100

Dynamics, Chaos & Special Relativity

PHYS2101

Advanced Dynamics and Special Relativity



Gabriele TARTAGLINO MAZZUCHELLI

CHAOS

An evolving set of notes, with major contributions by:
M. J. Davis, J. Ginges, I. McCulloch, T. Nieminen, T. Sholtz

School of Mathematics and Physics
The University of Queensland

Semester 2, 2020

These notes are only for use as supporting material for the classes and should not be disclosed publicly. In fact, some material and pictures in these notes are not original and have been copied from several sources

Contents

Contents	i
1 Dynamical systems in phase space	1
1.1 Review	1
1.1.1 Lagrangian mechanics	1
1.1.2 Hamiltonian mechanics	2
1.2 Phase space	3
1.3 Flow vector field	3
1.4 Phase portraits	5
1.5 Fixed points and separatrices	6
1.6 Examples	6
1.6.1 Linear potential	7
1.6.2 Quadratic potential (SHO)	8
1.6.3 Linear Repulsive Force	9
1.6.4 General potential	11
1.6.5 Further examples: Cubic potentials	12
1.6.6 Summary	14
2 Periodic motion	15
2.1 Libration (oscillation)	15
2.2 Rotation	15
2.3 Free particle rotating in a plane	15
2.3.1 Pendulum	16
2.4 APPENDIX: Computational mechanics and phase portraits	20
3 Dynamics near fixed points	29
3.1 Autonomous/non-autonomous systems	29
3.1.1 Non-autonomous Hamiltonian systems	30
3.1.2 Few degrees of freedom	31
3.2 Fixed points and linearization	32
3.3 Classification of linear systems	32
3.3.1 Eigenvalue/eigenvector equation for a 2×2 real matrix and ODE solutions	33
3.3.2 Bifurcation diagram and non-linear stability	39
3.3.3 Final comments: conservative hamiltonian systems	40
4 More on Hamiltonian mechanics	43

4.1	Canonical transformations and Poisson brackets	43
4.1.1	Properties of the Poisson bracket	45
4.1.2	Time dependence of observables	46
4.1.3	Generalisation to many degrees of freedom	46
4.2	Area (volume) preservation of canonical transformations	48
4.3	Volume preserving flows	49
4.4	Hamiltonian flow as a one parameter family of canonical transformations	51
4.5	Aside	52
4.6	Action-angle variables	52
4.7	Integrable systems	56
5	Examples and back to free pendulum	59
5.1	Simple harmonic oscillator	59
5.2	Linear repulsive force	63
5.3	Back to the pendulum	66
5.3.1	Rotations: $\Lambda > 1$	69
5.3.2	Full solution: $\phi(t)$	70
5.3.3	Aside: Jacobi elliptic functions	70
5.3.4	Full solution: $\ell(t)$	71
5.3.5	Limiting cases	72
5.3.6	Case: $\Lambda \ll 1$	72
5.3.7	Case: $\Lambda = 1$	72
5.3.8	Case: $\Lambda \gg 1$	72
5.4	APPENDIX: On generating functional of canonical transformations	73
6	Attractors	77
6.1	Chaos	77
6.1.1	Defining “chaos”	77
6.1.2	Lyapunov exponent	77
6.2	Attractors	79
6.3	Types of attractors	80
6.3.1	Fixed point attractor	80
6.3.2	Limit cycle attractors	80
6.3.3	A limit torus attractor	80
6.4	Defining chaos revisited	80
6.4.1	Lorenz System	82
7	The logistic map	85
7.1	One-dimensional maps	85
7.2	The logistic map and relation to population dynamics	86
7.3	Geometrical representation of logistic map	87
7.4	Fixed points	87
7.5	Unstable fixed points and n -cycles	90
7.6	More on period doubling	91
7.6.1	Lyapunov exponent	92
8	Fractals	101
8.1	Cantor Set	101
8.1.1	Cardinality	102
8.1.2	Self-similarity	103

8.2 Dimensions	103
8.2.1 Box counting dimension of the Cantor set	105
8.2.2 Koch curve	105
8.2.3 Box counting dimension of Logistic map	106
8.2.4 Box counting dimension of the Lorenz attractor	106
9 The driven pendulum, Recurrence plots and Poincaré sections	109
9.1 Hamiltonian for the driven pendulum	109
9.2 Equations of motion	110
9.3 Behaviour of the driven pendulum	111
9.4 Driven damped pendulum	115
9.5 Recurrence plots and Poincaré sections	117
9.6 Irrational Recurrence Plots	120
9.7 Recurrence plots with rational frequencies	120
9.8 Transition to chaos	120
9.9 Non-sinusoidal driving forces	122
9.9.1 The restricted 3-body problem	122
10 The double pendulum	125
10.1 Small oscillations	126
10.2 Hamilton's Equations	127
10.3 Poincaré sections	128
10.3.1 Low energy	129
10.3.2 Mid-range energy	129
10.3.3 Higher energy	130
10.4 KAM Theorem	130
11 Other chaotic systems	135
11.1 Non-linear coupled oscillators	135
11.1.1 Aperiodic motion	137
11.2 Lyapunov exponents	139
11.3 Turbulence	141
11.4 Lasers	142
11.5 Cardiac rhythms	142

CHAPTER 1

Dynamical systems in phase space

1.1 Review

A mechanical system is known as *conservative* if

$$\oint \mathbf{F} \cdot d\mathbf{r} = 0. \quad (1.1.1)$$

Frictional or dissipative systems do not satisfy equation (1.1.1).

Using vector analysis, it can be shown that if the force is a *field* – i.e., it depends only on position – then equation (1.1.1) implies that there exists a potential function such that

$$\mathbf{F} = -\nabla V(\mathbf{r}). \quad (1.1.2)$$

for some $V(\mathbf{r})$. In particular, conservative systems have *time-independent* potentials.

A *holonomic constraint* is a constraint written in terms of an equality, e.g.

$$|\mathbf{r}| = a, \quad a > 0. \quad (1.1.3)$$

A non-holonomic constraint is written as an inequality, e.g. $|\mathbf{r}| \geq a$.

1.1.1 Lagrangian mechanics

For a mechanical system of N particles with k holonomic constraints, there are a total of $3N - k$ degrees of freedom.

The system can be represented by $3N - k$ generalised coordinates $q_1, q_2, \dots, q_{3N-k}$, such that

$$\mathbf{r} = \mathbf{r}(q_1, q_2, \dots, q_{3N-k}, t)$$

where we indicated the possibility to also have time dependence in non-conservative systems or for time-dependent systems of generalised coordinates.

For a *conservative* system with $V = V(q_1, q_2, \dots, q_{3N-k})$, the Lagrangian is defined as

$$\mathcal{L} = T - V, \quad (1.1.4)$$

and the dynamics of the system can be found from the Euler-Lagrange equations

$$\frac{d}{dt} \left(\frac{\partial \mathcal{L}}{\partial \dot{q}_i} \right) - \frac{\partial \mathcal{L}}{\partial q_i} = 0. \quad (1.1.5)$$

The *generalized force* is

$$Q_j = \sum_i \mathbf{F}_i \cdot \frac{\partial \mathbf{r}_i}{\partial q_j}. \quad (1.1.6)$$

If the forces are derived from a scalar potential, $\mathbf{F}_i = -\nabla_i V$, then the generalized forces are

$$\begin{aligned} Q_j &= -\sum_i \nabla_i V \cdot \frac{\partial \mathbf{r}_i}{\partial q_j} \\ &= -\frac{\partial V}{\partial q_j} \end{aligned} \quad (1.1.7)$$

[Lagrange's equations can be used even if the forces are *not* obtained from a scalar potential function V , as long as they can be obtained from a function $U(q_j, \dot{q}_j)$, by the prescription

$$Q_j = -\frac{\partial U}{\partial q_j} + \frac{d}{dt} \left(\frac{\partial U}{\partial \dot{q}_j} \right), \quad (1.1.8)$$

that is, our potential U can depend explicitly on the generalized velocities, and the generalized forces are obtained from the Lagrangian

$$\mathcal{L} = T - U. \quad (1.1.9)$$

This kind of potential is called a *generalized potential*, or a *velocity-dependent potential*. *Magnetism* fits into this formation. However, we will not consider such systems in this course.]

1.1.2 Hamiltonian mechanics

The Hamiltonian formulation of mechanics does not add any new physics. However it provides a method that in some ways is more versatile than the Lagrangian approach. It is a crucial framework for extending the theory into other fields such as statistical mechanics and quantum mechanics: fundamental areas of physics that you will cover in detail in 3rd year. Moreover, the hamiltonian formulation hints at extended geometrical structures that helps solving its dynamics and played a central role in the developing of mathematical physics.

Lagrange's equations form a system of $n = 3N - k$ *second-order* differential equations requiring $2n$ initial conditions to obtain a unique solution. The Hamiltonian formulation is based upon Hamilton's equations

$$\dot{q}_i = \frac{\partial H}{\partial p_i}, \quad \dot{p}_i = -\frac{\partial H}{\partial q_i}, \quad (1.1.10)$$

which form a system of $2n$ *first-order* differential equations, again requiring $2n$ boundary conditions for a unique solution. The generalised momentum is defined as

$$p_i = \frac{\partial \mathcal{L}}{\partial \dot{q}_i} \quad (1.1.11)$$

and the Hamiltonian for the system is

$$H = H(\mathbf{q}, \mathbf{p}, t) = \sum_i q_i p_i - \mathcal{L}(\mathbf{q}, \dot{\mathbf{q}}, t) \quad (1.1.12)$$

where $\mathbf{q} = (q_1, q_2, \dots, q_n)$ and $\mathbf{p} = (p_1, p_2, \dots, p_n)$. Note that \mathbf{q} and \mathbf{p} are treated as *independent* variables. In general, Hamiltonian and Lagrangian equations prove to be equivalent.

For simple conservative mechanical systems you will have already shown that

$$H = T + V, \quad (1.1.13)$$

which says that H is the total mechanical energy of the system, and this will be the case for the majority of systems that we look at. It is also worth noting that the Hamiltonian of a conservative system has no explicit time dependence, i.e. $H = H(\mathbf{q}, \mathbf{p})$.

1.2 Phase space

The “space” of the (\mathbf{q}, \mathbf{p}) coordinates specifying a dynamical system is referred to as the “phase space”, and is a very important concept in physics. The complete specification of all phase space co-ordinates is sometimes called a “microstate” and contains all you can possibly know about the system. This concept generalises to statistical mechanics and quantum mechanics.

In Hamiltonian mechanics, the dynamics is defined by the evolution of points in phase space. For a system with n degrees of freedom, the phase space coordinates are made up of n generalised position coordinates \mathbf{q} and n generalised momentum coordinates \mathbf{p} , and so its phase space has a total of $2n$ dimensions.

$$\mathbf{q} = (q_1, q_2, \dots, q_n), \quad (1.2.14)$$

$$\mathbf{p} = (p_1, p_2, \dots, p_n). \quad (1.2.15)$$

Example: Bead moving on a frictionless and stationary wire under the influence of gravity.

The trajectory of the bead is a curve in (q, p) space parameterised by time. It can be drawn out by following a point travelling with a certain “velocity”. It is not a true velocity as its components are time derivatives of generalised position and momentum coordinates.

1.3 Flow vector field

If we consider a system with one degree of freedom, the velocity is

$$\mathbf{v} = (\dot{q}, \dot{p}), \quad (1.3.16)$$

and making use of Hamilton’s equations

$$\mathbf{v} = \left(\frac{\partial H}{\partial p}, -\frac{\partial H}{\partial q} \right). \quad (1.3.17)$$

For a general system with n degrees of freedom

$$\mathbf{v}(\mathbf{q}, \mathbf{p}) = (\dot{q}_1, \dot{q}_2, \dots, \dot{q}_n, \dot{p}_1, \dot{p}_2, \dots, \dot{p}_n), \quad (1.3.18)$$

$$= \left(\frac{\partial H}{\partial p_1}, \frac{\partial H}{\partial p_2}, \dots, \frac{\partial H}{\partial p_n}, -\frac{\partial H}{\partial q_1}, -\frac{\partial H}{\partial q_2}, \dots, -\frac{\partial H}{\partial q_n} \right) \quad (1.3.19)$$

So Hamilton’s equations are enough to define $\mathbf{v}(\mathbf{q}, \mathbf{p})$.

For every point of phase space there is a velocity vector. In other words there exists a velocity field $\mathbf{v}(q, p)$, usually referred to as the “flow vector field”. In principle the flow vector field enables the dynamics of the system to be completely determined. It is important to note that, assuming good regularity properties of the vector field (continuity, differentiability), due to the theorem of existence and uniqueness of differential equations, then for each point of the phase space there is only one curve passing which will be tangent to the vector field.

Example: Simple Harmonic Oscillator (SHO) in 1D

$$H = \frac{p^2}{2m} + \frac{m\omega^2}{2}q^2. \quad (1.3.20)$$

Hamilton's equations give

$$\dot{q} = \frac{\partial H}{\partial p} = \frac{p}{m}, \quad \dot{p} = -\frac{\partial H}{\partial q} = -m\omega^2 q, \quad (1.3.21)$$

so the hamiltonian vector flow field is

$$\mathbf{v} = \left(\frac{p}{m}, -m\omega^2 q \right). \quad (1.3.22)$$

If we set $m = \omega = 1$ then we can represent this graphically: $\mathbf{v} = (p, -q)$ as in Figure 1.1.

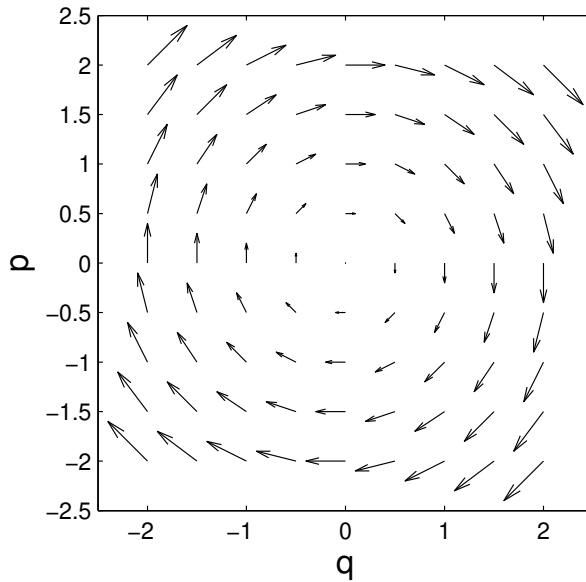


Figure 1.1: Vector flow field for the SHO with $m = \omega = 1$.

Note that we have been assuming that the flow vector field \mathbf{v} is not a function of time. This is true when H is time independent. But if, for example we have

$$H = \frac{p^2}{2m} + q \cos \omega t \quad (1.3.23)$$

then

$$\mathbf{v} = (p/m, -\cos \omega t), \quad (1.3.24)$$

which is a *time-varying* flow vector field.

1.4 Phase portraits

Our focus will initially be mostly on systems with time independent Hamiltonians, for which there is the useful result that the velocity vectors \mathbf{v} are always tangential to lines of constant H (energy). For the SHO example with $m = \omega = 1$, the Hamiltonian is

$$H = \frac{1}{2}(p^2 + q^2), \quad (1.4.25)$$

which describes a circle of radius $\sqrt{2H}$ as in Figure 1.2

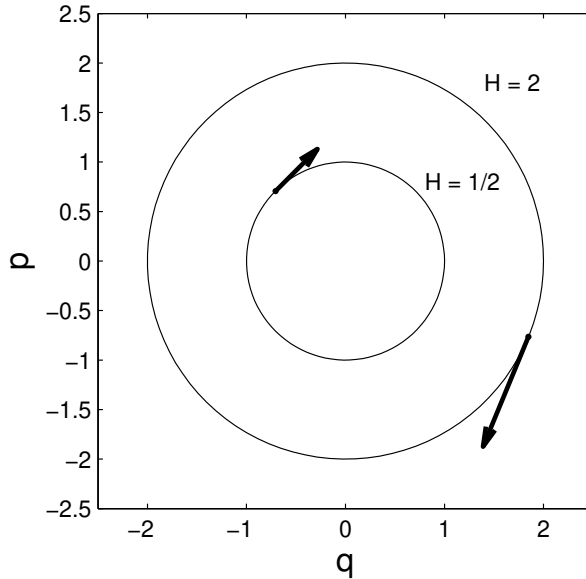


Figure 1.2: Lines of constant H for the SHO

To prove that \mathbf{v} is tangential to the lines of constant H , you need to make use of the well-known result from vector calculus, that the gradient of a scalar function f is perpendicular to lines of constant f . Then we find that

$$\begin{aligned} (\dot{q}, \dot{p}) &= \mathbf{v} = \left(\frac{\partial H}{\partial p}, -\frac{\partial H}{\partial q} \right), \quad \nabla H = \left(\frac{\partial H}{\partial q}, \frac{\partial H}{\partial p} \right), \\ \mathbf{v} \cdot \nabla H &= \frac{\partial H}{\partial p} \frac{\partial H}{\partial q} - \frac{\partial H}{\partial q} \frac{\partial H}{\partial p} = 0 \end{aligned} \quad (1.4.26)$$

so \mathbf{v} is perpendicular to ∇H . But ∇H is also perpendicular to lines of constant H , so \mathbf{v} must be *tangential* to lines of constant H .

A *phase portrait* is a geometric representation of the trajectories of a dynamical system in the phase plane. Each set of initial conditions is represented by a different curve, or point. Phase portraits are an invaluable tool in studying dynamical systems. In the case of conservative systems, lines of constant H are extremely important for time independent Hamiltonians as they define *trajectories* (or paths) through phase space for the system. To demonstrate this we first show that if H has no explicit time dependence ($\partial H / \partial t = 0$) then it has no implicit time dependence either ($dH / dt = 0$).

If $\partial H / \partial t = 0$ then

$$\frac{d}{dt} H(q, p) = \frac{\partial H}{\partial q} \dot{q} + \frac{\partial H}{\partial p} \dot{p} = \mathbf{v} \cdot \nabla H = 0. \quad (1.4.27)$$

Thus we must have that $H = \text{constant}$, and that a particle will move along a line of constant H . For higher-dimensional conservative systems and phase spaces, similar arguments apply and H is still a constant of motion. As a result orbits of motion will lie in $(2n - 1)$ -dimensional subspaces defined by $H = \text{constant}$.

In systems with one degree of freedom, and hence a 2D phase space, lines of constant H completely characterise the *phase portraits*. They are simply paths in phase space.

Our analysis here has essentially been a proof that energy is conserved in a system with a time independent Hamiltonian. (Note that it was assumed that H was not a function of \dot{p} or \dot{q} .)

Phase portraits are an excellent means of visualising the dynamics of a mechanical system and understand many exact and qualitative information of a dynamical system. We will spend a significant part of this section of the course learning how to construct them, and understanding what they tell us about the dynamics of the system.

1.5 Fixed points and separatrices

For many systems there may be special points in phase space where the velocity vector \mathbf{v} is zero. These are known as *fixed points*, and provide a starting point for the analysis of dynamical systems.

If $\mathbf{v} = (0, 0)$ then $\dot{q} = 0$ and $\dot{p} = 0$ and hence $\nabla H = (\partial H / \partial q, \partial H / \partial p) = (0, 0)$. When the system resides at a fixed point it is in *mechanical equilibrium*.

Fixed points only occur for $p = 0$ in simple mechanical systems where we have $T = p^2/2m$ and the potential $V = V(q)$ only, since $\dot{q} = p/m$. We will come back to this type of systems but first let us look at relevant examples.

An important question in the study of dynamical system is to understand the nature of fixed points. There are several different definitions that can be used to characterise fixed points and whether they are stable or unstable. For most of our purposes, a stable fixed point is such that there exists a region of the phase space which includes the fixed point such that every orbit close to the fixed point remains confined in that region. An unstable fixed point is one that has at least an orbit moving away from the fixed point.

Other notions of stability are: *positive/negative time stability* meaning that a fixed point is stable for positive/negative times only; *asymptotic stability* meaning that all orbits in a region surrounding a fixed point converge asymptotically to a fixed point. In these notes whenever we refer to stability we will mean positive time stability.

Separatrices are orbits in phase space that connect unstable fixed points. They play a very important role in separating different regions of the phase space and dynamical regimes.

1.6 Examples

Unless otherwise specified, we consider Hamiltonians of the form

$$H(q, p) = \frac{p^2}{2m} + V(q). \quad (1.6.28)$$

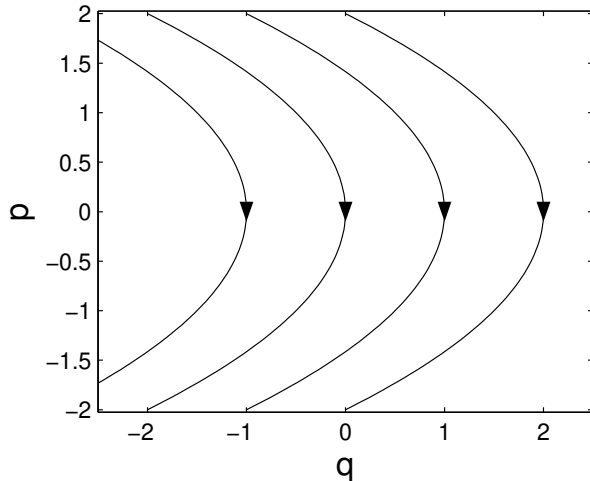


Figure 1.3: Phase portrait for a linear potential ($a = m = 1$) and $H = -1, 0, 1, 2$. Note that all trajectories in a phase portrait must have an arrow indicating the direction.

1.6.1 Linear potential

$$V(q) = aq, \quad a \neq 0. \quad (1.6.29)$$

The phase portrait can be found by fixing H and plotting p as a function of q (or vice versa). In general we have

$$p(q) = \pm \sqrt{2m} \sqrt{H - V(q)}. \quad (1.6.30)$$

For the current example we have

$$p = \pm \sqrt{2m(H - aq)}, \quad \text{or} \quad q = \frac{H}{a} - \frac{p^2}{2ma}. \quad (1.6.31)$$

Thus the trajectories are parabolas, which makes sense seeing as the potential is like the gravitational potential. The phase portrait is in Figure 1.3.

Note also that this potential has no fixed points.

We now solve Hamilton's equations for this potential. We have

$$\dot{q} = \frac{\partial H}{\partial p} = \frac{p}{m}, \quad \dot{p} = -\frac{\partial H}{\partial q} = -a. \quad (1.6.32)$$

We need boundary conditions to find a specific solution: let's say that at time $t = t_0$ we have $q = q(t_0)$ and $p = p(t_0)$. For this simple situation we can directly integrate the equation for \dot{p} in Eqs. (1.6.32) to give

$$p(t) = p(t_0) + \int_{t_0}^t (-a) dt' = p(t_0) - a(t - t_0). \quad (1.6.33)$$

We can use Eq. (1.6.33) to solve for $q(t)$

$$\begin{aligned} q(t) &= q(t_0) + \int_{t_0}^t dt' \frac{p(t')}{m} \\ &= q(t_0) + \frac{1}{m} \int_{t_0}^t dt' [p(t_0) - a(t' - t_0)], \\ &= q(t_0) + \frac{p(t_0)}{m}(t - t_0) - \frac{a}{2m}(t - t_0)^2. \end{aligned} \quad (1.6.34)$$

It is not difficult to show that if the solutions Eqs. (1.6.33) and (1.6.34) are substituted back into the Hamiltonian that the result is time independent.

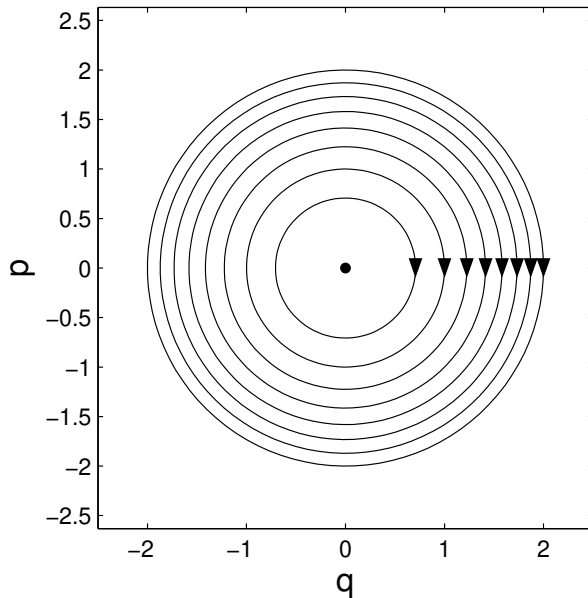


Figure 1.4: Phase portrait for a SHO ($m = \omega = 1$), for $H = 0.25$ to $H = 2$ in steps of 0.25. Note that in general the trajectories are ellipses.

1.6.2 Quadratic potential (SHO)

The simple harmonic oscillator (or SHO) is an extremely important model in physics. The Hamiltonian is

$$H = \frac{p^2}{2m} + \frac{m\omega^2}{2}q^2, \quad (1.6.35)$$

and the phase portrait is shown in Fig. 1.4. We first determine the fixed points. Hamilton's equations are

$$\dot{q} = \frac{\partial H}{\partial p} = \frac{p}{m}, \quad \dot{p} = -\frac{\partial H}{\partial q} = -m\omega^2q, \quad (1.6.36)$$

so that $\dot{q} = 0$ when $p = 0$ and $\dot{p} = 0$ when $q = 0$. Hence there is only one fixed point for this system at the origin: $(q, p) = (0, 0)$. This is classified as an *elliptic* fixed point—a fixed point that is encircled by a line of constant H . Elliptic fixed points are *stable*—any small perturbation of initial conditions away from equilibrium remains contained in a small region about the fixed point.

We can now solve for arbitrary trajectories by differentiating the equation for \dot{q} with respect to t and substituting in for \dot{p} . This gives

$$\ddot{q} = -\omega^2q, \quad (1.6.37)$$

which has the general solution

$$q(t) = A \cos(\omega t + \delta), \quad (1.6.38)$$

where the constants A and δ are determined by the boundary conditions.

The momentum is then determined from the equation for \dot{q} as

$$p(t) = m\dot{q}(t) = -m\omega A \sin(\omega t + \delta). \quad (1.6.39)$$

The motion is obviously oscillatory with period $T = 2\pi/\omega$ which is independent of the oscillation amplitude A . This may not seem like a big deal, but for a general potential the period of motion usually depends on the amplitude, and we will spend quite some time later developing a method to calculate the period of motion for confining potentials.

The energy H of the system is determined by the amplitude A . By substituting the solutions into the Hamiltonian we find (you should check this!)

$$H = \frac{1}{2}m\omega^2 A^2. \quad (1.6.40)$$

At the elliptic fixed point it is clear that $H = 0$.

The phase space trajectories are in general ellipses in phase space with where the positive turning points are $p_{max} = \sqrt{2mH}$ and $q_{max} = \sqrt{2H/m\omega^2}$. The area of the ellipse in phase space is $Area = \pi p_{max} q_{max}$, and defining the new variable $I = Area/2\pi$ we have

$$I = \frac{1}{2\pi} \times \pi \times \sqrt{\frac{2H}{m\omega^2}} \times \sqrt{2mH} = \frac{H}{\omega}. \quad (1.6.41)$$

The variable I is a generalised momentum variable that we call the *action*. Thus we find that here we have

$$\omega = \frac{\partial H}{\partial I}, \quad (1.6.42)$$

which is a specific example of a general result that we will derive later.

1.6.3 Linear Repulsive Force

In this situation we have

$$F(q) = aq, \quad a > 0. \quad (1.6.43)$$

Since $F(q) = -\partial V/\partial q$ we can integrate to find

$$V(q) = -\frac{1}{2}aq^2. \quad (1.6.44)$$

which is an inverted parabola. (Question for you: what about the constant of integration?) Thus the Hamiltonian is

$$H = \frac{p^2}{2m} - \frac{1}{2}aq^2. \quad (1.6.45)$$

To plot the phase portrait, we rearrange Eq. 1.6.45 to obtain

$$2mH = p^2 - m^2\gamma^2q^2, \quad \left(\gamma = \sqrt{\frac{a}{m}}\right). \quad (1.6.46)$$

This is the equation of a hyperbola.

Hamilton's equations for the system are

$$\dot{q} = \frac{\partial H}{\partial p} = \frac{p}{m}, \quad \dot{p} = -\frac{\partial H}{\partial q} = aq. \quad (1.6.47)$$

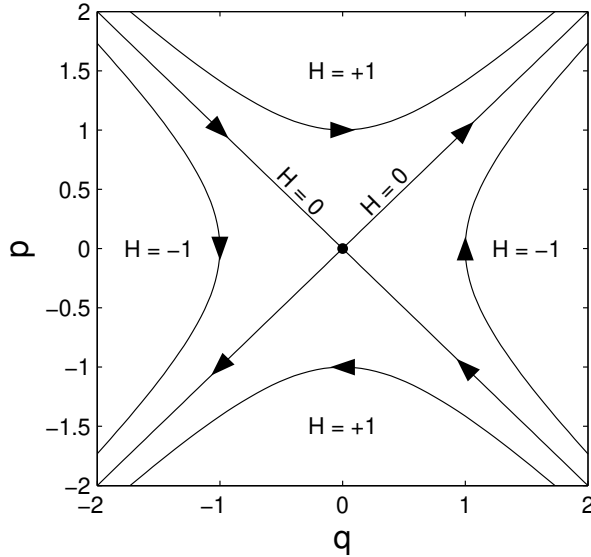


Figure 1.5: Phase portrait for a linearly repulsive force ($m = a = 1$) for $H = 0, \pm 1$.

Setting these to zero to find the fixed points we find that there is only one and it is at the origin $(q, p) = (0, 0)$. This is a different type of fixed point compared to the one we found for the SHO—it is known as a *hyperbolic* fixed point. Hyperbolic fixed points are *unstable*, as any small perturbation of the initial condition from equilibrium will grow.

Any curve in phase space that meets a hyperbolic fixed point is known as a *separatrix*, as they “separate” different types of motion. The determination of separatrices is an important part of determining global dynamics. The separatrices have $H = 0$ and satisfy

$$0 = p^2 - m^2\gamma^2 q^2, \quad (1.6.48)$$

implying

$$p = \pm m\gamma q \quad (1.6.49)$$

which are straight lines passing through the origin/fixed-point.

Solutions for this system can be found by the same method as for the SHO. We find

$$\ddot{q} = \gamma^2 q, \quad (1.6.50)$$

which has the general solution

$$q(t) = A_1 e^{\gamma t} + A_2 e^{-\gamma t}, \quad (1.6.51)$$

with the constants A_1 and A_2 determined by the boundary conditions. Correspondingly, the momentum is

$$p(t) = m\gamma(A_1 e^{\gamma t} - A_2 e^{-\gamma t}). \quad (1.6.52)$$

Note that

$$H = -2aA_1A_2. \quad (1.6.53)$$

The motion is unbounded in general, as $q(t)$ and $p(t) \rightarrow \pm\infty$.

1.6.4 General potential

Let us get back to the general Hamiltonian for a 1D conservative system with potential $V(q)$:

$$H(q, p) = \frac{p^2}{2m} + V(q). \quad (1.6.54)$$

As mentioned before, a first step to analyse the dynamics of the system is to find the fixed points. In this case they are with

$$0 = \dot{q} = \frac{\partial H}{\partial p} = \frac{p}{m}, \quad 0 = \dot{p} = -\frac{\partial H}{\partial q} = -V'(q). \quad (1.6.55)$$

It is clear that in this cases critical fixed-points are described by points in q where the first derivative of the potential $V(q)$ is zero. Calling \bar{q} a point such that

$$\left. \frac{dV(q)}{dq} \right|_{q=\bar{q}} = 0$$

the hamiltonian near the fixed point $(\bar{q}, 0)$ takes the form

$$H(q, p) = \frac{p^2}{2m} + V(\bar{q}) + \frac{1}{2}(q - \bar{q})^2 V''(\bar{q}) + \dots \quad (1.6.56)$$

where we have assumed that \bar{q} is an isolated zero of $V'(q)$ and

$$V''(\bar{q}) \neq 0.$$

Hamilton's equations near the fixed-point are then

$$\dot{q} = \frac{\partial H}{\partial p} = \frac{p}{m}, \quad \dot{p} = -\frac{\partial H}{\partial q} = -(q - \bar{q}) V''(\bar{q}) + \dots \quad (1.6.57)$$

These imply

$$\ddot{q} = -\lambda(q - \bar{q}) + \dots, \quad \lambda := \frac{V''(\bar{q})}{m} \quad (1.6.58)$$

Depending on the sign of λ , hence the sign of $V''(\bar{q})$ assuming positive masses, we have the system is approximated either by the SHO with solution

$$q(t) = \bar{q} + A \cos(\omega t + \delta) + \dots, \quad \omega = \sqrt{\frac{\lambda}{m}} = \sqrt{\frac{V''(\bar{q})}{m^2}}, \quad V''(\bar{q}) > 0 \quad (1.6.59)$$

or

$$q(t) = \bar{q} + A_1 e^{\sqrt{-\lambda}t} + A_2 e^{-\sqrt{-\lambda}t} + \dots, \quad V''(\bar{q}) < 0, \quad (1.6.60)$$

which indicates that in this case the behaviour of the approximate solution is the one of an hyperbolic fixed point and in fact the orbits move away from the fixed points (except for $A_1 = 0$ which is one of the separatrix).

Simple arguments based on conservation of energy (H) can be used to show that this approximate behaviour correctly indicates that near a local minimum of the potential, $V''(\bar{q}) > 0$, $(q, p) = (\bar{q}, 0)$ is an elliptic fixed-point with orbits that are closed curves of constant energy H . Instead near a local maximum of the

potential, $V''(\bar{q}) < 0$, $(q, p) = (\bar{q}, 0)$ is an hyperbolic fixed point with separatrices described by orbits that are solutions of the equation

$$V(\bar{q}) = \frac{p^2}{2m} + V(q). \quad (1.6.61)$$

Note that the degenerate cases with a potential such that $V'(\bar{q}) = V''(\bar{q}) = 0$ can lead to different behaviour. We suggest the reader to think about this as an exercise. For example consider the behaviour near an isolated fixed point with $V'(\bar{q}) = V''(\bar{q}) = \dots = V^{(n-1)}(\bar{q}) = 0$ and $V^{(n)}(\bar{q}) \neq 0$. Consider both the cases with n even and odd.

1.6.5 Further examples: Cubic potentials

$$V(q) = \frac{1}{2}m\omega^2 q^2 - \frac{1}{3}A m q^3, \quad \omega \neq 0, A > 0. \quad (1.6.62)$$

Hamilton's equations are

$$\dot{q} = \frac{\partial H}{\partial p} = \frac{p}{m}, \quad \dot{p} = -\frac{\partial H}{\partial q} = -m\omega^2 q + A m q^2, \quad (1.6.63)$$

Fixed points

$$\dot{q} = p/m = 0 \Rightarrow p = 0, \quad (1.6.64)$$

$$\dot{p} = mq(Aq - \omega^2) = 0 \Rightarrow q = 0, \omega^2/A. \quad (1.6.65)$$

So there are two fixed points $(q, p) = (0, 0), (\omega^2/A, 0)$.

To determine if they are elliptic or hyperbolic it is sufficient to analyse their local region in phase space.

Fixed point $(0, 0)$: In the vicinity of $q = 0$ we have $|q| \ll 1$, and so to a good approximation

$$H = \frac{p^2}{2m} + \frac{m\omega^2}{2}q^2 + \dots \quad (1.6.66)$$

This is the Hamiltonian for the SHO: and we have found already that the fixed point for this type of potential is a elliptic fixed point that is stable.

Fixed point $(\omega^2/A, 0)$: By using the results given before for a general potential, since

$$V''(q) = m(\omega^2 - 2Aq), \quad V''(\omega^2/A) = -m\omega^2 < 0,$$

this means $(\omega^2/A, 0)$ is a hyperbolic fixed point.

The phase portrait for the system is shown in Fig. 1.6. The energy at each fixed point can be found by substituting it directly into the Hamiltonian. We find

$$\text{For } (q, p) = (0, 0) : \quad H = 0, \quad (1.6.67)$$

$$\text{For } (q, p) = (\omega^2/A, 0) : \quad H = \frac{m\omega^2}{2} \frac{\omega^4}{A^2} - \frac{1}{3}Am \frac{\omega^6}{A^3} = \frac{m\omega^6}{6A^2} \quad (1.6.68)$$

Since all paths in phase space for this system have fixed values of H , this means the separatrices are defined by the equation

$$\frac{m\omega^6}{6A^2} = \frac{p^2}{2m} + \frac{1}{2}m\omega^2 q^2 - \frac{1}{3}Am q^3. \quad (1.6.69)$$

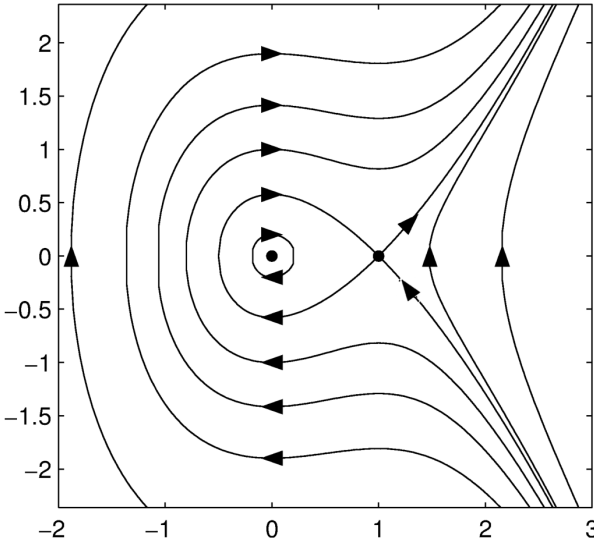


Figure 1.6: Phase portrait for a cubic potential with $m = \omega = A = 1$.

An interesting feature is that the left branch of the separatrices form a closed orbit with a turning point described by the negative solution of the equation:

$$\frac{m\omega^6}{6A^2} = \frac{1}{2}m\omega^2q^2 - \frac{1}{3}Amq^3 \iff -\frac{1}{3}Am\left(q - \frac{\omega^2}{A}\right)^2\left(q + \frac{\omega^2}{2A}\right), \quad (1.6.70)$$

indicating that the turning point is at $q_- = -\omega^2/(2A)$. Note also that the fact that the previous equation has a double zero in $\bar{q} = \omega^2/A$ reflect the nature of the fixed point.

As a good exercise study the potential $V(q) = -\frac{1}{3}Amq^3$, you will notice that the fixed point in $(q, p) = 0$ is hyperbolic though a branch of separatrices disappear compared to the linear repulsive force. This is a general behaviour close of of potentials having $V'(\bar{q}) = V''(\bar{q}) = \dots = V^{(n-1)}(\bar{q}) = 0$ and $V^{(n)}(\bar{q}) \neq 0$ with n an odd integer.

Exercises : (these examples are studied in the first half of Lecture two, I suggest to look at the lecture slides)

- As a good exercise study the phase portrait for the following hamiltonian

$$H(q, p) = \frac{1}{2}p^2 - \frac{a}{2}q^2 + \frac{1}{4}q^4.$$

The study of the position of fixed points show how there is a bifurcation structure at $a = 0$ of the types and positions of fixed points. We will see again these types of bifurcations in the behaviour of systems in examples leading to chaotic behaviour. The description of this example is given in the slides of the second lecture and the student is recommended to look at such material.

- As a second exercise study the dynamics for the following hamiltonian

$$H(q, p) = \frac{1}{2}p^2 + \frac{1}{3}q^3.$$

This is the simple example of a system admitting a fixed point \bar{q} with $V''(\bar{q}) = 0$ while $V^{(3)}(\bar{q}) \neq 0$. This is particularly interesting since it exhibit an unstable fixed point in the origin that qualitatively differs from the hyperbolic one described before.

1.6.6 Summary

Through the previous examples we have introduced the methods typically used in the analysis of a conservative Hamiltonian system with one degree of freedom. For this course a complete analysis can be summarised as follows:

1. Construct the Hamiltonian $H(q, p)$ where

$$H = T + V, \quad p = \frac{\partial \mathcal{L}}{\partial \dot{q}}.$$

2. Write down Hamilton's equations for the system

$$\dot{p} = -\frac{\partial H}{\partial q}, \quad \dot{q} = \frac{\partial H}{\partial p},$$

3. Find all of the fixed points (q, p) such that $(\dot{q}, \dot{p}) = (0, 0)$.
4. Determine the stability of the dynamics in the vicinity of the fixed point. If the coordinate $q(t)$ does not, in general, become large with increasing time then it is stable, otherwise it is unstable.
5. For hyperbolic fixed points: determine the equations of the separatrices.
6. Plot the phase portrait, for instance plotting the curves of constant H .
7. Solve Hamilton's equations when possible.
8. Discuss the behaviour of the system depending on the value of free parameters (we will see examples later in lectures and tutorials).

Aside: In the study of dynamical systems other types of fixed points are possible, in particular stable or unstable “nodes”, “stars” and “spirals”. However, these do not occur for conservative Hamiltonian systems. We will sketch examples later during the course.

CHAPTER 2

Periodic motion

There are two types of periodic motion that can occur in Hamiltonian dynamics—*libration* and *rotation*.

2.1 Libration (oscillation)

Libration is closed motion, where the system retraces its steps periodically so that q and p are periodic functions of time with the same frequency. The name “libration” comes from astronomy. A pendulum in a clock is a classic example, and the trajectories form closed loops in a phase portrait. A prototypical example of libration is given by the standard harmonic oscillator with closed curves surrounding an elliptic fixed point.

2.2 Rotation

Here p is some periodic function of q with a period q_0 , but q is not a periodic function of time. The most familiar example is rotation of a rigid body, with q as the angle of rotation and $q_0 = 2\pi$.

2.3 Free particle rotating in a plane

Imagine a particle of mass m attached to one end of a rigid, massless rod of length a that is able to pivot about the other end that is fixed. The configuration space of the system can be represented by the angle ϕ that it makes to the vertical axis as shown in Fig. 2.1. This is a simple system that can display rotational dynamics, for which we already know

$$\text{Moment of inertia: } J = ma^2, \quad (2.3.1)$$

$$\text{Angular momentum: } \ell = |\underline{\ell}| = J\dot{\phi}, \quad (2.3.2)$$

$$\text{Lagrangian: } \mathcal{L} = T = \frac{1}{2}J\dot{\phi}^2. \quad (2.3.3)$$

For the generalised coordinate ϕ the generalised momentum is $\partial\mathcal{L}/\partial\dot{\phi} = J\dot{\phi}$, which is simply the angular momentum ℓ as given above. Assuming there are no forces acting on the system thus the Hamiltonian takes the form

$$H = \frac{\ell^2}{2J}. \quad (2.3.4)$$

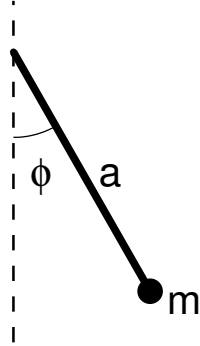


Figure 2.1: Configuration for a free particle rotating in a plane. (The configuration is the same for a pendulum, with the addition of the gravitational force mg acting downwards.)

Hamilton's equations

$$\dot{\ell} = -\frac{\partial H}{\partial \phi} = 0 \quad \Rightarrow \quad \ell \text{ is conserved.} \quad (2.3.5)$$

$$\dot{\phi} = \frac{\partial H}{\partial \ell} = \frac{\ell}{J}, \quad (2.3.6)$$

which is consistent with what we wrote down above. As ℓ is constant, Eq. (2.3.6) can be solved to give

$$\phi(t) = \omega(t - t_0) + \phi(t_0), \quad \omega = \frac{\ell}{J}, \quad T = \frac{2\pi}{\omega} = \frac{2\pi J}{\ell}. \quad (2.3.7)$$

Here we have indicated the frequency and period of rotation with ω and T , respectively. Later we will see that a similar description in terms of angle variable applies also to other 1D conservative hamiltonian systems, including for example the SHO.

2.3.1 Pendulum

The configuration for the pendulum is again as in Fig. 2.1, but with the gravitational force acting on the mass in the downwards direction. The gravitational potential is in this case given by

$$V(\phi) = -mga \cos \phi. \quad (2.3.8)$$

Thus the Lagrangian is

$$\mathcal{L} = T - V = \frac{1}{2}J\dot{\phi}^2 + mga \cos \phi. \quad (2.3.9)$$

The conjugate momentum is the same as in the previous section and so the Hamiltonian is

$$H(\phi, \ell) = \frac{\ell^2}{2J} - mga \cos \phi. \quad (2.3.10)$$

Hamilton's equations

$$\dot{\ell} = -\frac{\partial H}{\partial \phi} = -mga \sin \phi, \quad (2.3.11)$$

$$\dot{\phi} = \frac{\partial H}{\partial \ell} = \frac{\ell}{J}. \quad (2.3.12)$$

The fixed points are where $(\dot{\phi}, \dot{\ell}) = (0, 0)$, and so we have

$$\dot{\phi} = 0 \quad \text{when} \quad \ell = 0, \quad (2.3.13)$$

$$\dot{\ell} = 0 \quad \text{when} \quad \phi = 0, \pm\pi, \pm 2\pi, \dots, \quad (2.3.14)$$

however of course ϕ is periodic and so there are only two physically distinct fixed points $(\phi, \ell) = (0, 0)$ and $(\pi, 0)$. These correspond to the pendulum hanging downwards and "hanging upwards".

Intuitively you might guess that $(0, 0)$ is a stable fixed point and that $(\pi, 0)$ is unstable. To show this mathematically we need only consider motion in the vicinity of the fixed point.

2.3.1.1 Fixed point $(0, 0)$

For small ϕ we can approximate $\sin \phi \approx \phi$, and so Eq. (2.3.11) becomes

$$\dot{\ell} = -mga\phi. \quad (2.3.15)$$

Differentiating Eq. (2.3.12) with respect to time, and substituting in Eq. (2.3.15) gives

$$\ddot{\phi} = -\frac{mga}{J}\phi = -\omega_0^2\phi, \quad \omega_0 = \left(\frac{mga}{J}\right)^{1/2} = \sqrt{\frac{g}{a}}, \quad (2.3.16)$$

which has the general solution of the SHO

$$\phi(t) = A \cos(\omega_0 t + \delta), \quad (2.3.17)$$

and again the constants A and δ are determined by the boundary conditions. As the solution is the same as for the SHO then this must be a stable elliptic fixed point.

2.3.1.2 Fixed point $(\pi, 0)$

In the vicinity of $\phi = \pi$, we have

$$\sin(\phi) = \sin(\pi - \phi) \approx \pi - \phi, \quad (2.3.18)$$

so Eq. (2.3.11) becomes

$$\dot{\ell} = mga(\pi - \phi). \quad (2.3.19)$$

Differentiating Eq. (2.3.12) with respect to time, and substituting in Eq. (2.3.19) gives

$$\ddot{\phi} = \frac{mga}{J}(\phi - \pi). \quad (2.3.20)$$

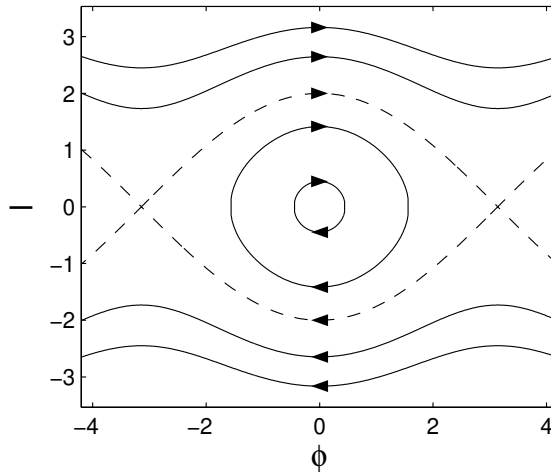


Figure 2.2: Phase portrait for the pendulum. The separatrices are indicated by the dashed lines.

If we make the change of coordinate $\gamma = \phi - \pi$ then Eq. (2.3.20) becomes

$$\dot{\gamma} = \omega_0^2 \gamma, \quad (2.3.21)$$

that has the general solution

$$\gamma(t) = A_1 e^{\omega_0 t} + A_2 e^{-\omega_0 t}. \quad (2.3.22)$$

Thus we have

$$\phi(t) = \pi + A_1 e^{\omega_0 t} + A_2 e^{-\omega_0 t}. \quad (2.3.23)$$

This is the same situation as we had for the repulsive linear force: this is a hyperbolic fixed point and is unstable.

2.3.1.3 Phase portrait

The phase portrait for the pendulum is shown in Fig. 2.2. The separatrix divides the phase space into three types of motion:

1. Above the upper separatrix the pendulum rotates about its pivot point in an anticlockwise direction.
2. Below the lower separatrix the pendulum rotates about its pivot point in a clockwise direction.
3. Between the separatrices the pendulum oscillates (librates) back and forth.

Note that the pendulum is NOT the simple harmonic oscillator except for the limiting case where the amplitude of oscillation is very small and hence $|\phi| \ll 1$ (you should check this!).

2.3.1.4 Separatrices

The energy of the system on the separatrices is given by substituting the coordinates of the hyperbolic fixed point $(\phi, \ell) = (\pi, 0)$ back into the expression for the Hamiltonian Eq. (2.3.10). We find that

$$H(\pi, 0) = m g a, \quad (2.3.24)$$

which would have been expected: this is the gravitational potential energy at this point.

Thus, when the energy of the system exceeds mga the pendulum rotates and the motion is of type (1) or (2) described earlier. If the energy is less than mga then the motion is of type (3).

The general solution of Hamilton's equations for the pendulum cannot be expressed in terms of simple functions. However, they can be for the special case of the separatrices, where from the Hamiltonian Eq. (2.3.10) we have

$$mga = \frac{\ell^2}{2J} - mga \cos \phi, \quad (2.3.25)$$

$$\Rightarrow \ell = \pm [2Jmga(1 + \cos \phi)]^{1/2}. \quad (2.3.26)$$

However, using the double angle formula $\cos 2\theta = \cos^2 \theta - \sin^2 \theta$ we can have

$$(1 + \cos \phi)^{1/2} = \sqrt{2} \cos(\phi/2), \quad (2.3.27)$$

and so

$$\ell = \pm 2(Jmga)^{1/2} \cos(\phi/2). \quad (2.3.28)$$

Substituting Eq. (2.3.28) into Eq. (2.3.13) for $\dot{\phi}$ gives the differential equation

$$\dot{\phi} = \pm 2\omega_0 \cos(\phi/2), \quad (2.3.29)$$

where use was made of the definition for ω_0 from Eq. (2.3.17). Equation (2.3.29) is a separable differential equation of first order and can be written

$$\frac{d\phi}{\cos(\phi/2)} = \pm 2\omega_0 dt. \quad (2.3.30)$$

Integrating both sides with the help of the result from tables, that

$$\int \frac{dz}{\cos z} = \ln[\tan(\pi/4 + z/2)], \quad (2.3.31)$$

gives

$$2 \ln[\tan(\pi/4 + \phi/4)] = \pm 2\omega_0 t + C, \quad (2.3.32)$$

where C is a constant that depends on the boundary conditions. If we choose $\phi(t=0) = 0$ then on rearranging Eq. (2.3.32) we have

$$\phi(t) = 4 \tan^{-1}[\exp(\pm\omega_0 t)] - \pi. \quad (2.3.33)$$

Physically this corresponds to travelling from the bottom of the separatrix to the hyperbolic point. The crucial point is that it takes an infinite time to reach the fixed-point, consistently with the uniqueness of the solutions.

We can now find the solution for the momentum. From Eq. (2.3.12) we have

$$\ell(t) = J\dot{\phi}(t). \quad (2.3.34)$$

Using the chain rule on Eq. (2.3.33) and

$$\frac{d}{dz} \tan^{-1} z = \frac{1}{1+z^2}, \quad (2.3.35)$$

we find that

$$\ell(t) = \pm \frac{2J\omega_0}{\cosh(\omega_0 t)}. \quad (2.3.36)$$

Note that as $t \rightarrow \infty$ then $\ell(t) \rightarrow 0$. These solutions are shown in Fig 2.3.

Wasn't that a fun bunch of mathematics! There are some different approaches, for example the general solution using action-angle variables in later lectures.

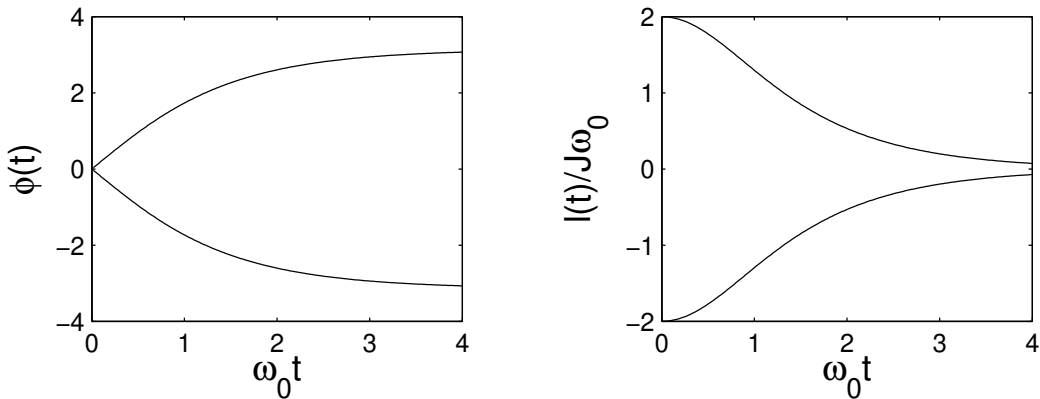


Figure 2.3: The solutions for $\phi(t)$ and $\ell(t)$ for the pendulum on the separatrix

2.4 APPENDIX: Computational mechanics and phase portraits

We will often encounter cases where we cannot find an analytical solution. In these cases, we can still obtain useful information using numerical solutions. Therefore, we will briefly look at computational methods for solving dynamics problems.

Mechanics as an initial value problem

If we have an Hamiltonian H , then Hamilton's equations

$$\dot{q}_i = \frac{\partial H}{\partial p_i}, \quad \dot{p}_i = -\frac{\partial H}{\partial q_i} \quad (2.4.37)$$

are a system of 1st order ODEs. With initial conditions $q_i(0) = A_i$ and $p_i(0) = B_i$, we can solve the system by integrating over time from the initial conditions.

We could also begin with

$$\dot{\mathbf{x}} = \mathbf{F}/m \quad (2.4.38)$$

and, substituting $\mathbf{v} = \dot{\mathbf{x}}$, obtain a system of coupled 1st order ODEs:

$$\dot{\mathbf{x}} = \mathbf{v}, \quad (2.4.39)$$

$$\dot{\mathbf{v}} = \mathbf{F}/m. \quad (2.4.40)$$

Given a differential equation we can write as

$$\dot{y}(t) = f(t, y(t)), \quad (2.4.41)$$

we can solve this for $t = 0$ to $t = t_{\text{final}}$, given a boundary condition $y(0) = y_0$ (i.e., we have an *initial value* problem). The basic method of solution is straightforward—integrate! We can write the solution as

$$y(t) = \int_0^t \dot{y}(z) dz + y_0. \quad (2.4.42)$$

Euler's method

We can perform the integration above numerically by using the forward difference approximation for the derivative:

$$\dot{y} \approx \frac{y(t + \Delta t) - y(t)}{\Delta t}. \quad (2.4.43)$$

Our integral can then be performed in a series of discrete steps:

$$y(t + \Delta t) = y(t) + \Delta t \dot{y} = y(t) + \Delta t f(t, y(t)). \quad (2.4.44)$$

This is *Euler's method*.

For the SHO, we can implement Euler's method in Matlab:

```
t = 0:0.01:2*pi;
x = zeros(size(t));
v = zeros(size(t));
x(1) = 1;
v(1) = 0;
% Euler's method
for n = 2:length(t)
    x(n) = x(n-1) + (t(n)-t(n-1))*v(n-1);
    v(n) = v(n-1) + -(t(n)-t(n-1))*x(n-1);
end
```

The path in phase space for 1 cycle is shown in Figure 2.4. Note that the cycle is not closed. This is due to numerical error. If we were to integrate for many cycles, we would obtain an outward spiral rather than periodic motion. We can reduce the numerical error by reducing the time step, as shown in Figure 2.5, but the cost in computational time and memory can be excessive.

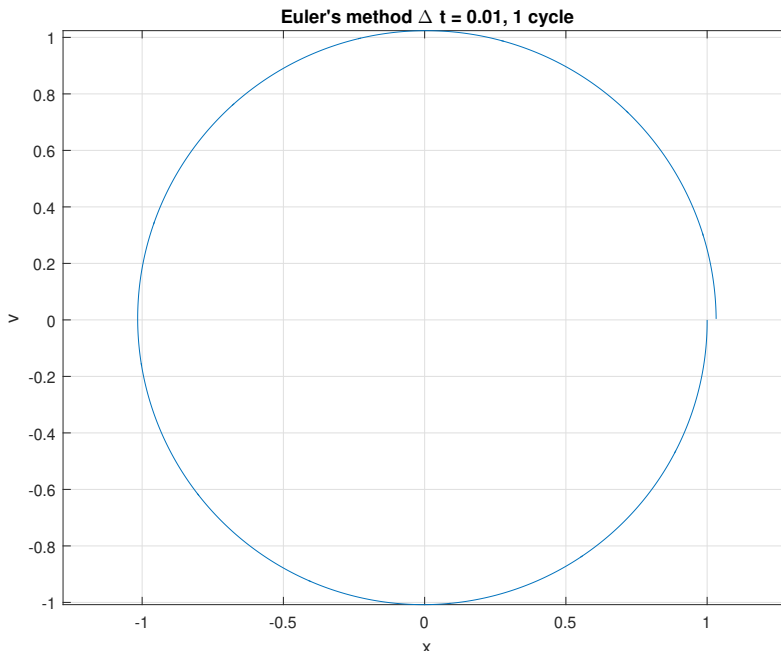


Figure 2.4: 1 cycle in phase space for the SHO with Euler's method. Note that the cycle is not closed—this is due to numerical error.

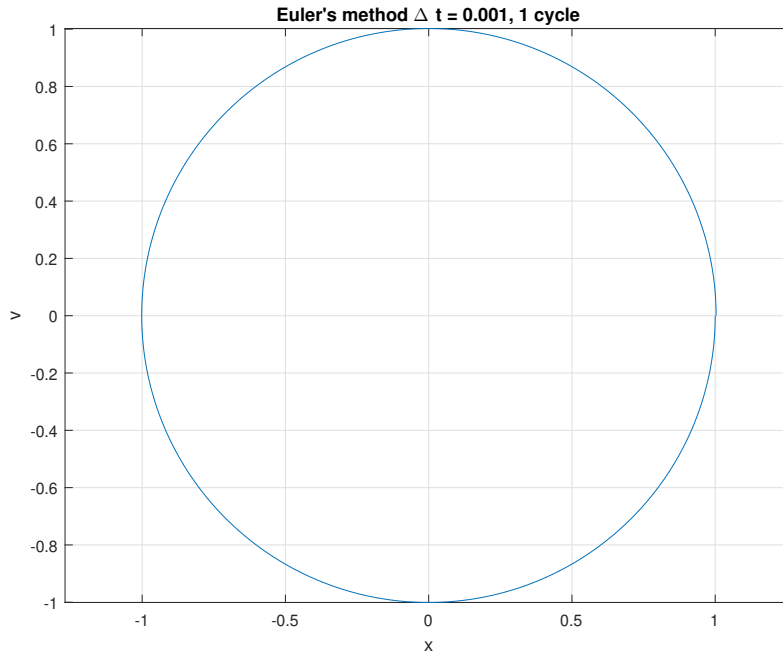


Figure 2.5: 1 cycle in phase space for the SHO with Euler’s method. This uses a smaller step size, and the numerical error is smaller.

Higher-order one-step methods—the Runge–Kutta family

When we want to have solutions more accurate than those provided by Euler’s method (or other low-order methods), we can use higher-order methods. The most common are the Runge–Kutta family of methods.

Of this family, two methods stand out as providing an excellent compromise between simplicity, accuracy, and robustness:

- 4th order Runge–Kutta (fixed step size)
- Order 4/5 Runge–Kutta–Fehlberg (variable step size, Matlab’s `ode45`)

These methods are also called *predictor–corrector methods*. Essentially, we can use a prediction of the derivative at the next point to correct our prediction of the value of the function at the point (rather than just using the derivative at our initial point, as in Euler’s method).

The two methods above are so widely used that either, especially the first, is often called “*the* Runge–Kutta method”.

In Matlab, it is convenient to use the function `ode45`. This solver uses adaptive choice of step size, so we don’t need to specify a time step. It’s usually safe to use the default settings for target accuracy. To use `ode45`, we need to define a function to calculate the derivatives, either as a separate m-file or as an inline function as in this example:

```
% Function to calculate the derivatives
dd = @(t,x) [x(2); -x(1)];
% time interval
tt = [0 2*pi];
% initial conditions
```

```
x0 = [ 1; 0 ];
[t,x] = ode45(dd,tt,x0);
figure;
plot(x(:,1),x(:,2),'-');
```

While this (usually) results in a reduction in the numerical error, compared to Euler's method with a similar time step, we can often still see outward spiralling of our solution if we calculate it for many cycles. If we only calculate it for 1 cycle, or a small number of cycles, our numerical error can be invisible, or almost so, on the scale of our graph, as shown in Figure 2.6.

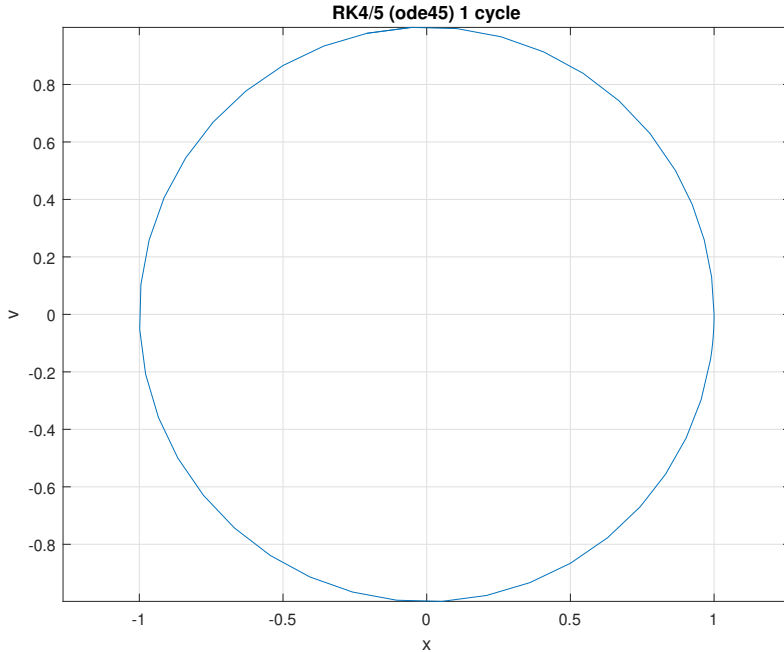


Figure 2.6: 1 cycle in phase space for the SHO using Matlab's `ode45`, a 4/5th order Runge–Kutta solver.

Methods designed for conservative system—Verlet integration

It is worth mentioning a method that is very well-behaved for conservative systems: Verlet integration. Since it produces time-reversible solutions, it avoids the outward (or inward, depending on the system) paths seen using Euler's method or Runge–Kutta methods. The most useful method for ODEs of the type we are interested in here is the *velocity Verlet method*. Given a position \mathbf{x} , velocity $\mathbf{v} = \dot{\mathbf{x}}$ and acceleration $\mathbf{a} = \dot{\mathbf{v}} = \ddot{\mathbf{x}}$, we can implement this as two sequential steps:

$$\mathbf{x}(t + \Delta t) = \mathbf{x}(t) + \mathbf{v}(t)\Delta t + \frac{1}{2}\mathbf{a}(t)\Delta t^2 \quad (2.4.45)$$

$$\mathbf{v}(t + \Delta t) = \mathbf{v}(t) + \frac{1}{2}(\mathbf{a}(t) + \mathbf{a}(t + \Delta t))\Delta t \quad (2.4.46)$$

if the acceleration only depends on the position \mathbf{x} and not the velocity \mathbf{v} . (What does this mean in terms of the Hamiltonian and Hamilton's equations?)

In Matlab, our SHO becomes

```
t = 0:0.01:2*pi;
x = zeros(size(t));
v = zeros(size(t));
x(1) = 1;
v(1) = 0;
for n = 2:length(t)
    dt = (t(n)-t(n-1));
    x(n) = x(n-1) + dt*v(n-1) + -dt^2/2*x(n-1);
    v(n) = v(n-1) + -dt*(x(n-1)+x(n))/2;
end
```

Typical results are shown in Figure 2.7; we can extend this calculation for many cycles and find that we have avoided spiralling paths.

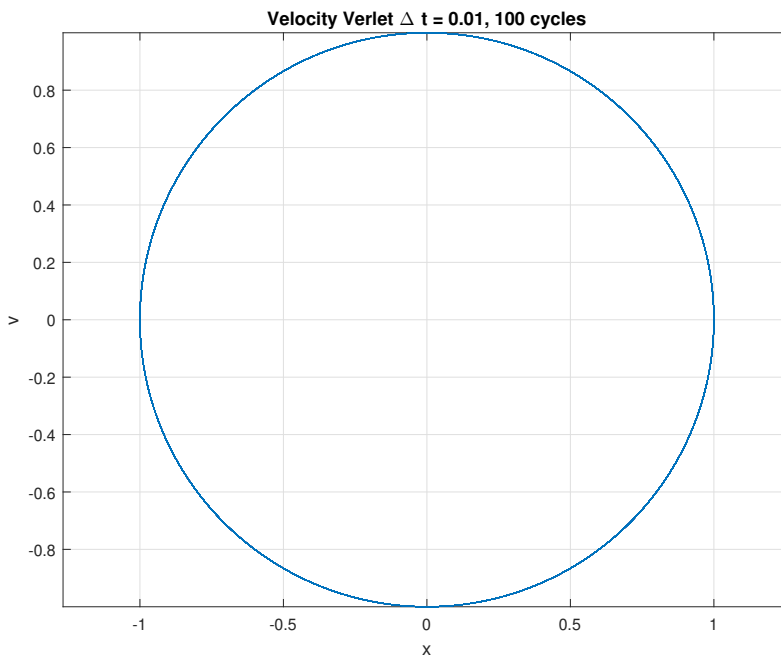


Figure 2.7: 100 cycles in phase space for the SHO using a velocity Verlet integrator.

The pendulum

Armed with the above tools, we can investigate the pendulum. If we choose a suitable set of initial conditions (which is easier said than done – see the code that generates these figures), we can generate the phase portrait, as shown in Figure 2.8.

However, for a conservative system, we can generate the phase portrait with solving the ODEs. Since the Hamiltonian is independent of time, and only depends on q and p , we can plot $H(q, p)$, shown in Figure 2.9.

Since H is constant along a path, the paths are contours of constant H , and we can generate the phase portrait using Matlab's `contour` function (Figure 2.10).

We can then use numerical differentiation to calculate the gradient of $H(q, p)$, shown in Figure 2.11. Rotating the gradient vectors 90 degrees clockwise, we obtain the flow field (Figure 2.12).

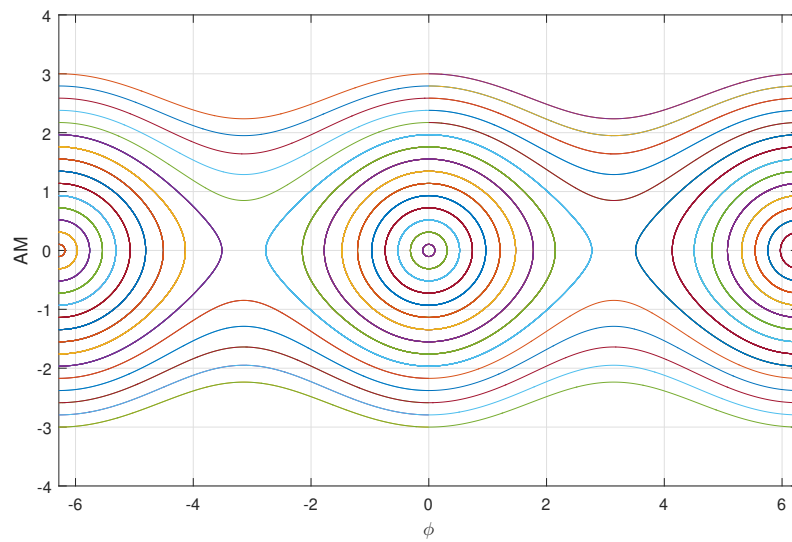


Figure 2.8: Phase portrait for pendulum using 90 initial conditions (why can't we see 90 paths?), using velocity Verlet integration.

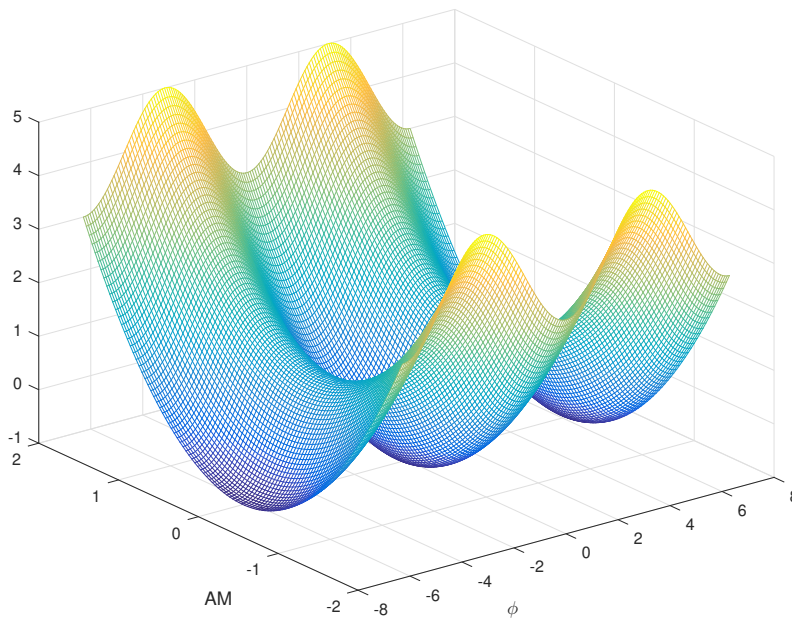


Figure 2.9: $H(q, p)$ for pendulum.

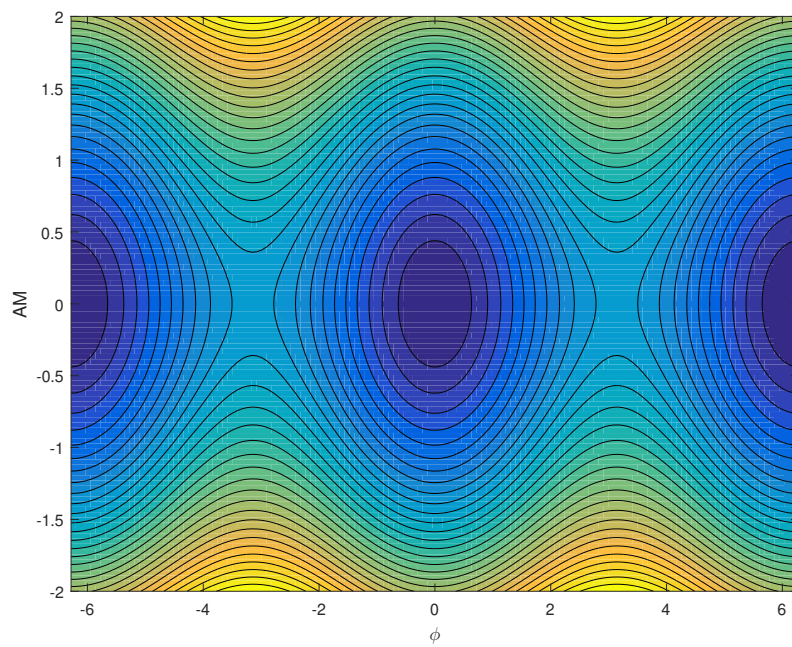


Figure 2.10: Phase portrait as contours of $H(q, p)$ for pendulum.

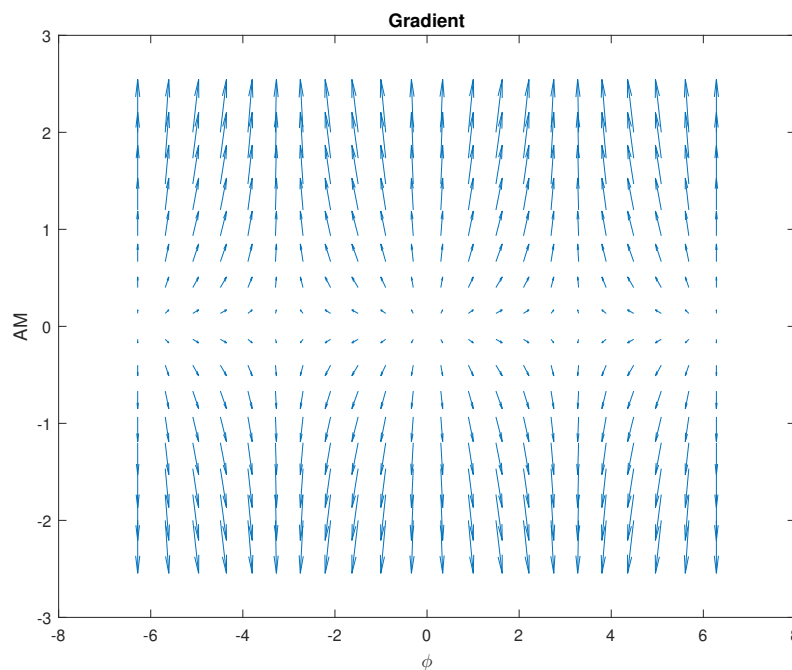


Figure 2.11: Gradient of $H(q, p)$ for pendulum.

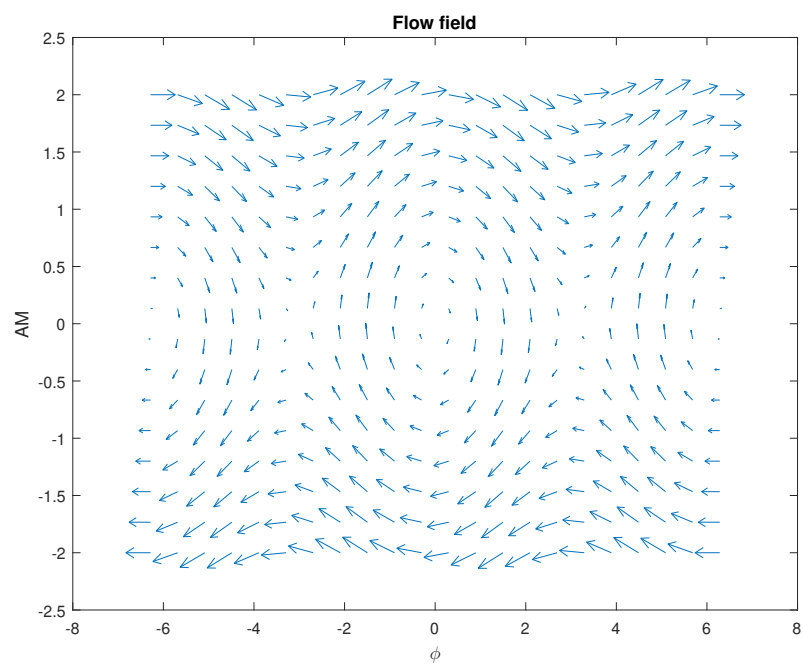


Figure 2.12: Flow field for pendulum.

CHAPTER 3

Dynamics near fixed points

In this chapter we want to extend some of the analysis made in the previous chapters for more general phase spaces whose dynamics is not necessarily hamiltonian. Examples of chaotic systems are of this form and we will see later they possess types of “attracting” points and regions (we’ll discuss attractors in some of the coming chapters) which largely characterise the qualitative and quantitative behaviour of a dynamical system. Fixed points still play an essential role and here we want to look at more general cases than the ones described before. For simplicity we will restrict our analysis to a two-dimensional system. An example we have seen before in the phase space of a one dimensional hamiltonian system described by a generic hamiltonian $H(q, p, t)$ and hamilton’s equations

$$\dot{q} = \frac{\partial H}{\partial p}(q, p, t), \quad \dot{p} = -\frac{\partial H}{\partial q}(q, p, t), \quad (3.0.1)$$

with q and p the phase space coordinates. This an example of 2D a system of a *non-autonomous system* ordinary differential equations written in normal form:

$$\begin{aligned} \dot{q} &= f_1(q, p, t) \\ \dot{p} &= f_2(q, p, t) \end{aligned} \quad (3.0.2)$$

In the particular case of a 1D hamiltonian system f_1 and f_2 are partial derivative of a single function, the hamiltonian. Let us now move for a while to more general cases, we will get back to Hamiltonian systems in next lectures.

3.1 Autonomous/non-autonomous systems

An *autonomous system* in normal form is a system of ordinary differential equations (ODEs), of the form

$$\begin{aligned} \dot{x} &= f_1(x, y, z, \dots) \\ \dot{y} &= f_2(x, y, z, \dots) \\ \dot{z} &= f_3(x, y, z, \dots) \\ &\vdots \end{aligned} \quad (3.1.3)$$

Or, in more compact form,

$$\dot{\mathbf{x}} = \mathbf{f}(\mathbf{x}) \quad (3.1.4)$$

The right hand side is *not* a function of time.

A *non-autonomous system* is a system of ODEs where the f s functions can depend on time.

$$\dot{\mathbf{x}} = \mathbf{f}(\mathbf{x}, t) \quad (3.1.5)$$

However, given a non-autonomous system (i.e., a system with an explicit time dependence) we can always construct a corresponding autonomous system, which will have higher order, by introducing one or more auxiliary variables. In fact, it is enough to extend the system to

$$\begin{aligned}\dot{\mathbf{x}} &= \mathbf{f}(\mathbf{x}, \tau) \\ \dot{\tau} &= 1\end{aligned} \quad (3.1.6)$$

which is equivalent to (3.1.5) though it has an extra degree of freedom which is the coordinate τ . For example, suppose we had a periodic driving term $\dot{x} = f(x) + A \sin \omega t$. We could introduce a new variable τ and construct an autonomous system as

$$\begin{aligned}\dot{x} &= g(x) + A \sin \tau \\ \dot{\tau} &= \omega\end{aligned} \quad (3.1.7)$$

plus the boundary condition $\tau(t = 0) = 0$, at the cost of going from a system with 1 degrees of freedom to one with two.

3.1.1 Non-autonomous Hamiltonian systems

It is worth noticing that the same trick works also for hamiltonian systems. Suppose to have a time dependent Hamiltonian $H(q_i, p_i, t)$ of a system with n degrees of freedom and $2n$ -dimensional phase space. Then define the following Hamiltonian

$$\tilde{H}(q_i, \tau, p_i, \rho) := H(q_i, p_i, \tau) + \rho \quad (3.1.8)$$

where τ , which is the time variable, is lifted to be a new generalised coordinate with conjugate momenta described by the coordinate ρ . The Hamiltonian $\tilde{H}(q_i, \tau, p_i, \rho)$ has $(2n + 1)$ degrees of freedom and its hamilton's equations are

$$\begin{aligned}\dot{q}_i &= \frac{\partial \tilde{H}}{\partial p_i}(q_j, \tau, p_k, \rho) = \frac{\partial H}{\partial p_i}(q_j, \tau, p_k) \\ \dot{\tau} &= \frac{\partial \tilde{H}}{\partial \rho}(q_j, \tau, p_k, \rho) = 1 \\ \dot{p}_i &= -\frac{\partial \tilde{H}}{\partial q_i}(q_j, p_k, \tau, \rho) = -\frac{\partial H}{\partial q_i}(q_j, p_k, \tau) \\ \dot{\rho} &= -\frac{\partial \tilde{H}}{\partial \tau}(q_j, p_k, \tau, \rho) = -\frac{\partial H}{\partial \tau}(q_j, p_k, \tau)\end{aligned} \quad (3.1.9)$$

The first three equations are equivalent to Hamilton's equations for the original Hamiltonian $H(q_i, p_j, t)$ while the last equation is trivial. In fact we know that for an Hamiltonian independent of time it holds $H(q_i(t), p_j(t)) = \text{constant}$, meaning that the Hamiltonian evaluated on the solution is a constant independent of time. This immediately tells us that¹

$$\text{constant} = C = \tilde{H}(q_i(t), t, p_i(t), \rho(t)) = H(q_i(t), p_i(t), t) + \rho(t) \quad (3.1.10)$$

which identifies

$$\rho(t) = -H(q_i(t), p_i(t), t) + C.$$

This proves the equivalence between a non-autonomous hamiltonian system and an autonomous one with more more degree of freedom. Let's now get back to general autonomous systems

¹For simplicity we assumed initial conditions for $\dot{\tau} = 1$ given by $t_0 = 0$ hence $\tau(t) = t$.

3.1.2 Few degrees of freedom

Autonomous systems with 1 or 2 degrees of freedom can generally be solved analytically. For example, in 1D,

$$\dot{x} = f(x) \quad (3.1.11)$$

is separable so it can be solved by rearranging and integrating,

$$\int \frac{dx}{f(x)} = \int dt, \quad \int_{x(t_0)}^{x(t)} \frac{ds}{f(s)} = t - t_0. \quad (3.1.12)$$

Another interesting example is the second-order equation

$$\ddot{x} = f(x, \dot{x}) \quad (3.1.13)$$

can be solved by first converting into a normal form of two first order equations,

$$\begin{aligned} \dot{x} &= v \\ \dot{v} &= f(x, v) \end{aligned} \quad (3.1.14)$$

Using the chain rule, $d^2x/dt^2 = dv/dt = (dv/dx)(dx/dt) = v(dv/dx)$ so we get again an implicit equation

$$v \frac{dv}{dx} = f(x, v) \quad (3.1.15)$$

which is first order and contains no reference to time, so its solution provides v as a function of x . If one is able to solve for $v(t)$ (which might not be possible in general), since $\dot{x} = v$, we can then solve for $x(t)$ in the same way we did for Eq.3.1.11. For instance, the special case of the second order system

$$\ddot{x} = f(x) \quad (3.1.16)$$

where the right hand side is *not* a function of velocity, is an example of a conservative Hamiltonian system that we studied in the previous chapters. From Newton's second law, $\ddot{x} = F/m = -\nabla V/m$, where m is the mass. Hence the potential V is the solution of

$$\frac{\partial V}{\partial x} = -mf(x). \quad (3.1.17)$$

Note that we will see that also general conservative 1D Hamiltonian systems can always be in principle solved by integrating. However, in general autonomous systems are not conservative and non-hamiltonian. There are no general solution methods for more general second order autonomous systems and for third and higher orders. These are systems that can exhibit chaotic behaviour.

Let us now turn our attention to understanding some qualitative properties of general two-dimensional first order autonomous system and in particular extract information about their fixed points. We will turn to examples of more general systems later on though we will not repeat any detailed analysis for linearization, fixed points etc with ODEs of dimension higher than two (some similar techniques and results hold though the complexity of the systems, even linear ones, largely increases with the dimension).

3.2 Fixed points and linearization

Consider the general two-dimensional first order ODEs

$$\begin{aligned}\dot{x} &= f(x, y) \\ \dot{y} &= g(x, y)\end{aligned}\tag{3.2.18}$$

where x, y, f, g are all taking real values. A fixed point of this dynamical system is given by (\bar{x}, \bar{y}) such that

$$\begin{aligned}0 = \dot{\bar{x}} &= f(\bar{x}, \bar{y}) \\ 0 = \dot{\bar{y}} &= g(\bar{x}, \bar{y})\end{aligned}\tag{3.2.19}$$

Similarly to the hamiltonian cases that we have studied before, we are interested to understand the dynamics close to the fixed points. We then expand the vector field (f, g) and the differential equation around the fixed points obtaining

$$\begin{aligned}\dot{x} &= (x - \bar{x}) \frac{\partial f(x, y)}{\partial x} \Big|_{(x, y) = (\bar{x}, \bar{y})} + (y - \bar{y}) \frac{\partial f(x, y)}{\partial y} \Big|_{(x, y) = (\bar{x}, \bar{y})} + \dots \\ \dot{y} &= (x - \bar{x}) \frac{\partial g(x, y)}{\partial x} \Big|_{(x, y) = (\bar{x}, \bar{y})} + (y - \bar{y}) \frac{\partial g(x, y)}{\partial y} \Big|_{(x, y) = (\bar{x}, \bar{y})} + \dots\end{aligned}\tag{3.2.20}$$

where the ellipsis represent higher-order in the Taylor expansion of f and g . Note that once defined the shifted coordinates

$$u_1 := (x - \bar{x}), \quad u_2 := (y - \bar{y}), \quad \mathbf{u} := (u_1, u_2)$$

the linearised system (3.2.20) can be rewritten in the compact form

$$\dot{\mathbf{u}} = A\mathbf{u} + \dots\tag{3.2.21}$$

where A is a constant matrix defined by the Jacobian matrix at the fixed points

$$A := \begin{pmatrix} \frac{\partial f(x, y)}{\partial x} & \frac{\partial f(x, y)}{\partial y} \\ \frac{\partial g(x, y)}{\partial x} & \frac{\partial g(x, y)}{\partial y} \end{pmatrix} \Big|_{(x, y) = (\bar{x}, \bar{y})}.\tag{3.2.22}$$

Assuming we can ignore the \dots in (3.2.20), we can study the dynamics near the fixed points by solving (3.3.24) which can actually be solved exactly. We will comment later whether this approximation is sensible or not to describe the behaviour of the fixed points for the entire non-linear equation (3.2.18).

3.3 Classification of linear systems

Let us classify the solutions of the linear first order ODE

$$\dot{\mathbf{u}} = A\mathbf{u}\tag{3.3.23}$$

where we will parametrize the constant matrix A as

$$A := \begin{pmatrix} a & b \\ c & d \end{pmatrix}.\tag{3.3.24}$$

Note that this equation has always a fixed point in the origin of the phase space.

The general solution can be found by separation of variables and linearity. First, we assume that the solution factorises as

$$\mathbf{u}(t) = T(t)\mathbf{w} \quad (3.3.25)$$

Since $T(t) \neq 0$, which follows from the fact that we want $\mathbf{u}(t) \neq 0$ different than the central fixed point for all time, the previous equation is equivalent to

$$\frac{\dot{T}(t)}{T(t)}\mathbf{w} = A\mathbf{w}. \quad (3.3.26)$$

Since the left hand side is independent of time, the previous equation is equivalent to the following two separate equations

$$\frac{\dot{T}(t)}{T(t)} = \lambda, \quad A\mathbf{w}_\lambda = \lambda\mathbf{w}_\lambda. \quad (3.3.27)$$

The second equation is the eigenvalue/eigenvector equation for the matrix A . Assuming we have solved it for a (in general complex) eigenvalue λ and eigenvector \mathbf{w}_λ , then the solution of $\dot{T}(t) = \lambda T(t)$ is simply given by

$$T(t) = T_0 e^{\lambda t}. \quad (3.3.28)$$

If $\lambda = 0$, but $\mathbf{w} \neq 0$, the solution of the original linearized differential equation is simply the constant $\mathbf{u}(t) = T_0\mathbf{w}_0$. For a real nonzero eigenvalue λ we get $\mathbf{u}(t) = T_0 e^{\lambda t}\mathbf{w}_\lambda$ and the solution diverges from or converges to the fixed point at the origin if $\lambda > 0$ or $\lambda < 0$, respectively. For complex eigenvalues the solution is not real and we need some more care. We will classify all these cases but first let's remind the reader how the general solution of the eigenvector equations for a 2×2 real matrix goes.

3.3.1 Eigenvalue/eigenvector equation for a 2×2 real matrix and ODE solutions

A necessary condition for the equation

$$A\mathbf{w}_\lambda = \lambda\mathbf{w}_\lambda$$

to be satisfied is that the matrix $(A - \lambda I)$, where I is the 2×2 identity matrix, has a nonzero Kernel, which means that the characteristic equation

$$\det[A - \lambda I] = 0. \quad (3.3.29)$$

Expressed in terms of the components of A the characteristic equation takes the form

$$\lambda^2 - (a + d)\lambda + (ad - bc) = 0 \iff \lambda^2 - \text{Tr}[A]\lambda + \det[A] = 0, \quad (3.3.30)$$

where $(a + d) = \text{Tr}[A]$ is the trace of the matrix A while $(ad - bc) = \det[A]$ is its determinant. Since (3.3.30) is a second order algebraic equation in a complex variable λ we know that it can always be solved. There are different types of solution depending on the value of the discriminant of the quadratic equation:

$$\Delta = (\text{Tr}[A])^2 - 4\det[A]. \quad (3.3.31)$$

Three separate cases leads to different solutions and types of fixed points at the origin of phase space.

3.3.1.1 $\Delta > 0$: nodes and saddle points (“hyperbolic” fixed points)

In this case the eigenvalue(s) are real and given by

$$\lambda_1 = \frac{\text{Tr}[A] - \sqrt{\Delta}}{2}, \quad \lambda_2 = \frac{\text{Tr}[A] + \sqrt{\Delta}}{2} \quad (3.3.32)$$

moreover the two eigenvectors \mathbf{w}_{λ_1} and \mathbf{w}_{λ_2} are necessarily linearly independent. This means that we have two independent solutions and the general solution can be written as the following linear combination

$$\mathbf{u}(t) = \alpha_0 e^{\lambda_1 t} \mathbf{w}_{\lambda_1} + \beta_0 e^{\lambda_2 t} \mathbf{w}_{\lambda_2}. \quad (3.3.33)$$

Since, as already mentioned, \mathbf{w}_{λ_1} and \mathbf{w}_{λ_2} in this case are linearly independent, for any possible initial condition $\mathbf{u}(0) = \mathbf{u}_0$ there are real constants α and β such that $\mathbf{u}_0 = \alpha \mathbf{w}_{\lambda_1} + \beta \mathbf{w}_{\lambda_2}$. This implies that (3.3.38) is the most general solution of $\dot{\mathbf{u}} = A\mathbf{u}$ when $\Delta > 0$. There are still different interesting subcases when $\Delta > 0$.

- $0 < \lambda_1 < \lambda_2$ or $\lambda_2 < \lambda_1 < 0$:

In this case $(0, 0)$ is called a *node*. With positive eigenvalues, $0 < \lambda_1 < \lambda_2$, we have an unstable node, each orbit diverges from the origin for positive times. With $\lambda_1 < \lambda_2 < 0$ we have a stable node, each orbit converge to the origin for positive times. Two directions, the ones parallel to the two eigenvectors, are straight lines. The other orbits approximate the straight line of the slow direction of \mathbf{w}_{λ_1} for $t \simeq 0$ while move in the same direction of the fast eigenvalue \mathbf{w}_{λ_2} asymptotically in the past and future $t \rightarrow \pm\infty$.

It is straightforward to have an idea of the phase portrait of the two curves considering that, assuming a general solution is given by

$$\mathbf{u}(t) = \alpha(t) \mathbf{w}_{\lambda_1} + \beta(t) \mathbf{w}_{\lambda_2}, \quad \alpha(t) = \alpha_0 e^{\lambda_1 t}, \quad \beta(t) = \beta_0 e^{\lambda_2 t} \quad (3.3.34)$$

then it holds (assuming both α and β are nonzero, hence we are not considering a straight line normal direction)

$$\frac{\beta}{\beta_0} = \left(\frac{\alpha}{\alpha_0} \right)^{\lambda_2/\lambda_1}. \quad (3.3.35)$$

This can be considered as a solution of β as a function of α , though keep in mind that the axes described by \mathbf{w}_{λ_1} and \mathbf{w}_{λ_2} are in general not orthogonal and do not coincide with the q and p axes. Note also that the shape is the same for both attractive and repulsive nodes. Through an appropriate change of coordinates, for nodes it is always possible to diagonalise the system and choose \mathbf{w}_{λ_1} and \mathbf{w}_{λ_2} orthogonal and coinciding with the q and p axes. A picture of an attractive node is given in figure 3.1.

- $\lambda_1 < 0 < \lambda_2$:

In this case the eigenvalues have different sign. The origin is an unstable fixed point which is denoted as *saddle point*. This is qualitatively the same case as an hyperbolic fixed point that we discussed before. A typical trajectory approaches the \mathbf{w}_{λ_2} unstable line $t \rightarrow +\infty$ while it approaches the \mathbf{w}_{λ_1} stable line as $t \rightarrow -\infty$. The behaviour of the orbits is described by the relation

$$\beta = c \alpha^{-|\lambda_2|/|\lambda_1|}, \quad c := \beta_0 \alpha_0^{|\lambda_2|/|\lambda_1|}. \quad (3.3.36)$$

Figure 3.2 shows an example of the phase portrait for a saddle point.

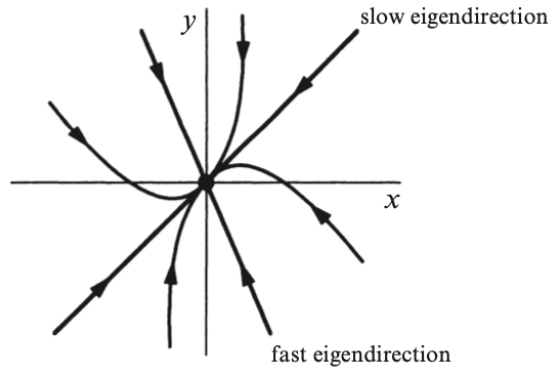


Figure 3.1: Attractive node.

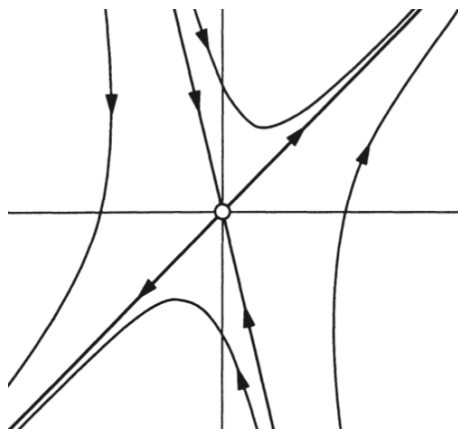


Figure 3.2: Saddle point.

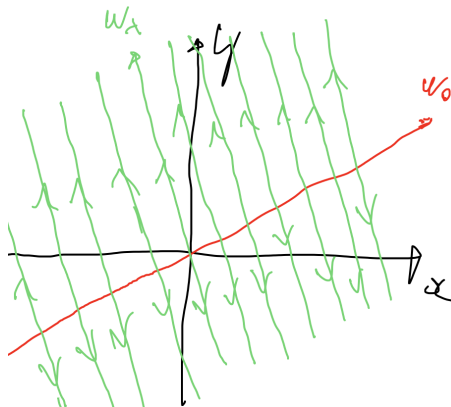


Figure 3.3: Degenerate unstable case, one line of fixed points.

- $\lambda_1 = 0; \lambda_2 := \lambda \neq 0$:

In this case the matrix still admits two eigenvectors but one has zero eigenvalue, we assume to be $\lambda_1 = 0$ and rename λ_2 as λ . In this case the whole line described by w_λ is made of fixed points while it is simple to see that the phase portrait is described by straight lines parallel to the eigenvector w_λ and passing through every point of the straight line described by w_0 . For $\lambda > 0$ each trajectory diverges from the unstable line of fixed points, while for $\lambda < 0$ we have a line of stable fixed points. An example of a degenerate case with a line of unstable fixed points is shown in figure 3.3.

3.3.1.2 $\Delta < 0$: centers (elliptic fixed points) and spirals

In this case there are in general two complex eigenvalues. Since the characteristic polynomial is real, the two eigenvalues are complex conjugate one of the other. We denote them as

$$\lambda = \mu + i\omega, \quad \lambda^* = \mu - i\omega, \quad \mu := \frac{\text{Tr}[A]}{2}, \quad \omega := \frac{\sqrt{-\Delta}}{2} \quad (3.3.37)$$

By assumption $\omega \neq 0$ and the general solution of (3.3.23) is now taking complex values and it is given by

$$\mathbf{u}(t) = \alpha_0 e^{\lambda t} \mathbf{w} + \beta_0 e^{\lambda^* t} \mathbf{w}^*, \quad (3.3.38)$$

where we have used the fact that the eigenvector associated to λ^* is the complex conjugate of \mathbf{w} . Note also that by assumption \mathbf{w} and \mathbf{w}^* have to be linearly independent complex vectors. (if they were parallel, then $\lambda = \lambda^*$ which is against the assumption of $\omega \neq 0$). It is not difficult to construct a general real solution out of the previous complex one by noticing that

$$\mathbf{w} = \text{Re}[\mathbf{w}] + i\text{Im}[\mathbf{w}] \quad (3.3.39)$$

where $\text{Re}[\mathbf{w}]$ and $\text{Im}[\mathbf{w}]$ are the real and imaginary parts of \mathbf{w} respectively. Importantly, $\text{Re}[\mathbf{w}]$ and $\text{Im}[\mathbf{w}]$ are linearly independent as real vectors (if not, it's easy to show that \mathbf{w} and \mathbf{w}^* would be the same up to a complex number, which contradicts the fact that they have to be linearly independent). To restrict to a generic solution with real $\mathbf{u}(t)$ it is enough to choose

$$\alpha_0 = \frac{\rho_0}{2} e^{i\varphi_0}, \quad \beta_0 = (\alpha_0)^* = \frac{\rho_0}{2} e^{-i\varphi_0}, \quad \rho_0 \geq 0, \quad 0 \leq \varphi_0 < 2\pi \quad (3.3.40)$$

and

$$\mathbf{u}(t) = \frac{\rho_0}{2} e^{i\varphi_0} e^{\lambda t} \mathbf{w} + \frac{\rho_0}{2} e^{-i\varphi_0} e^{\lambda^* t} \mathbf{w}^* \quad (3.3.41)$$

$$\mathbf{u}(t) = \rho_0 e^{\mu t} \left[\text{Re}[\mathbf{w}] \cos(\omega t + \varphi_0) - \text{Im}[\mathbf{w}] \sin(\omega t + \varphi_0) \right]. \quad (3.3.42)$$

Note that this real solution is parametrised by two independent real constants ρ_0 and φ_0 , which is the right number we would expect for a two dimensional first order ODE. Moreover, it is simple to show that every point of the real two-dimensional plane can be uniquely written as (a version of polar coordinates where, however, $\text{Re}[\mathbf{w}]$ and $\text{Im}[\mathbf{w}]$ are in general not orthonormal to each other)

$$\mathbf{u}(0) = \rho_0 \left[\text{Re}[\mathbf{w}] \cos(\varphi_0) - \text{Im}[\mathbf{w}] \sin(\varphi_0) \right]. \quad (3.3.43)$$

Hence, due to uniqueness, its clear that (3.3.42) is a general real solution with $\Delta < 0$. We rewrite it in “polar” coordinates as

$$\mathbf{u}(t) = \rho(t) \left[\text{Re}[\mathbf{w}] \cos(\varphi(t)) - \text{Im}[\mathbf{w}] \sin(\varphi(t)) \right], \quad (3.3.44)$$

$$\rho(t) = \rho_0 e^{\mu t}, \quad \varphi(t) = \omega t + \varphi_0. \quad (3.3.45)$$

By eliminating the time from $\rho(t)$ and $\varphi(t)$ we find the curve in polar coordinates given by

$$\rho = \rho_0 e^{\mu(\varphi - \varphi_0)/\omega} \quad (3.3.46)$$

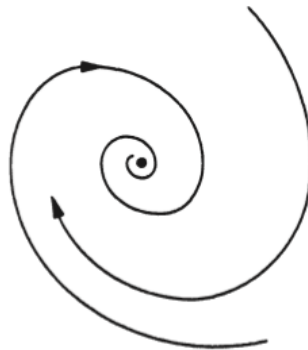


Figure 3.4: Stable spiral.

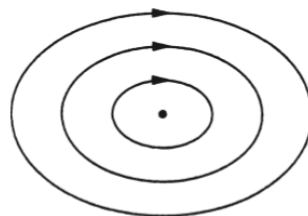


Figure 3.5: Center ("elliptic fixed point").

which, for $\mu \neq 0$ is called "logarithmic spiral". With $\mu = 0$ the solution is periodic with period $T = 2\pi/\omega$ and describe a circle, up to distortions due to general $Re[\mathbf{w}]$ and $Im[\mathbf{w}]$ – this case is also called a center. The sign of μ indicate whether the solutions converge to or diverge from the origin of phase space. The sign of ω determines the direction of rotation. Summarising, we have qualitatively three cases with $\Delta < 0$:

- $\mu < 0$, *stable spiral*

In this case the origin of phase space is stable and the phase portrait is a logarithmic spiral. An example is given in figure 3.4. A prototypical case of stable spiral is given by the damped simple harmonic oscillator.

- $\mu = 0$, *center (elliptic fixed point)*

In this case the orbits are periodic and the behaviour is qualitatively equivalent to the elliptic fixed point we described in the previous chapters. The origin is a stable fixed point (sometimes called neutral fixed point to distinguish from stable spirals where solutions asymptotically converge to the fixed point.) An example of a center is given in figure 3.5.

- $\mu > 0$, *unstable spiral*

In this case the origin of phase space is unstable with the phase portrait a logarithmic spiral. An example is the same as figure 3.4 but with reversed direction of the vector field flow.

3.3.1.3 $\Delta = 0$: stars, degenerate nodes

When $\Delta = 0$ the characteristic equation has only one solution given by

$$\lambda = \frac{\text{Tr}[A]}{2} \quad (3.3.47)$$

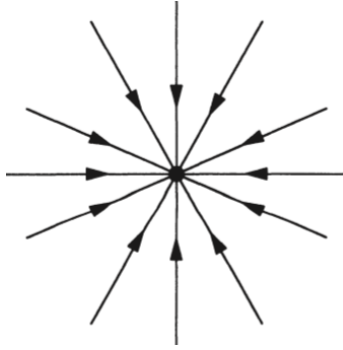


Figure 3.6: Stable star.

We have two non-trivial cases:

- *Two eigenvectors: stars*

We assume λ to be nonzero, otherwise the whole plane would be given by fixed points. In this case it is simple to show that the matrix A is necessarily proportional to the identity matrix

$$A := \begin{pmatrix} \lambda & 0 \\ 0 & \lambda \end{pmatrix}. \quad (3.3.48)$$

The solution is given by

$$\mathbf{u}(t) = \mathbf{u}_0 e^{\lambda t}, \quad (3.3.49)$$

for every vectors \mathbf{u}_0 in the real 2D plane. The phase portrait are straight lines coming from the origin and directing to or from the origin depending on the sign of λ . These are called star fixed points. $\lambda > 0$ it is an unstable star while for $\lambda < 0$ the origin is a stable star. Figure 3.6 is the phase portrait for a stable star.

- *One eigenvector: degenerate nodes*

This is the most tricky example. A typical example is given by the matrix A of the form

$$A := \begin{pmatrix} \lambda & b \\ 0 & \lambda \end{pmatrix}, \quad b \neq 0. \quad (3.3.50)$$

The solution of the ODE in this case is schematically of the following form (we choose $b = 1$ here)

$$u_1(t) = u_1(0)e^{\lambda t} + u_2(0)te^{\lambda t}, \quad u_2(t) = u_2(0)e^{\lambda t} \quad (3.3.51)$$

we simply comment that in this case, with $\lambda < 0$, the phase portrait has the shape given in figure 3.7 indicating that the origin is a stable fixed point (for $\lambda > 0$ it is unstable). Note that there is only one straight line (the eigendirection) passing through the origin and all the other trajectories become parallel to the one available eigendirection for $t \rightarrow \pm\infty$.

A good way to think about the degenerate node is to imagine that it has been created by deforming an ordinary node. The ordinary node has two independent eigendirections; all trajectories are parallel to the slow eigendirection as $t \rightarrow -\infty$ and to the fast eigendirection as $t \rightarrow +\infty$ (Figure 3.8).

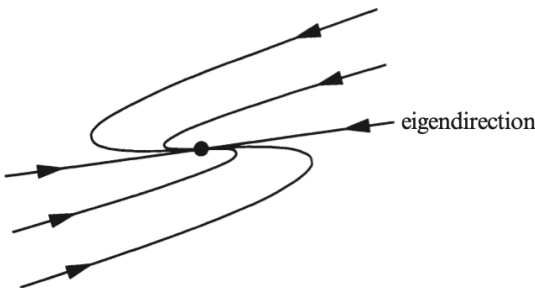


Figure 3.7: Degenerate node.

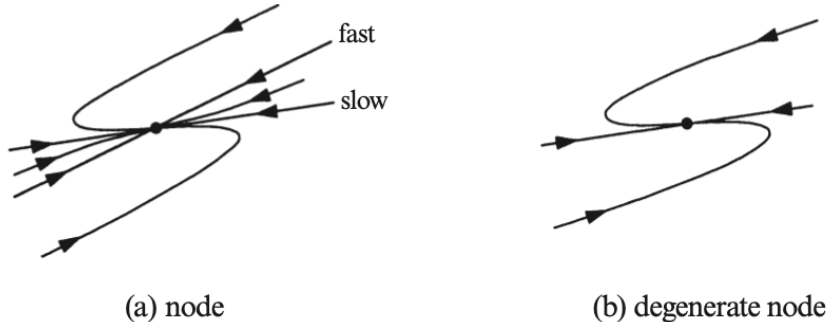


Figure 3.8: Degenerate node from limit of standard node.

For $\lambda = 0$ the trajectories degenerate even more and the solutions are of the form

$$u_1(t) = u_1(0) + u_2(0)t, \quad u_2(t) = u_2(0) \quad (3.3.52)$$

where one line is made of unstable fixed points and the rest of the phase portrait is made by parallel straight lines (this is very much the phase portrait of a free 1D particle).

3.3.2 Bifurcation diagram and non-linear stability

The previous analysis is quite rich and indicates that depending on the trace and determinant of the matrix A the physical system, and its fixed point at the origin, can have largely different dynamical behaviours. These can be summarised by the bifurcation diagram described by figure 3.9.

Coming back to the original non-linear ODE (3.2.21). Can we state that the nature of the non-linear fixed point is the same as described by the linearization? In other words, does the linearized system give a qualitatively correct picture of the phase portrait near the fixed point? The answer is yes, as long as the fixed point for the linearized system is not one of the borderline cases. In other words, if the linearized system predicts a saddle, node, or a spiral, then the fixed point really is a saddle, node, or spiral for the original nonlinear system. We don't attempt to prove this here. The borderline cases (centers, degenerate nodes, stars, or non-isolated fixed points) are much more delicate. They can be altered by small nonlinear terms. A nice exception to the previous statement are centers (elliptic fixed points) for conservative hamiltonian systems whose nature remains the same in the non-linear case as their linearization. Let's close this chapter (that works as an illustrative detour to prepare the reader to exotic objects like strange

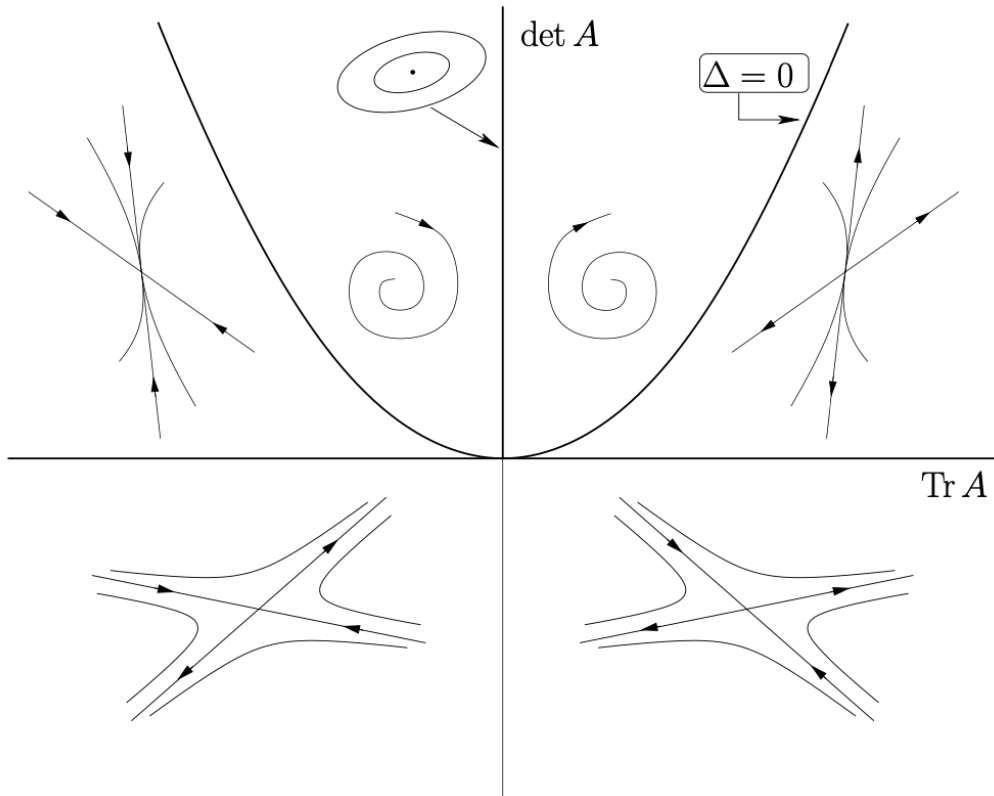


Figure 3.9: Bifurcation diagram for linear first order ODE.

attractors and systems exhibiting chaotic behaviour) by looking back at hamiltonian systems.

3.3.3 Final comments: conservative hamiltonian systems

Consider a conservative hamiltonian system with hamilton's equations given by

$$\dot{q} = \frac{\partial H(q, p)}{\partial p}, \quad \dot{p} = -\frac{\partial H(q, p)}{\partial q}, \quad (3.3.53)$$

Assuming that (\bar{q}, \bar{p}) is a fixed point, then the Jacobian at the fixed point for the linearization of the system about the fixed point is

$$A_H := \begin{pmatrix} \frac{\partial^2 H(q, p)}{\partial q \partial p} & \frac{\partial^2 H(q, p)}{\partial p^2} \\ -\frac{\partial^2 H(q, p)}{\partial q^2} & -\frac{\partial^2 H(q, p)}{\partial q \partial p} \end{pmatrix} \Big|_{(q, p) = (\bar{q}, \bar{p})}. \quad (3.3.54)$$

We see that in this case

$$\text{Tr}[A_H] \equiv 0 \quad (3.3.55)$$

This implies that the bifurcation diagram completely collapse only to the vertical line! This can be seen as a reason why for conservative 2D hamiltonian system elliptic fixed points (centers) are well classified by the linearization analysis. Perturbations cannot change the phases (as for instance turning a center in a spiral), there is no space for that. The only point where the stability analysis remain subtle is the one with both $\text{Tr}[A_H] = 0$ and $\det[A_H] = 0$. To make clear contact to

our previous analysis, let's restrict to the case in which the hamiltonian is

$$H(q, p) = \frac{p^2}{2m} + V(q) \quad (3.3.56)$$

Hence it holds

$$A_H := \begin{pmatrix} 0 & \frac{1}{m} \\ -V''(\bar{q}) & 0 \end{pmatrix}. \quad (3.3.57)$$

The condition $\det[A_H] = 0$ is then identical to $V''(\bar{q}) = 0$ which we have already seen to be a case in which the linearization fails to address the nature of the dynamics near the fixed point. From the bifurcation diagram of the general conservative one dimensional hamiltonian systems it's clear that the dynamics close to isolated fixed point is very restricted and it is hard to imagine these systems can have chaotic behaviour. In fact they cannot since these systems are the simplest example of *integrable* systems (we will explain in the next section what integrable means). To obtain chaotic dynamics it's necessary to have at least a conservative two dimensional hamiltonian system (or, essentially equivalently, a 1D non-conservative hamiltonian system or a system of nonlinear ODEs with at least three degrees of freedom). Before turning our attention to overview some chaotic systems it's useful to give some more information about hamiltonian mechanics.

Exercise: (at exam and assessments you will not have to draw phase portraits other then for conservative hamiltonian systems but it's good to see at least some more general cases).

As a nice exercise to try at least ones to study a phase portrait for a nonconservative and nonhamiltonian system you can study the classic Lotka-Volterra model of competition between two species (for example rabbits against sheeps but in a covid year you might play thinking about humans against virus). Here we remain hoptimistic and stick with rabbits and sheeps. Suppose that both species are competing for the same food supply (grass) and the amount available is limited. Furthermore, ignore all other complications, like predators, seasonal effects, and other sources of food. Then there are two main effects we should consider:

1. Each species would grow to its carrying capacity in the absence of the other. This can be modelled by assuming logistic growth for each species (we will consider logistic maps and growth later). Rabbits have a legendary ability to reproduce, so perhaps we should assign them a higher intrinsic growth rate.

2. When rabbits and sheep encounter each other, trouble starts. Sometimes the rabbit gets to eat, but more usually the sheep nudges the rabbit aside and starts nibbling (on the grass, that is). We'll assume that these conflicts occur at a rate proportional to the size of each population. (If there were twice as many sheep, the odds of a rabbit encountering a sheep would be twice as great.) Furthermore, we assume that the conflicts reduce the growth rate for each species, but the effect is more severe for the rabbits.

An ODE that incorporates these assumptions is:

$$\begin{aligned} \dot{x} &= x(3 - x - 2y) \\ \dot{y} &= y(2 - x - y) \end{aligned} \quad (3.3.58)$$

where $x(t)$ is the population of rabbits while $y(t)$ is the population of sheeps. Find the fixed points, analyse their linearized stability properties and try to infer

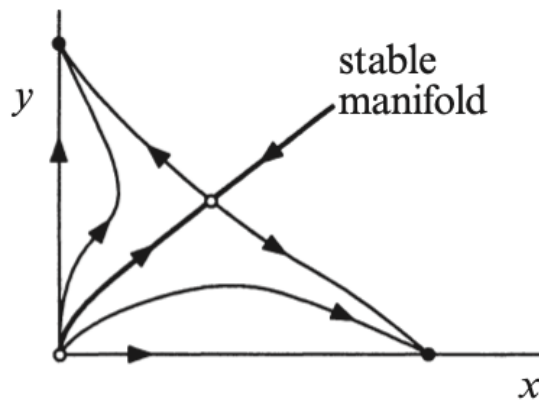


Figure 3.10: Rabbits vs Sheeps.

what the phase portrait could look like. Alternatively, you might use a calculator and see that the dynamics look like in figure 3.10. Note that, while in this case the dynamics is quite simple and leads in almost all situations to the extinction of one of the two species, more general Lotka-Volterra systems with different species actually present chaotic behaviour.

CHAPTER 4

More on Hamiltonian mechanics

During the last part of the Dynamics section of the course you have already seen the concept of Canonical transformations and Poisson brackets. These are absolutely crucial concepts in understanding the power of hamiltonian mechanics vs the Lagrangian and Newtonian one. Canonical transformations are the correct extension of coordinate transformations in Hamiltonian systems and preserve very important geometrical structures of phase space. Let us start by reviewing results that you have already seen in the Dynamics part, then we will further develop the hamiltonian/canonical formalism. This will be the appropriate language to understand various important examples of chaotic systems.

4.1 Canonical transformations and Poisson brackets

For simplicity, let's start by considering a system with one degree of freedom with generalised coordinates and momentum q, p . Let $H(q, p)$ be the Hamiltonian. We recall Hamilton's equations

$$\dot{q} = \frac{\partial H}{\partial p} \quad \dot{p} = -\frac{\partial H}{\partial q} \quad (4.1.1)$$

Take a transformation to a new set of coordinates (Q, P) where $Q = Q(q, p)$ and $P = P(q, p)$. Then the Hamiltonian may be expressed in terms of P, Q

$$H'(Q, P) = H(q(Q, P), p(Q, P)) \iff H(q, p) = H'(Q(q, p), P(q, p)).$$

Our aim here is to determine conditions on such a transformation so that Hamilton's equations hold for H' with Q and P ,

$$\dot{Q} = \frac{\partial H'}{\partial P} \quad \dot{P} = -\frac{\partial H'}{\partial Q}.$$

Such a transformation is called a *canonical transformation*. Using Hamilton's equations (4.1.1) it holds

$$\dot{Q} = \{Q, H\}$$

where $\{ , \}$ is called the Poisson bracket. We will sometimes use also the notation $\{ , \}_{(q,p)}$ if we want to stress that the Poisson brackets are computed in terms of the coordinates (q, p) of phase space.

Given functions $F(q, p)$, $G(q, p)$ their Poisson bracket is defined by

$$\{F, G\} = \frac{\partial F}{\partial q} \frac{\partial G}{\partial p} - \frac{\partial F}{\partial p} \frac{\partial G}{\partial q}.$$

Note that $\{F, G\} = -\{G, F\}$ (antisymmetry of the Poisson bracket) so that $\{F, F\} = 0$.

Now $H(q, p) = H'(Q(q, p), P(q, p))$ means that we have

$$\frac{\partial H}{\partial p} = \frac{\partial H'}{\partial Q} \frac{\partial Q}{\partial p} + \frac{\partial H'}{\partial P} \frac{\partial P}{\partial p}$$

and similarly for $\frac{\partial H}{\partial q}$. Thus substituting into the above expression for \dot{Q} we have

$$\begin{aligned}\dot{Q} &= \frac{\partial Q}{\partial q} \left(\frac{\partial H'}{\partial Q} \frac{\partial Q}{\partial p} + \frac{\partial H'}{\partial P} \frac{\partial P}{\partial p} \right) - \frac{\partial Q}{\partial p} \left(\frac{\partial H'}{\partial Q} \frac{\partial Q}{\partial q} + \frac{\partial H'}{\partial P} \frac{\partial P}{\partial q} \right) \\ &= \frac{\partial H'}{\partial P} \left(\frac{\partial Q}{\partial q} \frac{\partial P}{\partial p} - \frac{\partial Q}{\partial p} \frac{\partial P}{\partial q} \right) \\ \dot{Q} &= \{Q, P\} \frac{\partial H'}{\partial P}\end{aligned}$$

Similarly,

$$\dot{P} = -\{Q, P\} \frac{\partial H'}{\partial Q}.$$

Thus, assuming $H'(Q, P) = H(q(Q, P), p(Q, P))$ (equivalent to $H(q, p) = H'(Q(q, p), P(q, p))$), Q, P obey Hamilton's equations if and only if

$$\{Q, P\} = 1.$$

This is the condition such that the variable change transformation $(q, p) \rightarrow (Q, P)$ is canonical.

Note: The Jacobian determinant of this transformation is given by

$$\begin{aligned}J &\equiv \left| \frac{\partial(Q, P)}{\partial(q, p)} \right| = \begin{vmatrix} \frac{\partial Q}{\partial q} & \frac{\partial Q}{\partial p} \\ \frac{\partial P}{\partial q} & \frac{\partial P}{\partial p} \end{vmatrix} \\ &= \frac{\partial Q}{\partial q} \frac{\partial P}{\partial p} - \frac{\partial Q}{\partial p} \frac{\partial P}{\partial q} \\ &= \{Q, P\}.\end{aligned}$$

So a canonical transformation is one in which the Jacobian determinant is $J = 1$.

Example: Suppose that for one degree of freedom we have the transformation

$$\begin{aligned}Q &= q \cos \alpha + p \sin \alpha \\ P &= -q \sin \alpha + p \cos \alpha\end{aligned}$$

Then

$$\{Q, P\} = \frac{\partial Q}{\partial q} \frac{\partial P}{\partial p} - \frac{\partial Q}{\partial p} \frac{\partial P}{\partial q} = \cos^2 \alpha + \sin^2 \alpha = 1, \quad \{Q, Q\} = \{P, P\} = 0$$

so the transformation is canonical.

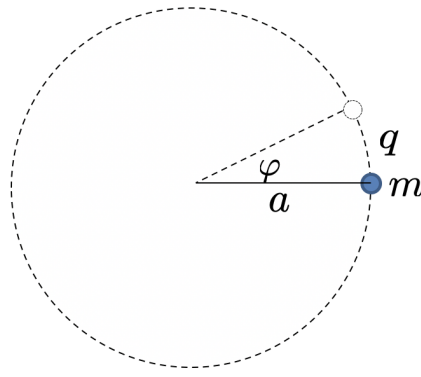


Figure 4.1: Mass on circle.

The fact that in hamiltonian mechanics q and p are treated on equal footing, and in fact canonical transformations typically mix them, is a crucial feature and allow for great simplifications and understanding of quantitative and qualitative features of a classical dynamical systems. Hamilton's equations could not be reduced to their simplest form by only making a change of coordinates in q , which is the one that is typically used to simplify Lagrangians.

Example: We again consider a freely rotating mass. We may choose our set of generalised coordinates as (q, p) where q is the distance around the circumference of the pivot from a fixed point, and $p = m\dot{q}$ (see Figure 4.1).

An alternative set of coordinates is (ϕ, ℓ) as considered in Section 2.3 and defined as the angle ϕ and the angular momenta ℓ . The transformation between the coordinates is

$$\phi = \frac{q}{a}, \quad \ell = ma^2\dot{\phi} = ma\dot{q} = ap. \quad (4.1.2)$$

The Jacobian determinant is

$$\left| \begin{array}{c} \partial(\phi, \ell) \\ \partial(q, p) \end{array} \right| = \left| \begin{array}{cc} \frac{\partial\phi}{\partial q} & \frac{\partial\phi}{\partial p} \\ \frac{\partial\ell}{\partial q} & \frac{\partial\ell}{\partial p} \end{array} \right| = \left| \begin{array}{cc} 1/a & 0 \\ 0 & a \end{array} \right| = \frac{1}{a} \times a - 0 \times 0 = 1. \quad (4.1.3)$$

4.1.1 Properties of the Poisson bracket

1. Antisymmetry:

$$\{u, v\} = -\{v, u\}.$$

2. Linearity:

$$\{au + bv, w\} = a\{u, w\} + b\{v, w\}, \quad a, b \in \mathbb{R}.$$

3. Derivation (Leibniz rule):

$$\{uv, w\} = \{u, w\}v + u\{v, w\}.$$

4. Jacobi's identity:

$$\{u, \{v, w\}\} + \{v, \{w, u\}\} + \{w, \{u, v\}\} = 0.$$

That is, the sum of cyclic permutation of the double Poisson bracket of three functions is zero.

I suggest you to prove the following identities as an instructive exercise

4.1.2 Time dependence of observables

The Poisson brackets play also a fundamental role in identifying the time dependence of “observables” (that in classical mechanics are functions in phase space and eventually time). In fact, given an arbitrary function u in the Poisson bracket formulation its total derivative with respect to time is

$$\frac{du}{dt} = \{u, H\} + \frac{\partial u}{\partial t}.$$

If u is a constant of the motion then from the above we have

$$\{H, u\} = \frac{\partial u}{\partial t}.$$

In this way we may identify the constants of motion. And conversely, the Poisson bracket of H with any constant of the motion must be equal to the explicit time derivative of the constant function. This is a very strong conceptual improvement in the search of constants of the motions. It streamlines the problem in solving a set of differential equation. We will not discuss it here (as Noether’s theorem and its relation to symmetries were not discussed in the Dynamics part) but it is worth shortly mentioning that this descriptions of constants of the motions and Poisson brackets proves to give a simple perspective on symmetries in hamiltonian mechanics.

If u, v are two constants of the motion and not explicit functions of t , then setting $w = H$ and using linearity, the Jacobi identity gives us that

$$\{H, \{u, v\}\} = 0.$$

(Poisson’s theorem: The Poisson bracket of any two constants of the motion is also a constant of the motion.) Assuming $\{u, v\}$ is a nontrivial function, this property can in principle be used to construct new constants of the motions by pure algebraic operations in terms of Poisson brackets.

4.1.3 Generalisation to many degrees of freedom

Above it was shown that for a system with one degree of freedom that the transformation (we will denote with \mathfrak{C} canonical transformations)

$$\mathfrak{C}: (q, p) \rightarrow (Q, P), \quad Q = Q(q, p), \quad P = P(q, p)$$

is canonical provided $\{Q, P\} = 1$ where $\{\cdot, \cdot\}$ denotes the Poisson bracket. Also by antisymmetry, we have $\{Q, Q\} = \{P, P\} = 0$. Now consider a system with m degrees of freedom with generalised coordinates and momenta q_i, p_i , ($1 \leq i \leq m$) which we will denote as

$$\mathbf{s} = (\mathbf{q}, \mathbf{p}) = (q_1, \dots, q_m, p_1, \dots, p_m), \quad \mathbf{s} \in \mathbb{R}^{2m}$$

Let then $H = H(q_i, p_i)$ be the Hamiltonian of the system and consider a transformation to new coordinates

$$\mathbf{S} = \mathfrak{C}(\mathbf{s}): Q_i = Q_i(q_j, p_j), \quad P_i = P_i(q_j, p_j)$$

where we introduced $\mathbf{S} = (Q_1, \dots, Q_m, P_1, \dots, P_m)$. In terms of these the Hamiltonian may be expressed as

$$H(q_i(Q_j, P_j), p_i(Q_j, P_j)) = H'(Q_j, P_j) \iff H(q_i, p_i) = H'(Q_j(q_i, p_i), P_j(q_i, p_i))$$

or in compact notations

$$H(\mathfrak{C}^{-1}(\mathbf{s})) = H'(\mathbf{s}) \iff H(\mathbf{s}) = H'(\mathfrak{C}(\mathbf{s})).$$

Then the coordinate transformation $\mathfrak{C}(\mathbf{s})$, given by Q_i, P_i , is canonical if they obey Hamilton's equations for H' and provided that they satisfy

$$\{Q_i, P_j\} = \delta_{ij}, \quad \{Q_i, Q_j\} = \{P_i, P_j\} = 0,$$

where the Poisson bracket of two functions $F(q_j, p_j), G(q_j, p_j)$ is now defined by

$$\{F, G\} = \sum_{i=1}^m \left(\frac{\partial F}{\partial q_i} \frac{\partial G}{\partial p_i} - \frac{\partial F}{\partial p_i} \frac{\partial G}{\partial q_i} \right) = -\{G, F\}.$$

Above, δ_{ij} is the Kronecker delta function defined as

$$\delta_{ij} = \begin{cases} 1 & i = j \\ 0 & i \neq j. \end{cases}$$

These canonical transformations preserve Hamilton's equations in fact

$$\dot{q}_i = \frac{\partial H}{\partial p_i} \quad \dot{p}_i = -\frac{\partial H}{\partial q_i}$$

and one can show that it follows

$$\begin{aligned} \dot{Q}_i &= \sum_{j=1}^m \left(\frac{\partial Q_i}{\partial q_j} \dot{q}_j + \frac{\partial Q_i}{\partial p_j} \dot{p}_j \right) \\ &= \sum_{j=1}^m \left(\frac{\partial Q_i}{\partial q_j} \frac{\partial H}{\partial p_j} - \frac{\partial Q_i}{\partial p_j} \frac{\partial H}{\partial q_j} \right) \\ &= \sum_{j=1}^m \frac{\partial Q_i}{\partial q_j} \sum_{k=1}^m \left(\frac{\partial H'}{\partial Q_k} \frac{\partial Q_k}{\partial p_j} + \frac{\partial H'}{\partial P_k} \frac{\partial P_k}{\partial p_j} \right) - \sum_{j=1}^m \frac{\partial Q_i}{\partial p_j} \sum_{k=1}^m \left(\frac{\partial H'}{\partial Q_k} \frac{\partial Q_k}{\partial q_j} + \frac{\partial H'}{\partial P_k} \frac{\partial P_k}{\partial q_j} \right) \\ &= \sum_{k=1}^m \frac{\partial H'}{\partial Q_k} \sum_{j=1}^m \left(\frac{\partial Q_i}{\partial q_j} \frac{\partial Q_k}{\partial p_j} - \frac{\partial Q_i}{\partial p_j} \frac{\partial Q_k}{\partial q_j} \right) + \sum_{k=1}^m \frac{\partial H'}{\partial P_k} \sum_{j=1}^m \left(\frac{\partial Q_i}{\partial q_j} \frac{\partial P_k}{\partial p_j} - \frac{\partial Q_i}{\partial p_j} \frac{\partial P_k}{\partial q_j} \right) \\ &= \sum_{k=1}^m \frac{\partial H'}{\partial Q_k} \{Q_i, Q_k\} + \sum_{k=1}^m \frac{\partial H'}{\partial P_k} \{Q_i, P_k\} \\ &= \frac{\partial H'}{\partial P_i}. \end{aligned}$$

Similarly it can be shown that

$$\dot{P}_i = -\frac{\partial H'}{\partial Q_i}.$$

As before, we call a transformation to new coordinates Q_i, P_i satisfying Hamilton's equations for $H'(Q_j, P_j) = H(q_i(Q_j, P_j), p_i(Q_j, P_j))$, a canonical transformation \mathfrak{C} .

Note: It can be shown that such a transformation in phase space is such that the determinant of its Jacobian is equal to unity.

Consider a function $F(q_i, p_i)$ of generalised coordinates and momenta. Then from Hamilton's equations we have

$$\begin{aligned}\dot{F} &= \sum_{i=1}^m \left(\frac{\partial F}{\partial q_i} \dot{q}_i + \frac{\partial F}{\partial p_i} \dot{p}_i \right) \\ &= \sum_{i=1}^m \left(\frac{\partial F}{\partial q_i} \frac{\partial H}{\partial p_i} - \frac{\partial F}{\partial p_i} \frac{\partial H}{\partial q_i} \right) = \{F, H\}.\end{aligned}$$

Thus the time evolution of a dynamical function $F(q_i, p_i)$ is governed by the Poisson bracket with H . In particular we have

$$\dot{q}_i = \{q_i, H\}, \quad \dot{p}_i = \{p_i, H\},$$

so Hamilton's equations may be expressed in terms of the Poisson bracket as

$$\{q_i, H\} = \frac{\partial H}{\partial p_i}, \quad \{p_i, H\} = -\frac{\partial H}{\partial q_i}.$$

Define an operator D_H by

$$D_H F(q_i, p_i) = \{F, H\}.$$

Thus D_H is a first order differential operator given by

$$D_H = \sum_{i=1}^m \left(\frac{\partial H}{\partial p_i} \frac{\partial}{\partial q_i} - \frac{\partial H}{\partial q_i} \frac{\partial}{\partial p_i} \right).$$

Then we have

$$\dot{F} = D_H F, \quad \ddot{F} = D_H \dot{F} = D_H^2 F, \dots, \frac{d^n F}{dt^n} = D_H^n F.$$

Using a Taylor series expansion, we have

$$\begin{aligned}F(t) &= \sum_{r=0}^{\infty} \frac{F^{(r)}(0)}{r!} t^r \\ &= \sum_{r=0}^{\infty} \frac{t^r D_H^r}{r!} F(0) = e^{t D_H} F(0)\end{aligned}$$

where $F(t) = F(q_i(t), p_i(t))$. In this way, given the value of a function at $t = 0$ we may determine its value at any subsequent time t , at least in principle.

So far we have also considered canonical transformations that are not dependent upon the time t . In general one can consider time dependent canonical transformations and in fact these prove to be extremely useful in several cases. All the properties discussed here are the same in this case and you can use the equivalence of autonomous and non-autonomous systems to nicely prove it if you wish.

4.2 Area (volume) preservation of canonical transformations

Consider a region R with area A_R in (q, p) space. Suppose it is transformed to a region S with area A_S in the (Q, P) system, as depicted in Fig. 4.2. The area of the

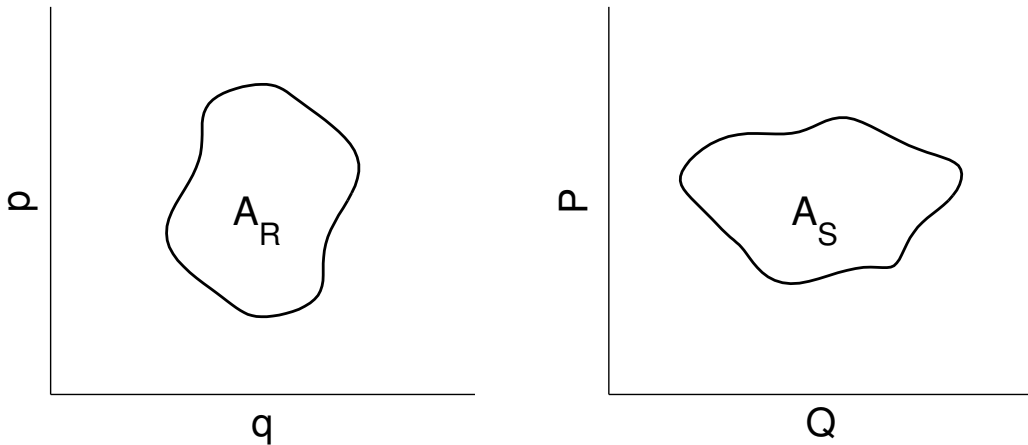


Figure 4.2: Coordinate transform of area A_R in (q, p) to area A_S in (Q, P) .

region R is

$$A_R = \int_R dq dp, \quad (4.2.4)$$

and the area of region S is

$$A_S = \int_S dQ dP, \quad (4.2.5)$$

In general there is no reason to assume that A_R and A_S will be the same. In fact, it can be shown that

$$\int_S dQ dP = \int_R dq dp \left| \frac{\partial(Q, P)}{\partial(q, p)} \right|. \quad (4.2.6)$$

where $\left| \frac{\partial(Q, P)}{\partial(q, p)} \right|$ is the Jacobian determinant of the transformation. Once more, for a canonical transformation it holds

$$\left| \frac{\partial(Q, P)}{\partial(q, p)} \right| = \begin{vmatrix} \frac{\partial Q}{\partial q} & \frac{\partial Q}{\partial p} \\ \frac{\partial P}{\partial q} & \frac{\partial P}{\partial p} \end{vmatrix} = \frac{\partial Q}{\partial q} \frac{\partial P}{\partial p} - \frac{\partial Q}{\partial p} \frac{\partial P}{\partial q} = \{Q, P\}_{(q, p)} = 1. \quad (4.2.7)$$

Hence, canonical transformations are the subclass of coordinate transformations of phase space that preserve the area (Volume). The same important property holds for systems with m degrees of freedoms which preserve the $2m$ dimensional volume (canonical transformations in $m > 1$ preserve more geometric invariants than just the volume but we will not enter in these details).

4.3 Volume preserving flows

The concept of the conservation of volume in phase space is very important in Hamiltonian mechanics and that's also another reason why canonical transformations are so important in this context. We have mentioned that canonical transformations have the property to preserve the volume (Area) in phase space. Note that for a system with n degrees of freedom, volume is defined as

$$V = \int_{\Omega} d\mathbf{q} d\mathbf{p}, \quad (4.3.8)$$

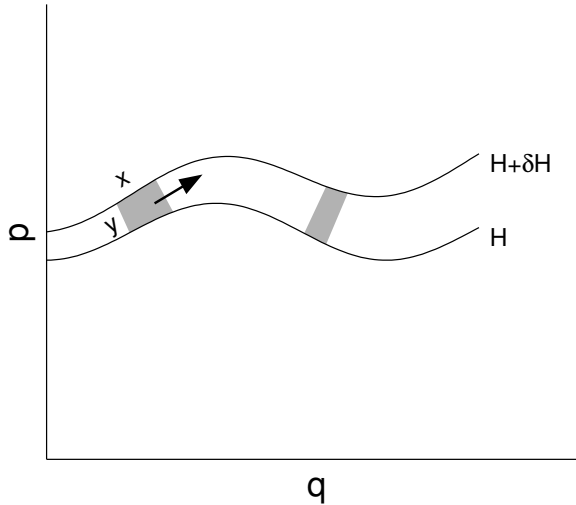


Figure 4.3: Volume preserving flows in phase space.

where Ω is the integration volume. Thus for a system with one degree of freedom, the volume is an “area” with units $kg\ m^2\ s^{-1} \equiv Js$. Remarkably, the hamiltonian flow defined by the solution to hamilton’s equations also preserve the volume. This can be seen in several ways.

It holds the following important theorem:

Liouville’s theorem:

The volume of a phase space flow is conserved for Hamiltonian systems.

We can show this explicitly for a 1D conservative Hamiltonian system. The theorem holds for non conservative ones too and for generic number of degrees of freedoms. It is a fundamental property of hamiltonian mechanics and it has important implication for several branches of physics, as for instance statistical mechanics and thermodynamics.

Consider a small rectangular region bounded by two paths in phase space, with energies given by H and $H + \delta H$ respectively as depicted in Fig. 4.3. The magnitude of the flow vector field is given by

$$|\mathbf{v}| = \left| \left(\frac{\partial H}{\partial p}, -\frac{\partial H}{\partial q} \right) \right| = \left[\left(\frac{\partial H}{\partial p} \right)^2 + \left(\frac{\partial H}{\partial q} \right)^2 \right]^{1/2} = |\nabla H|. \quad (4.3.9)$$

Then the length x of the area A is simply

$$x \approx |\mathbf{v}| \delta t = |\nabla H| \delta t. \quad (4.3.10)$$

As ∇H is perpendicular to curves of constant H then it follows that

$$|\nabla H| \approx \frac{\delta H}{y}. \quad (4.3.11)$$

Thus the area A is given by

$$A = xy = |\nabla H| \delta t \times y = \frac{\delta H}{y} \delta t \times y = \delta H \delta t. \quad (4.3.12)$$

So what this means is that for *any* point along the two trajectories, the area will be given by $\delta H \delta t$, and these quantities are chosen by us. Thus the area of the element is conserved as it moves through phase space.

We already commented about the fact that canonical transformations preserve the volume. Let us look at this again and then reinterpret Liouville's theorem as a simple consequence of the fact that the flow defined by the solutions of Hamilton's equations defines a one parameter family of canonical transformations.

We have seen that the hamiltonian flow is preserving the Area (Volume), thanks to Liouville's theorem. This means that the hamiltonian flow is a canonical transformation. We can show this explicitly.

4.4 Hamiltonian flow as a one parameter family of canonical transformations

A very useful way to think about the solution of Hamilton's equation is that they represent a set of change of coordinates parametrised by the time. We can denote this as the function $\mathfrak{G}^{(t)} : \mathbb{R}^{2m} \rightarrow \mathbb{R}^{2m}$ given by $\mathbf{s} \rightarrow \mathfrak{G}^{(t)}(\mathbf{s}) = \mathbf{s}(t)$ with $\mathbf{s}(t)$ being the solution of hamilton's equation with $\mathbf{s} = \mathbf{s}(0)$ as initial conditions. For simplicity, we focus on 1D hamiltonian system but all the results are true in general. In terms of generalised coordinates it holds

$$\mathfrak{G}^{(t)}(q, p) = \left(Q^{(t)}(q, p), P^{(t)}(q, p) \right) := (q(t), p(t))$$

$$\mathfrak{G}^{(0)}(q, p) = \left(Q^{(0)}(q, p), P^{(0)}(q, p) \right) = (q(0), p(0)) := (q, p)$$

The meaning of the previous relations is that given any point in phase space (q, p) the coordinate transformation $\left(Q^{(t)}(q, p), P^{(t)}(q, p) \right)$ is defined by the solution of Hamilton's equations $(q(t), p(t))$ where the initial conditions at $t = 0$ are the points (q, p) . At least locally, this is a well defined one-parameter family of maps of phase space in itself and trivially satisfies the following composition relations

$$\left(Q^{(t_1)} \left(Q^{(t_2)}, P^{(t_2)} \right), P^{(t_1)} \left(Q^{(t_2)}, P^{(t_2)} \right) \right) = \left(Q^{(t_2)} \left(Q^{(t_1)}, P^{(t_1)} \right), P^{(t_2)} \left(Q^{(t_1)}, P^{(t_1)} \right) \right) , \quad (4.4.13)$$

$$= \left(Q^{(t_1+t_2)}(q, p), P^{(t_1+t_2)}(q, p) \right) , \quad (4.4.14)$$

$$= \left(Q^{(t_2)} \left(Q^{(t_1)}, P^{(t_1)} \right), P^{(t_2)} \left(Q^{(t_1)}, P^{(t_1)} \right) \right) \quad (4.4.15)$$

and

$$\left(Q^{(t)} \left(Q^{(-t)}, P^{(-t)} \right), P^{(t)} \left(Q^{(-t)}, P^{(-t)} \right) \right) = \left(Q^{(0)}(q, p), P^{(0)}(q, p) \right) = (q, p) . \quad (4.4.16)$$

In a more compact form, these are

$$\mathfrak{G}^{(t_1)} \cdot \mathfrak{G}^{(t_2)}(\mathbf{s}) = \mathfrak{G}^{(t_1)}[\mathfrak{G}^{(t_2)}(\mathbf{s})] = \mathfrak{G}^{(t_1+t_2)}(\mathbf{s}) = \mathfrak{G}^{(t_2)} \cdot \mathfrak{G}^{(t_1)}(\mathbf{s})$$

$$\mathfrak{G}^{(t)} \cdot \mathfrak{G}^{(-t)}(\mathbf{s}) = \mathfrak{G}^{(0)}(\mathbf{s}) = \mathbf{s} .$$

Without entering too much in the mathematical meaning of the previous relations, let us prove the original statement. To do so, first, we notice that for $t = 0$

the map is the identity $(Q^{(0)}(q, p), P^{(0)}(q, p)) = (q(0), p(0)) := (q, p)$ and then for sure it holds

$$\{Q^{(0)}, P^{(0)}\}_{(q,p)} = 1 \quad (4.4.17)$$

But since it holds

$$\{Q^{(t)}, P^{(t)}\}_{(q,p)} = e^{tD_H} \{Q^{(0)}, P^{(0)}\}_{(q,p)}, \quad (4.4.18)$$

and $\{Q^{(0)}, P^{(0)}\}_{(q,p)} = 1$ is a constant independent of (q, p) , we see immediately that

$$\{Q^{(t)}, P^{(t)}\}_{(q,p)} = \{Q^{(0)}, P^{(0)}\}_{(q,p)} = 1 \quad (4.4.19)$$

and the whole one-parameter family of transformations is canonical. This strengthens even more the reasons to understand in detail the structure of volume preserving change of coordinates in hamiltonian systems. These potentially exhibit chaotic behaviour as the hamiltonian flow of solutions does (not in 2D).

4.5 Aside

A lot of the formalism of classical Hamiltonian mechanics carries through to quantum mechanics. In particular, the Poisson bracket is replaced by the commutator. When it comes to considering the dynamics of an operator \hat{A} (in what is called the Heisenberg picture), we find that

$$\frac{d\hat{A}}{dt} = [\hat{A}, \hat{H}] + \frac{\partial \hat{A}}{\partial t}, \quad (4.5.20)$$

where \hat{H} is the Hamiltonian operator for the system, and the definition of the commutator is

$$[\hat{A}, \hat{H}] = \hat{A}\hat{H} - \hat{H}\hat{A}. \quad (4.5.21)$$

This is equivalent to the classical expression

$$\frac{dA}{dt} = \{A, H\} + \frac{\partial A}{\partial t}. \quad (4.5.22)$$

where now A and H are functions of phase space and H is the Hamiltonian of the system. Moreover, canonically conjugated operators, such as the position \hat{q} and momentum \hat{p} , satisfy the commutation relations

$$[\hat{q}, \hat{p}] = i\hbar \quad (4.5.23)$$

4.6 Action-angle variables

One of the main uses of a canonical transformation is to transform to a set of coordinates for which the equations of motion take on a particularly simple form.

For example, suppose we find a transformation $(q, p) \rightarrow (Q, P)$ such that (remember that $H'(Q, P) = H(q(Q, P), p(Q, P))$)

$$\frac{\partial H'}{\partial Q} = 0. \quad (4.6.24)$$

This has two important consequences:

1. Since $\dot{P} = -\partial H'/\partial Q$ then P is a constant of the motion, and $H' = H'(P)$ only.
2. Since $\dot{Q} = \partial H'/\partial P$, then $\dot{Q} = \text{constant}$ as $\partial H'/\partial P$ is a function of P alone. Thus the solution for Q has the simple form

$$Q(t) = a_1 t + a_2. \quad (4.6.25)$$

for some constants a_1 and a_2 that are determined by the boundary conditions.

The so called *action-angle* variables (θ, I) are designed specifically to be a transformation of this type. They are particularly powerful for application to systems displaying periodic motion since they encode important informations about the qualitative behaviour of the system.

Consider a conservative system. For simplicity we restrict to the Hamiltonian

$$H = H(q, p) = \frac{p^2}{2m} + V(q) \quad (4.6.26)$$

but the results hold in general with mild assumptions about the Hamiltonian. We have already shown that H is a constant of the motion. This can be rearranged to give¹

$$p(q, H) = \pm [2m(H - V(q))]^{1/2} \quad (4.6.27)$$

where you should think of H as a constant value that defines a particular trajectory. The sign of p depends on the region of phase space the solution is in.

If we assume that the orbits are closed, for example we are close to an elliptic fixed point, we can define the action variable

$$I = \frac{1}{2\pi} \oint p dq, \quad (4.6.28)$$

where the integral is over a complete period of the motion. From Eqs. (4.6.27) and (4.6.28) we can see that I is a function of H alone i.e. $I = I(H)$. Since H is a constant of the motion, then I will be as well.

Inverting the relationship, we can also see that H will be a function of I alone i.e. $H = H(I)$. If we define the generalised coordinate conjugate to I as θ , then from Hamilton's equations we have

$$\dot{\theta} = \frac{\partial H}{\partial I} = \omega \quad \Rightarrow \quad \theta(t) = \omega t + \delta, \quad (4.6.29)$$

for some (as yet undetermined) constants ω and δ .

Note that the action I is simply the area A enclosed by the trajectory with the particular value of H divided by 2π . Thus, we can equivalently write

$$I = \frac{1}{2\pi} \int_A dq dp = \frac{1}{2\pi} \oint p(q, H) dq = -\frac{1}{2\pi} \oint q(p, H) dp. \quad (4.6.30)$$

where the minus sign arises in the last expression on the right due to the change in direction of the contour when switching the p and q axes.

¹In the general case of $H(q, p)$, assuming $\partial H/\partial p \neq 0$ one can locally define $p = p(q, H)$ thanks to the implicit function theorem.

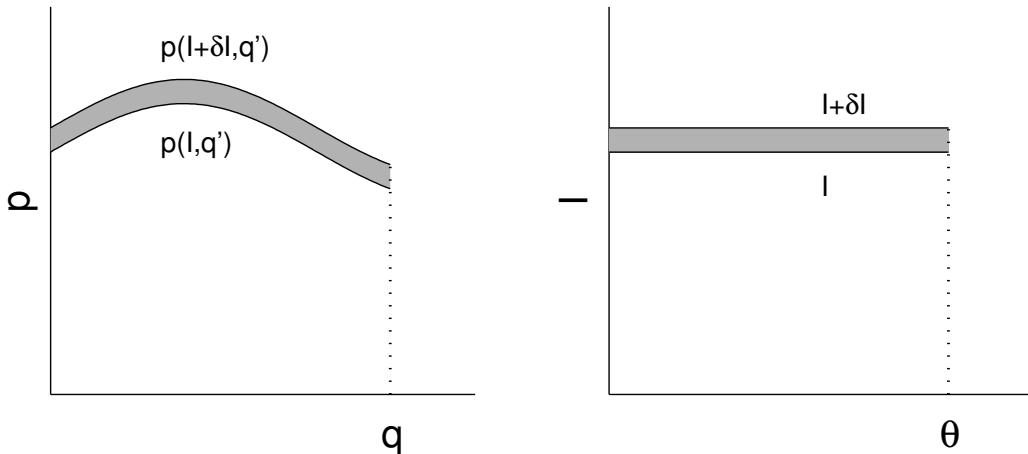


Figure 4.4: Determination of the variable θ in action-angle coordinates

To determine θ , which we assume to be canonically conjugated to I , and its connection to the parameters of periodic motion, consider the function S known as Hamilton's characteristic function

$$S = S(I, q) = \int_0^q p(I, q') dq' \quad (4.6.31)$$

which is a function of I (using the fact that $H = H(I)$) representing the new momentum, and of the coordinate q . This is essentially computing a part of Area associated to an orbit of action I . To determine the coordinate θ we need only impose the area preserving condition of a canonical transformation. We then impose the equivalence of the area between two curves with action I and $I + \delta I$ before and after the canonical transformation $(q, p) \rightarrow (\theta, I)$ and obtain

$$\text{Area: } \delta S = \int_0^q \delta p dq' = \delta I \theta. \quad (4.6.32)$$

As by definition the area is preserved for canonical transformations (see Fig. 4.4)

$$\delta S = \delta I \theta \Rightarrow \theta = \frac{\partial S}{\partial I}, \quad (4.6.33)$$

i.e. along this argument one obtains

$$\theta = \theta(q, I) = \frac{\partial S(I, q)}{\partial I} = \frac{\partial}{\partial I} \int_0^q p(I, q') dq'. \quad (4.6.34)$$

By construction it also holds

$$p = p(q, I) = \frac{\partial S(I, q)}{\partial q} = \frac{\partial}{\partial q} \int_0^q p(I, q') dq'. \quad (4.6.35)$$

which doesn't really add new informations since we already knew that $p = p(q, I) = p(q, H(I))$. Note that the previous definition works well locally in a region where the orbits are well defined in terms of p as a function of q . In general the previous set up might be defined locally, only in some regions, and it is necessary to patch together the procedure made in different regions to obtain the global behaviour. We'll not enter in these subtleties here.

Now, if we invert the equation $\theta = \theta(q, I)$ as $q = q(\theta, I)$ (where I is considered as a parameter and we invert the function θ with respect to the variable q) then one can in principle obtain the explicit expressions for the canonical transformation $(q, p) \rightarrow (\theta, I)$ as

$$q(\theta, I) = \theta^{-1}(\theta, I), \quad p(\theta, I) = p(q(\theta, I), I) \quad (4.6.36)$$

Similarly, if we invert the equation $p = p(q, I)$ as $I = I(q, p)$ (where q is considered as a parameter and we invert the function p with respect to the variable I) then one can in principle obtain the explicit expressions for the canonical transformation $(\theta, I) \rightarrow (q, p)$ as

$$I(q, p) = I^{-1}(q, p), \quad \theta(q, p) = \theta(q, I(q, p)) \quad (4.6.37)$$

From this point of view the function $S(I, q)$ is the main ingredient to construct the canonical transformation. It is an example of the so called *generating functions* of canonical transformations.

To obtain a physical interpretation of θ , consider the change in θ over one period of motion

$$\Delta\theta = \oint \frac{\partial\theta}{\partial q} dq = \oint \frac{\partial^2 S}{\partial q \partial I} dq = \frac{\partial}{\partial I} \oint \frac{\partial S}{\partial q} dq, \quad (4.6.38)$$

where we have used Eq. (4.6.33) and the fact that I is constant during the motion. From the definition of the characteristic function Eq. (5.1.14) we can see that

$$\oint \frac{\partial S}{\partial q} dq = \oint p dq = 2\pi I. \quad (4.6.39)$$

So this means that

$$\Delta\theta = 2\pi \quad (4.6.40)$$

and over the period of motion θ changes by 2π . But from Eq. (4.6.29) this means that ω must be 2π multiplied by the inverse of the period T . That is, ω is the frequency of periodic motion

$$\omega = \frac{2\pi}{T} = \frac{\partial H}{\partial I}. \quad (4.6.41)$$

Thus, one of the advantages of the action-angle coordinate system becomes clear: *without solving the equations of motion we can find the angular frequency of the motion – one of the main features characterising periodic motion.*

Furthermore, since θ changes by 2π through one period of motion then for any other set of coordinates that we may wish to use to describe the system (e.g. ϕ, ℓ) it follows that

$$\phi(\theta + 2\pi, I) = \phi(\theta, I), \quad \ell(\theta + 2\pi, I) = \ell(\theta, I). \quad (4.6.42)$$

The frequency is then a property of closed orbits which is invariant under change of coordinates and can be computed by simple geometrical means.

The previous analysis shows that 1D conservative hamiltonian systems can be in principle solved exactly via quadratures or, equivalently, by canonical transformations that turns the orbits into straight lines. In the case of regions with

periodic motion the phase portrait of this integrable system is equivalent to a circle S^1 (described by the angle variable θ) times a real coordinate $I \in \mathbb{R}$ which is the action/constant-of-motion. The dynamics in this case are then straight lines over a cylinder $S^1 \times \mathbb{R}$ with frequency of motion given by

$$\omega = \frac{2\pi}{T} = \frac{\partial H}{\partial I}. \quad (4.6.43)$$

This is a remarkably simple outcome which find their natural understanding in the context of hamiltonian and the canonical formalisms. More remarkable, similar results hold for systems with more degrees of freedom and high enough number of constants of the motion. We will close this chapter by looking at integrable hamiltonian systems with m degrees of freedom.

4.7 Integrable systems

Let's now consider a general autonomous hamiltonian system with m degrees of freedom (everything we are going to discuss here works also for non-autonomous systems once they are considered as autonomous hamiltonian systems with $m + 1$ degrees of freedom). The hamiltonian is

$$H(\mathbf{s}) = H(q_i, p_i)$$

Let's assume that there is a constant of the motion I for the system (note that H will always be an example) and then

$$\{H, I\} = 0$$

It is tempting to imagine that the procedure outlined in the previous section works also for more degrees of freedom. In fact, it can be shown (under some conditions that we'll skip here) that there exist a canonical transformation

$$\mathbf{s} \rightarrow (Q_1, \dots, Q_{m-1}, P_1, \dots, P_{m-1}, I, \theta)$$

that reduces the hamiltonian system to one degrees of freedom less with hamiltonian

$$H'(Q_1, \dots, Q_{m-1}, P_1, \dots, P_{m-1}, I) = H[\mathbf{s}(Q_1, \dots, Q_{m-1}, P_1, \dots, P_{m-1}, I, \theta)].$$

The variables I and θ are canonical. The new hamiltonian $H'(Q_1, \dots, Q_{m-1}, P_1, \dots, P_{m-1}, I, \theta)$ is independent of θ whose dynamics reduce to a straight line and decouples from the rest of hamilton's equations (separation of variables).

If there are more *independent* constant of the motion, than you can imagine that you can continue with the process of parallelisation of the orbits to action-angle variables proceeds and simplify over and over until the problem is in principle solved in terms of m action-angle variables. The condition of the constants of the motion I_1, I_2, I_3 etc to be independent turns out to be described by an algebraic relation in terms of Poisson brackets:

$$\{I_1, I_2\} = \{I_1, I_3\} = \{I_2, I_3\} = \dots = 0, \quad \{H, I_1\} = \{H, I_2\} = \dots = 0$$

meaning that all the Poisson brackets among all the constants of the motion are zero. If there are m constants of the motion (the same number as the number of

degrees of freedom of the system) that satisfy the previous mutual independency condition then the system is *integrable*. In this case, it can be proven that there exist (locally) a canonical transformation

$$(q_1, \dots, q_m, p_1, \dots, p_m) \rightarrow (\theta_1, \dots, \theta_m, I_1, \dots, I_m),$$

and the hamiltonian in the new action-angle coordinate has the simple form

$$H'(I_1, \dots, I_m)$$

Then hamilton's equations are

$$\dot{I}_i = 0, \quad \dot{\theta}_j = \omega_j(I_k), \quad \omega_j(I_k) = \frac{\partial H}{\partial I_j}$$

The dynamics is then a straight line

$$I_i(t) = I_i(0), \quad \theta_j(t) = \omega_j(I_k)t + \theta_j(0), \quad i, j, k = 1, \dots, m$$

Note that in general the various $\omega_j(I_k)$ represent the speed of the orbits in the action angle-variables. Such speed is not invariant under change of coordinates. In case of closed periodic orbits, one can choose the angles θ_i to be periodic $\theta_i = \theta_i + 2\pi$ and then all the $\omega_j(I_k)$ represent the various frequencies of oscillations in the m periodic directions – some of the most important information which instead is invariant under canonical transformations and the same in every coordinate systems. Moreover, it can be proven that if there is an entire region of phase space where the dynamics is described by closed periodic orbits (the generalisation of dynamics close to centers/elliptic fixed points), then all the angle variables are periodic. In this case phase space has the structure of an m -dimensional torus $\mathbb{T}^m = S^1 \times \dots \times S^1$ (the product of m circles) times \mathbb{R}^m which describe the values: *Phase – space* = $\mathbb{T}^m \times \mathbb{R}^m$. Orbits are “straight lines” over the torus. Pictures of how the orbits would look like on the a two-dimensional torus for an integral periodic motion with two degrees of freedom is given in Figures 4.7 and 4.5 where the torus is respectively described as a donut or as the flat square with double identification of the opposite lines. This statement generalised also for orbits that are confined to a compact region of phase space. More in general, the orbits might be “quasi-periodic” but are still equivalent (up to a canonical transformation) to curves on a m -dimensional torus $\mathbb{T}^m = S^1 \times \dots \times S^1$. The case of periodic curves are when all frequencies of motion in the action-angle variable ω_i are proportional to each other up to rational numbers (the frequencies are commensurate to each others). The case of quasi periodic motions occurs with frequencies that are irrational among each others (the frequencies are incommensurate). The quasi periodic orbits densely and homogeneously fill the torus.

Integrable systems have a pivotal role in theoretical and mathematical physics. Besides 1D conservative hamiltonian systems, important examples of integrable systems are for example systems of harmonic oscillators, and the two body problem and Kepler potential. Most of the physical systems we understand best are either integrable or perturbations of integrable systems. Some of the best understood chaotic systems are perturbations of integrable hamiltonian systems such as the forced pendulum or the double pendulum that we will look at later. Before focusing in the second part of the course on chaotic behaviour, let's give some examples in the next lecture where the power of hamiltonian and canonical formalism becomes evident.

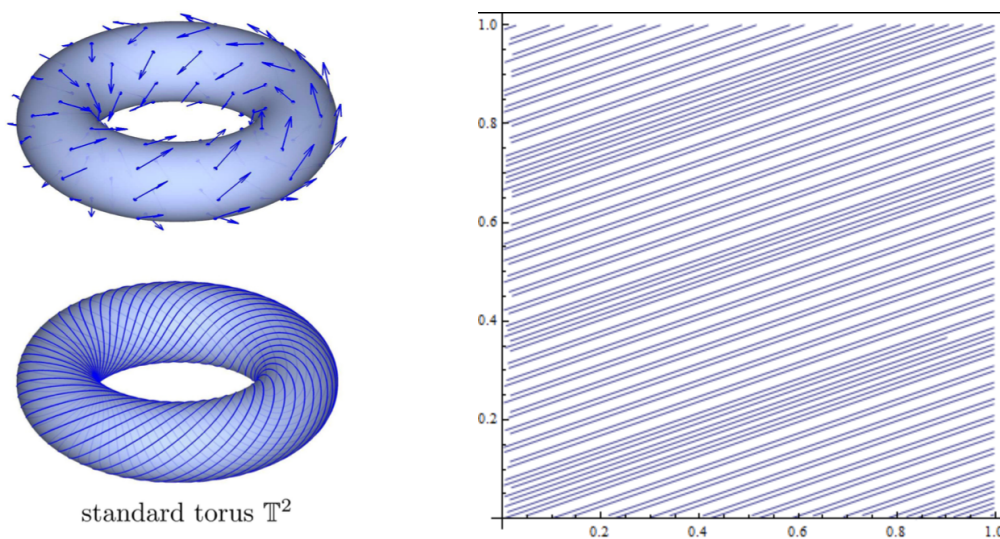


Figure 4.5: Dynamics on 2-torus

CHAPTER 5

Examples and back to free pendulum

Let's see the power of canonical formalism at work...

5.1 Simple harmonic oscillator

The Hamiltonian is

$$H = \frac{p^2}{2m} + \frac{1}{2}m\omega^2q^2, \quad (5.1.1)$$

and so

$$p = \pm(2mH - m^2\omega^2q^2)^{1/2}. \quad (5.1.2)$$

Remember the phase portrait is

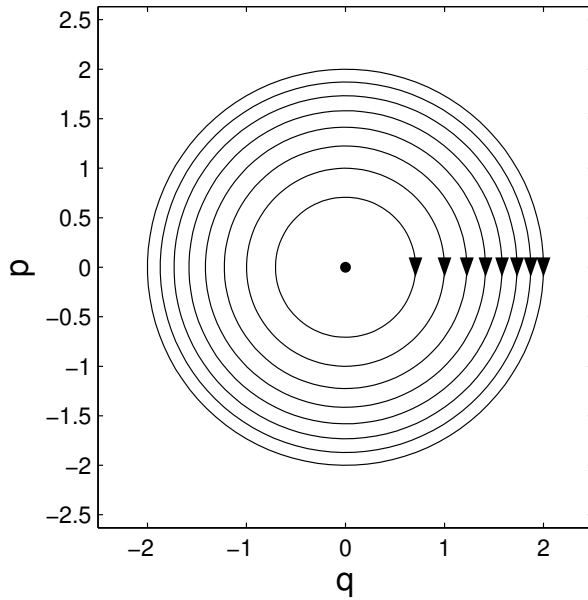


Figure 5.1: Phase portrait for a SHO ($m = \omega = 1$), for $H = 0.25$ to $H = 2$ in steps of 0.25. Note that in general the trajectories are ellipses.

The action variable is then

$$I = \frac{1}{2\pi} \oint p dq, \quad (5.1.3)$$

$$= \frac{1}{2\pi} \left[\int_{-q_1}^{q_1} (2mH - m^2\omega^2q^2)^{1/2} dq + \int_{q_1}^{-q_1} -(2mH - m^2\omega^2q^2)^{1/2} dq \right]. \quad (5.1.4)$$

However, because

$$\int_a^{-a} f(x)dx = - \int_{-a}^a f(x)dx, \quad (5.1.5)$$

then Eq. (5.1.4) becomes

$$I = \frac{1}{\pi} \int_{-q_1}^{q_1} (2mH - m^2\omega^2 q^2)^{1/2} dq. \quad (5.1.6)$$

The limit of integration q_1 is a turning point of the motion where $p = 0$. So from the Hamiltonian Eq. (5.1.2) we see that

$$q_1 = \sqrt{\frac{2H}{m\omega^2}}. \quad (5.1.7)$$

If we make the variable substitution

$$q = \sqrt{\frac{2H}{m\omega^2}} \sin \phi \quad \Rightarrow \quad dq = \sqrt{\frac{2H}{m\omega^2}} \cos \phi d\phi, \quad (5.1.8)$$

then Eq. (5.1.6) becomes

$$I = \frac{1}{\pi} \int_{-\pi/2}^{\pi/2} \left(2mH - m^2\omega^2 \frac{2H}{m\omega^2} \sin^2 \phi \right)^{1/2} \sqrt{\frac{2H}{m\omega^2}} \cos \phi d\phi, \quad (5.1.9)$$

$$= \frac{2H}{\pi\omega} \int_{-\pi/2}^{\pi/2} \cos^2 \phi d\phi, \quad (5.1.10)$$

$$= \frac{H}{\omega}, \quad (5.1.11)$$

where we have used the result that

$$\int_{-\pi/2}^{\pi/2} \cos^2 \phi d\phi = \frac{\pi}{2}.$$

The frequency of oscillation is given by $\partial H / \partial I$ and thus it is clear that ω represents the frequency of oscillation as before. Also

$$\theta(t) = \omega t + \delta, \quad (5.1.12)$$

where δ is determined by the boundary conditions. Thus we have solved the SHO in the action-angle coordinate system. We stress once more that for the SHO the frequency of oscillation doesn't depend on the action variable and the specific orbit.

We would like to find also the exact canonical transformations that bring the hamiltonian in action-angle form. For simplicity we set all constants to unity and consider the hamiltonian

$$H(q, p) = \frac{1}{2}(p^2 + q^2) \quad (5.1.13)$$

that has circular orbits. A natural guess to bring the hamiltonian in action-angle form (we have chosen $\omega = 1$)

$$I = H'(I) = H(q(\theta, I), p(\theta, I))$$

is

$$I(q, p) = H(q, p) = \frac{1}{2}(p^2 + q^2), \quad \theta(q, p) = \arctan \frac{q}{p}$$

whose inverse is

$$q = \sqrt{2I} \sin \theta, \quad p = \sqrt{2I} \cos \theta$$

Exercise: prove that this is a canonical transformation by computing explicitly the determinant of the Jacobian.

Let us use instead the generating function

$$S = S(I, q) = \int_0^q p(I, x) dx \quad (5.1.14)$$

to find the canonical transformation. To determine θ , we compute

$$S(I, q) = \int_0^q (2I - x^2)^{1/2} dx. \quad (5.1.15)$$

Once more, we make the substitution

$$x = \sqrt{2I} \sin y \quad \Rightarrow \quad dx = \sqrt{2I} \cos y dy, \quad (5.1.16)$$

the integral becomes

$$S(I, q) = \int_0^{\arcsin(q/\sqrt{2I})} \left(I - 2I \sin^2 y \right)^{1/2} \sqrt{2I} \cos y dy, \quad (5.1.17)$$

$$= 2I \int_0^{\arcsin(q/\sqrt{2I})} \cos^2 y dy, \quad (5.1.18)$$

$$(5.1.19)$$

and once used

$$\int \cos^2 y dy = \frac{1}{2}x + \frac{\sin x \cos x}{2} + constant \quad (5.1.20)$$

we obtain

$$S(I, q) = I \arcsin \frac{q}{\sqrt{2I}} + I \sin \left(\arcsin \frac{q}{\sqrt{2I}} \right) \cos \left(\arcsin \frac{q}{\sqrt{2I}} \right)$$

$$S(I, q) = I \arcsin \frac{q}{\sqrt{2I}} + \frac{qI}{\sqrt{2I}} \sqrt{1 - \frac{q^2}{I}}$$

$$S(I, q) = I \arcsin \frac{q}{\sqrt{2I}} + \frac{q}{2} \sqrt{2I - q^2} \quad (5.1.21)$$

As a consistency check we compute

$$p = p(q, I) = \frac{\partial S(I, q)}{\partial q} = I \frac{1}{\sqrt{2I}} \frac{1}{\sqrt{1 - \frac{q^2}{2I}}} + \frac{1}{2} \sqrt{2I - q^2} + \frac{q}{4} \frac{-2q}{\sqrt{2I - q^2}}$$

$$p = p(q, I) = \frac{2I - q^2}{2\sqrt{2I - q^2}} + \frac{1}{2} \sqrt{2I - q^2}$$

which correctly gives

$$p = p(q, I) = \sqrt{2I - q^2}$$

Moreover, we get

$$\begin{aligned}\theta = \theta(q, I) &= \frac{\partial S(I, q)}{\partial I} = \arcsin \frac{q}{\sqrt{2I}} + I \frac{-\frac{q}{2(2I)^{3/2}}}{\sqrt{1 - \frac{q^2}{2I}}} + \frac{q}{4} \frac{2}{\sqrt{2I - q^2}} \\ \theta = \theta(q, I) &= \frac{\partial S(I, q)}{\partial I} = \arcsin \frac{q}{\sqrt{2I}} - \frac{q}{2\sqrt{2I - q^2}} + \frac{q}{2} \frac{1}{\sqrt{2I - q^2}}\end{aligned}$$

which leads to the nice result

$$\theta = \theta(q, I) = \frac{\partial S(I, q)}{\partial I} = \arcsin \frac{q}{\sqrt{2I}} \quad (5.1.22)$$

we can then invert the previous function and obtain

$$q = q(\theta, I) = \sqrt{2I} \sin \theta \quad (5.1.23)$$

Moreover, it holds

$$\begin{aligned}p = p(\theta, I) &= p(q(\theta, I), I) = \sqrt{2I - (q(\theta, I))^2} = \sqrt{2I - 2I \sin^2 \theta} \\ p = p(\theta, I) &= \sqrt{2I} \cos \theta\end{aligned} \quad (5.1.24)$$

which finishes the derivation of our original guess.

It is then immediate to show that indeed it holds

$$H'(\theta, I) = H(q(\theta, I), p(\theta, I)) = I$$

Note that the canonical transformations

$$q = q(\theta, I) = \sqrt{2I} \sin \theta, \quad p = p(\theta, I) = \sqrt{2I} \cos \theta \quad (5.1.25)$$

are a well defined map of the entire (q, p) phase space plane except the origin, $\mathbb{R}^2 \setminus (0, 0)$, to the half cylinder $S^1 \times \mathbb{R}^+$. The fixed point is a degenerate point of the map. This is a general feature in moving to action-angle variables. Fixed points and separatrices are typically degenerate sets and separate regions that are regularly transformed into action-angle variables where the orbits are turned into straight lines. Let's give an example where this phenomena is even more pronounced.

If we now use the fact that the general solution (except the fixed point) in the action-angle coordinates is

$$\theta(t) = \omega t + \delta, \quad (5.1.26)$$

we can use the canonical transformation to see that such a solution in the original coordinates q, p is

$$q(t) = \sqrt{2H} \sin(\omega t + \delta), \quad p(t) = \sqrt{2I} \cos(\omega t + \delta) \quad (5.1.27)$$

which matches with our known result.

5.2 Linear repulsive force

The Hamiltonian is

$$H = \frac{p^2}{2} - \frac{1}{2}q^2, \quad (5.2.28)$$

and so

$$p = \pm(2H + q^2)^{1/2}. \quad (5.2.29)$$

The motion is not periodic and the action variable is not well defined (as Area within the orbits). However, the system is integrable and we know there should be a canonical transformation that brings it to a situation in which the orbits are straight lines. Remember that the phase portrait is the one of Figure 5.2 which

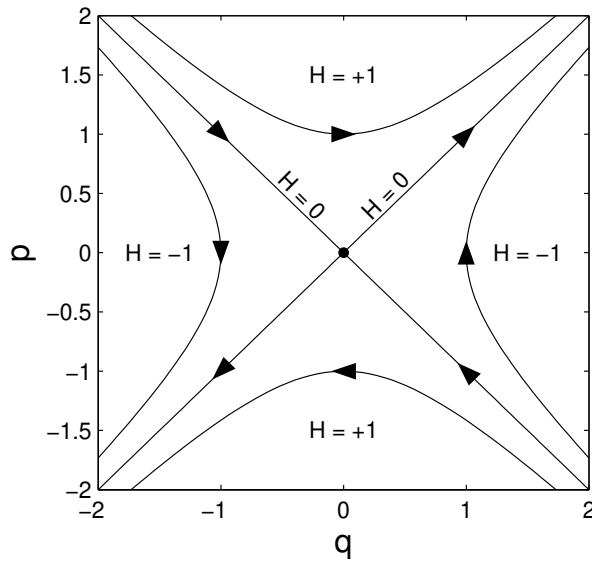


Figure 5.2: Phase portrait for a linearly repulsive force ($m = a = 1$) for $H = 0, \pm 1$.

indicates that we might have to deal with different canonical transformations for the four regions divided by the separatrices. This will be a nice example showing that the canonical transformations that make the orbits straight lines, and generating function used to extract them, are not necessarily defined on the entire phase space.

Let us consider the top region where we can certainly use

$$p = (2H + q^2)^{1/2}. \quad (5.2.30)$$

We then consider the generating function (we define from here on $I = H$)

$$S = S(I, q) = \int_0^q p(I, x) dx \quad (5.2.31)$$

and see if we can obtain an appropriate canonical transformation by using it. To determine θ , we compute

$$S(I, q) = \int_0^q (2I + x^2)^{1/2} dx = \int_0^{\frac{q}{\sqrt{2I}}} (2I + 2It^2)^{1/2} \sqrt{2I} dt$$

$$S(I, q) = 2I \int_0^{\frac{q}{\sqrt{2I}}} (1 + t^2)^{1/2} dt$$

The previous integral can be computed explicitly (use mathematica or similar for example)

$$\int \sqrt{1+x^2} dx = \frac{1}{2}x\sqrt{1+x^2} + \frac{1}{2}\ln[x + \sqrt{1+x^2}] + constant$$

equivalent to

$$\int \sqrt{1+x^2} dx = \frac{1}{2}x\sqrt{1+x^2} + \frac{1}{2}\sinh^{-1}[x] + constant$$

and then

$$S(I, q) = 2I \left\{ \frac{1}{2} \frac{q}{\sqrt{2I}} \sqrt{1 + \frac{q^2}{2I}} + \frac{1}{2} \sinh^{-1} \left[\frac{q}{\sqrt{2I}} \right] \right\}$$

$$S(I, q) = \frac{q}{2} \sqrt{2I + q^2} + I \sinh^{-1} \left[\frac{q}{\sqrt{2I}} \right] \quad (5.2.32)$$

As a consistency check we compute

$$\frac{\partial S(I, q)}{\partial q} = \frac{1}{2} \sqrt{2I + q^2} + \frac{q}{4} \frac{2q}{\sqrt{2I + q^2}} + I \frac{1}{\sqrt{2I}} \frac{1}{\sqrt{1 + \frac{q^2}{2I}}}$$

$$\frac{\partial S(I, q)}{\partial q} = \frac{1}{2} \sqrt{2I + q^2} + \frac{q^2}{2\sqrt{2I + q^2}} + \frac{2I}{2\sqrt{2I + q^2}}$$

$$\frac{\partial S(I, q)}{\partial q} = (2I + q^2)^{1/2} = p(I, q)$$

which is correct.

Moreover, we get

$$\theta = \theta(q, I) = \frac{\partial S(I, q)}{\partial I} = \sinh^{-1} \frac{q}{\sqrt{2I}} \quad (5.2.33)$$

we can then invert the previous function and obtain

$$q = q(\theta, I) = \sqrt{2I} \sinh \theta \quad (5.2.34)$$

Moreover, it holds

$$p = p(\theta, I) = p(q(\theta, I), I) = \sqrt{2I - (q(\theta, I))^2} = \sqrt{2I + 2I \sinh^2 \theta}$$

$$p = p(\theta, I) = \sqrt{2I} \cosh \theta \quad (5.2.35)$$

It is then immediate to show that it holds

$$H'(\theta, I) = I(q(\theta, I), p(\theta, I)) = I$$

If we now use the fact that the general solution (except the fixed point) in the action-angle coordinates for this quadrant is

$$\theta(t) = t + \delta, \quad (5.2.36)$$

we can use the canonical transformation to see that such a solution in the original coordinates q, p is

$$q(t) = \sqrt{2H} \sinh(t + \delta), \quad p(t) = \sqrt{2I} \cosh(t + \delta) \quad (5.2.37)$$

which matches with the known result.

Note that, differently from the SHO case, the canonical transformations (prove explicitly that $\{\theta, I\} = 1$)

$$q = q(\theta, I) = \sqrt{2I} \sinh \theta \quad (5.2.38)$$

$$p = p(\theta, I) = \sqrt{2I} \cosh \theta \quad (5.2.39)$$

is not suitable to map (almost) the whole phase space (almost the whole, since the origin doesn't work) $(q, p) \in \mathbb{R}^2 \setminus (0, 0)$ in a single region of $(\theta, I) \in \mathbb{R}^2$. This is due to the fact that $\cosh \theta \geq 1$ and $p > 0$ while θ is now an unbounded variable, not an angle. It is clear that the canonical transformation is appropriate to transform the whole top quarter of orbits to half of the plane $\mathbb{R} \times \mathbb{R}^+$. The canonical transformation is singular for $I = H = 0$ meaning that the separatrices and the fixed point at the origin (which describe the boundary of the region that have the same type of orbits) are not properly mapped in the new phase space and they lie all in the boundary of $\mathbb{R} \times \mathbb{R}^+$ described by the plane with $I = H = 0$, which is also degenerate. Besides the separatrices and fixed points, so far we are only reducing to action-angle variables one quarter of the whole orbits. It is not difficult to actually proceed similarly for the other three quarters.

First, we can clearly proceed in the same way as before for the bottom quarter of orbits where

$$p = -(2H + q^2)^{1/2}. \quad (5.2.40)$$

The generating function can then be chosen to be

$$S = S(I, q) \int_0^q p(I, x) dx \quad (5.2.41)$$

Everything works the same way and you can easily prove that

$$S(I, q) = -\frac{q}{2} \sqrt{2I + q^2} - I \sinh^{-1} \left[\frac{q}{\sqrt{2I}} \right] \quad (5.2.42)$$

and

$$\theta = \theta(q, I) = \frac{\partial S(I, q)}{\partial I} = -\sinh^{-1} \frac{q}{\sqrt{2I}} \quad (5.2.43)$$

we can then invert the previous function and obtain

$$q = q(\theta, I) = -\sqrt{2I} \sinh \theta \quad (5.2.44)$$

Moreover, it holds

$$p = p(\theta, I) = p(q(\theta, I), I) = -\sqrt{2I - (q(\theta, I))^2} = -\sqrt{2I + 2I \sinh^2 \theta}$$

$$p = p(\theta, I) = -\sqrt{2I} \cosh \theta \quad (5.2.45)$$

which finishes the derivation of a new canonical transformation. It also holds

$$H'(\theta, I) = I(q(\theta, I), p(\theta, I)) = I$$

To bring into action-angle variable the other half of the (q, p) phase space we can either guess the appropriate canonical transformation or find a new appropriate generating function. It's clear by symmetry arguments that all orbits are symmetric under reflection along the separatrices or, equivalently, under rotation by 90 degrees. We can then correctly guess that the following maps:

$$q = q(\theta, I) = \mp \sqrt{2I} \cosh \theta \quad (5.2.46)$$

$$p = p(\theta, I) = \mp \sqrt{2I} \sinh \theta \quad (5.2.47)$$

is canonical and appropriately look at the right and left other two quarters of orbits where the energy $H = I$ is negative. Here the only subtlety to keep in mind is that

$$H = -I$$

One can derive the previous results by using an alternative generating function. First note that for these two quadrants the appropriate solution of the hyperbola is

$$q(p, I) = \pm \sqrt{2I + p^2}, \quad I := -H \quad (5.2.48)$$

Then, due to the shape of the orbits it is natural to choose which is well defined in the whole quadrants under considerations

$$S = S(p, I) = - \int_0^p q(I, x) dx \quad (5.2.49)$$

All the previous calculations proceed in the same way as the case of the two other quadrant (up to some signs and exchanging q with p) and one finds exactly the transformations (5.2.47).

5.3 Back to the pendulum

We now use action-angle coordinates to find the general solutions for the dynamics of the pendulum. Remember the Hamiltonian is

$$H(\phi, \ell) = \frac{\ell^2}{2J} - mg a \cos \phi. \quad (5.3.50)$$

We define a new parameter

$$\Lambda = \left(\frac{\omega_1^2 + H}{2\omega_1^2} \right)^{1/2}, \quad \omega_1 = \sqrt{J}\omega_0 = \sqrt{mg a}. \quad (5.3.51)$$

where H represents the energy of a particular trajectory and remember that

$$\omega_0 = \left(\frac{mg a}{J} \right)^{1/2} = \sqrt{\frac{g}{a}}$$

is the natural frequency of the SHO which describe libration orbits very close to the origin. Note that from Eq. (2.3.24) ω_1^2 is the energy of the system on the separatrix. It follows that

$$\begin{aligned}\Lambda &= 1, & \Rightarrow & \text{on the separatrices,} \\ \Lambda &< 1, & \Rightarrow & \text{libration (within separatrices),} \\ \Lambda &> 1, & \Rightarrow & \text{rotation (outside separatrices).}\end{aligned}$$

where Figure 5.3 is, once more, the phase portrait for the pendulum

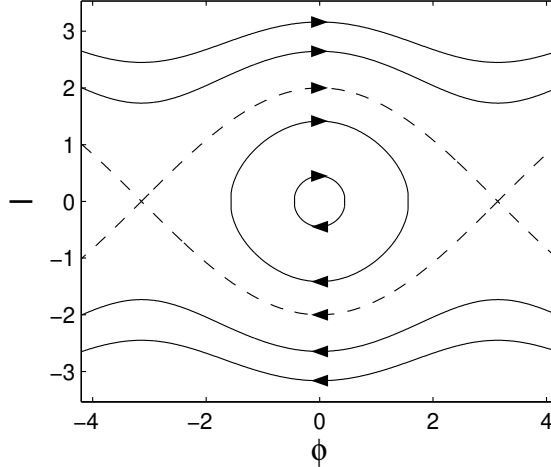


Figure 5.3: Phase portrait for the pendulum. The separatrices are indicated by the dashed lines.

We have already found the solution for motion on the separatrices. We now consider motion inside and outside.

5.3.0.1 Librations: $\Lambda < 1$

We begin by calculating the action

$$I(H) = \frac{1}{2\pi} \oint p dq. \quad (5.3.52)$$

For the pendulum the generalised coordinate and momentum are ϕ and ℓ and therefore

$$I(H) = \frac{1}{2\pi} \left(\int_{-\phi_1}^{\phi_1} |\ell| d\phi + \int_{\phi_1}^{-\phi_1} -|\ell| d\phi \right), \quad (5.3.53)$$

$$= \frac{1}{2\pi} \left(\int_{-\phi_1}^{\phi_1} \sqrt{2J(H + \omega_1^2 \cos \phi)} d\phi + \right. \quad (5.3.54)$$

$$\left. \int_{\phi_1}^{-\phi_1} -\sqrt{2J(H + \omega_1^2 \cos \phi)} d\phi \right), \quad (5.3.55)$$

where we have divided the integral over a complete period into two integrals for which $\ell > 0$ and $\ell < 0$. Due to the symmetry of the integrals this reduces to

$$I(H) = \frac{1}{\pi} \int_{-\phi_1}^{\phi_1} \sqrt{2J(H + \omega_1^2 \cos \phi)} d\phi. \quad (5.3.56)$$

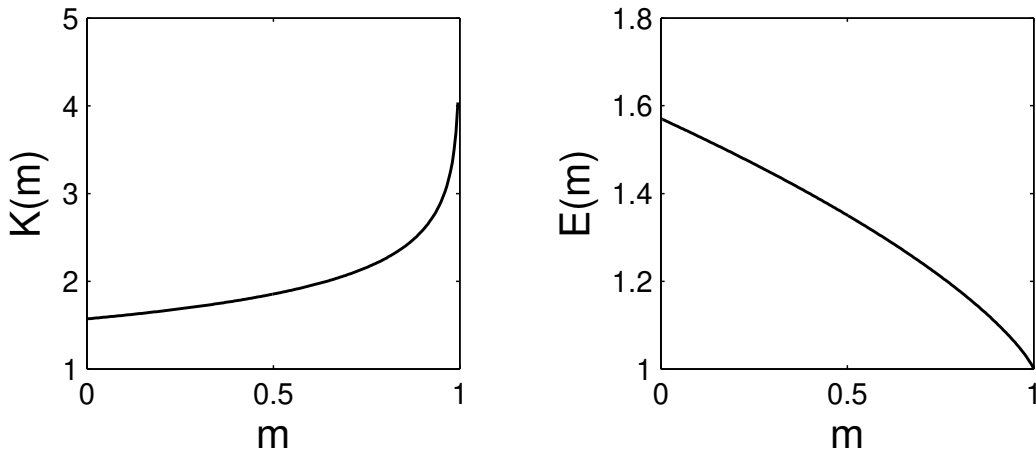


Figure 5.4: Complete elliptic integrals of the first $K(m)$ and second $E(m)$ kind.

The limit of integration ϕ_1 is the angle at the turning point of the motion (where $\ell = 0$). By making this substitution into the Hamiltonian we find that

$$\phi_1 = \cos^{-1} \left(-\frac{H}{\omega_1^2} \right) = 2 \sin^{-1} \Lambda. \quad (5.3.57)$$

The evaluation of the integral is rather lengthy, and instead we simply quote the result

$$I(H) = \frac{8J\omega_0}{\pi} \left[E(\Lambda^2) - (1 - \Lambda^2)K(\Lambda^2) \right], \quad \Lambda < 1, \quad (5.3.58)$$

where

$$K(m) = \int_0^{\pi/2} (1 - m \sin^2 \theta)^{-1/2} d\theta, \quad (5.3.59)$$

is a complete elliptic integral of the first kind, and

$$E(m) = \int_0^{\pi/2} (1 - m \sin^2 \theta)^{1/2} d\theta, \quad (5.3.60)$$

is a complete elliptic integral of the second kind. (See <http://mathworld.wolfram.com> for a handy reference to special functions such as these.) These functions are plotted in Fig. 5.4.

Earlier we showed that the angular frequency of motion ω is given by

$$\omega = \frac{\partial H}{\partial I} = \left[\frac{\partial I(H)}{\partial H} \right]^{-1}. \quad (5.3.61)$$

Using known properties of elliptic integrals we can differentiate Eq. (5.3.58) with respect to H to find

$$\omega(H) = \frac{\pi}{2} \frac{\omega_0}{K(\Lambda^2)}, \quad \Lambda < 1. \quad (5.3.62)$$

This result is plotted in Fig. 5.5 with $\Lambda < 1$.

5.3.1 Rotations: $\Lambda > 1$

As before we have

$$I(H) = \frac{1}{2\pi} \oint p dq = \frac{1}{2\pi} \int_{-\pi}^{\pi} \ell d\phi. \quad (5.3.63)$$

where now the pendulum explores all values of ϕ . We shall assume that the motion is in the anticlockwise direction, and so $\ell > 0$. The other case can be obtained simply by symmetry arguments. Thus

$$I(H) = \frac{1}{2\pi} \int_{-\pi}^{\pi} \sqrt{2J(H + \omega_1^2 \cos \phi)} d\phi. \quad (5.3.64)$$

Using the fact that cosine is an even function $\cos \phi = \cos(-\phi)$ and the result $\cos \phi = 1 - 2 \sin^2(\phi/2)$, we can write Eq. (5.3.64) as

$$I(H) = \frac{1}{\pi} \int_0^{\pi} [2J(H + \omega_1^2 - 2\omega_1^2 \sin^2 \phi/2)]^{1/2} d\phi, \quad (5.3.65)$$

$$= \frac{\sqrt{2J}}{\pi} (H + \omega_1^2)^{1/2} \int_0^{\pi} \left[1 - \frac{2\omega_1^2}{H + \omega_1^2} \sin^2 \frac{\phi}{2} \right]^{1/2} d\phi \quad (5.3.66)$$

Making the change of variable $\phi' = \phi/2$ we find

$$I(H) = \frac{\sqrt{2J \times 2\omega_1^2}}{\pi} \left(\frac{H + \omega_1^2}{2\omega_1^2} \right)^{1/2} \times 2 \int_0^{\pi/2} \left[1 - \frac{1}{\Lambda^2} \sin^2 \phi' \right]^{1/2} d\phi' \quad (5.3.67)$$

$$= \frac{4\omega_1 \sqrt{J}}{\pi} \Lambda E(1/\Lambda^2). \quad (5.3.68)$$

We find the angular frequency again according to Eq. (5.3.61) and obtain

$$\omega(H) = \frac{\pi \omega_1}{\sqrt{J}} \frac{\Lambda}{K(1/\Lambda^2)}, \quad \Lambda > 1. \quad (5.3.69)$$

Combining this result with the frequency for $\Lambda < 1$ from Eq. (5.3.62) we get Fig. 5.5. As well as producing this plot on a computer, we can get it from the series expansion of $K(k)$

$$K(m) = \frac{\pi}{2} \left[1 + \left(\frac{1}{2} \right)^2 m + \left(\frac{1 \cdot 3}{2 \cdot 4} \right)^2 m^2 + \left(\frac{1 \cdot 3 \cdot 5}{2 \cdot 4 \cdot 6} \right)^2 m^3 + \dots \right]. \quad (5.3.70)$$

and so we see $K(m) \rightarrow \pi/2$ as $m \rightarrow 0$. Thus we have the three limiting cases for the frequency

$$\begin{aligned} \omega(\Lambda) &\rightarrow \omega_0 && \text{as } \Lambda \rightarrow 0, \\ \omega(\Lambda) &\rightarrow 0 && \text{as } \Lambda \rightarrow 1, \\ \omega(\Lambda) &\rightarrow 2\Lambda\omega_0 && \text{as } \Lambda \rightarrow \infty. \end{aligned} \quad (5.3.71)$$

You should try to derive these results yourself.

Thus, we have exploited one of the advantages of action-angle coordinates: we have found the angular frequency of the pendulum without actually solving the equations of motion.

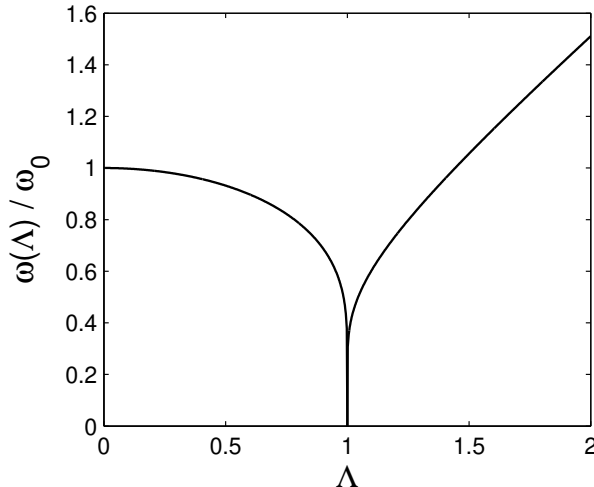


Figure 5.5: Angular frequency of a pendulum as a function of $\Lambda(H)$.

5.3.2 Full solution: $\phi(t)$

We can now work out the full solution to Hamilton's equations for $\ell(t)$ and $\phi(t)$. We apply Eq. (4.6.34) to the pendulum to find

$$\theta(\phi) = \frac{\partial}{\partial I} \int_0^\phi \ell(\phi', H) d\phi'. \quad (5.3.72)$$

If we solve this for $\phi(\theta, H)$ and substitute in

$$\theta(t) = \omega(H)t + \theta(0), \quad (5.3.73)$$

then the solutions are

$$\phi(t) = \begin{cases} 2 \cos^{-1}[\text{dn}(\omega_0 t, \Lambda^2)], & \Lambda \leq 1, \\ 2 \sin^{-1}[\text{sn}(\Lambda \omega_0 t, 1/\Lambda^2)], & \Lambda > 1, \end{cases} \quad (5.3.74)$$

where we have taken the boundary condition to be $\phi(0) = 0$. Here we have introduced the *Jacobi elliptic functions* dn and sn.

5.3.3 Aside: Jacobi elliptic functions

Adapted from <http://mathworld.wolfram.com/JacobiEllipticFunctions.html>

The Jacobi elliptic functions are standard forms of elliptic functions. The three basic functions are denoted $\text{cn}(u, m)$, $\text{dn}(u, m)$, and $\text{sn}(u, m)$, where $m = k^2$ and k is known as the elliptic modulus. They arise from the inversion of the elliptic integral of the first kind

$$u = K(\phi, m) = \int_0^\phi \frac{dt}{\sqrt{1 - m \sin^2 t}}, \quad (5.3.75)$$

where $0 < m < 1$, and $\phi = \text{am}(u, m) = \text{am}(u)$ is the Jacobi amplitude, giving $\phi = K^{-1}(u, m) = \text{am}(u, m)$.

From this, it follows that

$$\sin \phi = \sin(\text{am}(u, m)) \equiv \text{sn}(u, m), \quad (5.3.76)$$

$$\cos \phi = \cos(\text{am}(u, m)) \equiv \text{cn}(u, m), \quad (5.3.77)$$

$$\sqrt{1 - m \sin^2 \phi} = \sqrt{1 - m \sin^2(\text{am}(u, m))} \equiv \text{dn}(u, m). \quad (5.3.78)$$

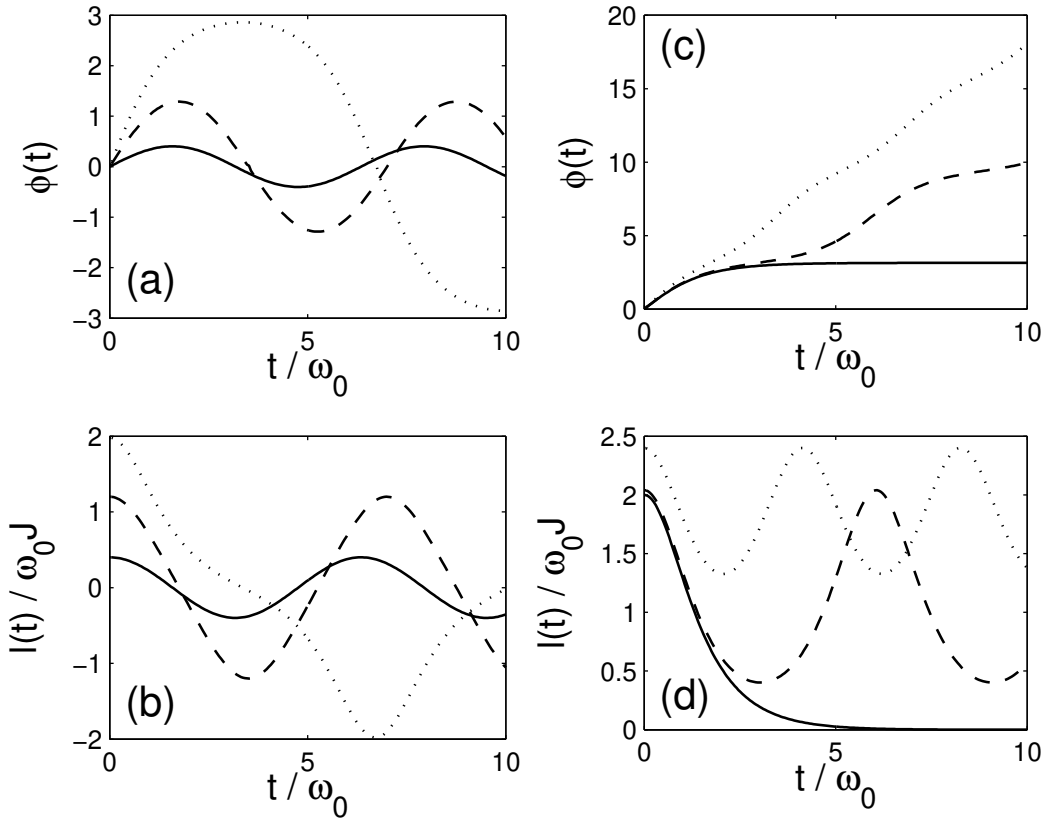


Figure 5.6: Solutions for the pendulum. (a) $\phi(t)$ and (b) $\ell(t)$ for $\Lambda = 0.2$ (solid), $\Lambda = 0.6$ (dashed), and $\Lambda = 0.99$ (dotted). (c) $\phi(t)$ and (d) $\ell(t)$ for $\Lambda = 1$ (solid), $\Lambda = 1.02$ (dashed), and $\Lambda = 1.2$ (dotted).

These functions are doubly periodic generalizations of the trigonometric functions satisfying

$$\text{sn}(u, 0) = \sin u, \quad \text{cn}(u, 0) = \cos u, \quad \text{dn}(u, 0) = 1. \quad (5.3.79)$$

5.3.4 Full solution: $\ell(t)$

With the boundary condition $\phi(0) = 0$, then we can see that at $t = 0$

$$H = \frac{\ell^2(0)}{2J} - m g a = \frac{\ell(0)^2}{2J} - \omega_1^2. \quad (5.3.80)$$

Inserting this into the definition of Λ from Eq. (5.3.51) we have

$$\Lambda^2 = \frac{\omega_1^2 + \ell(0)^2/2J - \omega_1^2}{2\omega_1^2}, \quad (5.3.81)$$

$$\Rightarrow \ell(0) = \pm 2\sqrt{J}\Lambda\omega_1. \quad (5.3.82)$$

Using this as the boundary condition we can then show that the angular momentum is

$$\ell(t) = \begin{cases} 2\omega_0 J \Lambda \text{cn}(\omega_0 t, \Lambda^2), & \Lambda \leq 1, \\ 2\omega_0 J \Lambda \text{dn}(\omega_0 t, 1/\Lambda^2), & \Lambda > 1. \end{cases} \quad (5.3.83)$$

This can be derived by, for example, substituting the solution Eq. (5.3.74) into the Hamiltonian and solving for $\ell(t)$. Examples of the solutions are shown in Fig. 5.6.

5.3.5 Limiting cases

The Jacobi elliptic functions can be written in terms of infinite expansions which allow us to find simple expressions for $\phi(t)$ and $\ell(t)$ in limiting cases.

$$\text{sn}(u, m) = u - (1 + m) \frac{u^3}{3!} + (1 + 14m + m^2) \frac{u^5}{5!} + \dots, \quad (5.3.84)$$

$$\text{cn}(u, m) = 1 - \frac{u^2}{2!} + (1 + 4m) \frac{u^4}{4!} - (1 + 44m + 16m^2) \frac{u^6}{6!} + \dots, \quad (5.3.85)$$

$$\text{dn}(u, m) = 1 - m \frac{u^2}{2!} + m(4 + m) \frac{u^4}{4!} - m(16 + 44m + m^2) \frac{u^6}{6!} + \dots \quad (5.3.86)$$

5.3.6 Case: $\Lambda \ll 1$

In this limit we find that

$$\text{cn}(u, \Lambda \rightarrow 0) = 1 - \frac{u^2}{2!} + \frac{u^4}{4!} - \frac{u^6}{6!} + \dots = \cos u, \quad (5.3.87)$$

and so we find for the angular momentum

$$\ell(t) = 2\omega_0 J \Lambda \cos(\omega_0 t), \quad (5.3.88)$$

which is the same as the SHO solution in the limit of small oscillations.

5.3.7 Case: $\Lambda = 1$

Here we find

$$\text{cn}(u, \Lambda = 1) = 1 - \frac{u^2}{2!} + 5 \frac{u^4}{4!} - 61 \frac{u^6}{6!} + \dots = \frac{1}{\cosh u}, \quad (5.3.89)$$

and so we have

$$\ell(t) = \frac{2\omega_0 J}{\cosh(\omega_0 t)}, \quad (5.3.90)$$

as we have already derived for the separatrix.

5.3.8 Case: $\Lambda \gg 1$

Here we have

$$\text{dn}(u, 1/\Lambda^2 \rightarrow 0) \approx 1 - \frac{1}{\Lambda^2} \frac{u^2}{2!} + \frac{1}{\Lambda^4} \frac{u^4}{4!} - \frac{1}{\Lambda^6} \frac{u^6}{6!} + \dots \approx 1. \quad (5.3.91)$$

Ignoring the terms of $O(1/\Lambda^2)$ and higher we have

$$\ell(t) = \frac{2\omega_0 J}{\Lambda}, \quad (5.3.92)$$

which is constant rotation as we might have expected.

5.4 APPENDIX: On generating functional of canonical transformations

Disclaimers:

This Material is only for the curious reader, not for exams

This is copied from lecture notes of an old MATH4104 course at UQ. Most books on hamiltonian systems have large sections on generating functions which we recommend to the interested reader.

Both Lagrange's equations of motion and Hamilton's equations of motion can be derived from Hamilton's principle of least action. That is that the realizable path is one that extremises the action

$$S[\mathbf{q}] = \int_{t_0}^{t_1} L(\mathbf{q}, \dot{\mathbf{q}}, t) dt$$

or in terms of the Hamiltonian

$$S[\mathbf{q}] = \int_{t_0}^{t_1} (\mathbf{p} \cdot \dot{\mathbf{q}} - H(\mathbf{q}, \mathbf{p}, t)) dt.$$

Suppose now that we transform to new canonical coordinates (\mathbf{Q}, \mathbf{P}) . Then the realizable path will also extremise

$$S'[\mathbf{Q}] = \int_{t_0}^{t_1} (\mathbf{P} \cdot \dot{\mathbf{Q}} - K(\mathbf{Q}, \mathbf{P}, t)) dt,$$

where $K(\mathbf{Q}, \mathbf{P}, t)$ is the new Hamiltonian. Note that if the transformation is independent of time then this is just the old Hamiltonian in terms of the new variables, but here we will include the possibility that the transformation is dependent on time.

Now recall that there remained some ambiguity in the Lagrangian we could use. We defined the Lagrangian as the difference between the kinetic and potential energies. But the alternative Lagrangian $L' = L + \frac{dF}{dt}$ for some function F also satisfied Hamilton's principle of least action. Similarly to extremise $S[\mathbf{q}]$ and $S'[\mathbf{Q}]$ does not necessarily imply that the integrands are equal, they may differ by a complete differential.

$$(\mathbf{p} \cdot \dot{\mathbf{q}} - H(\mathbf{q}, \mathbf{p}, t)) = (\mathbf{P} \cdot \dot{\mathbf{Q}} - K(\mathbf{Q}, \mathbf{P}, t)) + \frac{dF}{dt}$$

There are various sets of variables one can choose F to be a function of. Suppose we choose $F = F_1$ to be a function of the new and old angles.

$$F_1(\mathbf{q}, \mathbf{Q}, t) : \quad \text{then} \quad \frac{dF_1}{dt} = \text{grad}_{\mathbf{q}} F_1 \cdot \dot{\mathbf{q}} + \text{grad}_{\mathbf{Q}} F_1 \cdot \dot{\mathbf{Q}} + \frac{\partial F_1}{\partial t}$$

This implies that

$$(\mathbf{p} - \text{grad}_{\mathbf{q}} F_1) \cdot \dot{\mathbf{q}} + (K(\mathbf{Q}, \mathbf{P}, t) - H(\mathbf{q}, \mathbf{p}, t) - \frac{\partial F_1}{\partial t}) = (\mathbf{P} + \text{grad}_{\mathbf{Q}} F_1) \cdot \dot{\mathbf{Q}}$$

which is satisfied if

$$\mathbf{p} = \text{grad}_{\mathbf{q}} F_1, \quad \mathbf{P} = -\text{grad}_{\mathbf{Q}} F_1 \quad \text{and} \quad K(\mathbf{Q}, \mathbf{P}, t) = H(\mathbf{q}, \mathbf{p}, t) + \frac{\partial F_1}{\partial t}$$

Alternatively one could choose $F_2(\mathbf{q}, \mathbf{P}, t)$, $F_3(\mathbf{Q}, \mathbf{p}, t)$ or $F_4(\mathbf{p}, \mathbf{P}, t)$. Each type of generating function is useful in a different situation and can be related to $F_1(\mathbf{q}, \mathbf{Q}, t)$. The most commonly used is $F_2(\mathbf{q}, \mathbf{P}, t) = F_1(\mathbf{q}, \mathbf{Q}, t) + \mathbf{P} \cdot \mathbf{Q}(\mathbf{q}, \mathbf{P})$, which is a Legendre transform away from $-F_1(\mathbf{q}, \mathbf{Q}, t)$. (The new variables are active, with \mathbf{q} and t being passive. This means that, with respect to the active variables $\mathbf{P} = -\text{grad}_{\mathbf{Q}}F_1$ becomes $\mathbf{Q} = \text{grad}_{\mathbf{P}}F_2$ and with respect to the passive variables $\mathbf{p} = \text{grad}_{\mathbf{q}}F_1$ becomes $\mathbf{p} = \text{grad}_{\mathbf{q}}F_2$.) Alternatively one can substitute in as before

$$(\mathbf{p} \cdot \dot{\mathbf{q}} - H(\mathbf{q}, \mathbf{p}, t)) = (\mathbf{P} \cdot \dot{\mathbf{Q}} - K(\mathbf{Q}, \mathbf{P}, t)) + \frac{d(F_2 - \mathbf{P} \cdot \mathbf{Q})}{dt} = (-\dot{\mathbf{P}} \cdot \mathbf{Q} - K(\mathbf{Q}, \mathbf{P}, t)) + \frac{dF_2}{dt}$$

with

$$\frac{dF_2}{dt} = \text{grad}_{\mathbf{q}}F_2 \cdot \dot{\mathbf{q}} + \text{grad}_{\mathbf{P}}F_2 \cdot \dot{\mathbf{P}} + \frac{\partial F_2}{\partial t}.$$

This implies that

$$(\mathbf{p} - \text{grad}_{\mathbf{q}}F_2) \cdot \dot{\mathbf{q}} + K(\mathbf{Q}, \mathbf{P}, t) - H(\mathbf{q}, \mathbf{p}, t) - \frac{\partial F_2}{\partial t} = -\dot{\mathbf{P}} \cdot (\mathbf{Q} - \text{grad}_{\mathbf{P}}F_2)$$

which is satisfied if

$$\mathbf{p} = \text{grad}_{\mathbf{q}}F_2, \quad \mathbf{Q} = \text{grad}_{\mathbf{P}}F_2 \quad \text{and} \quad K(\mathbf{Q}, \mathbf{P}, t) = H(\mathbf{q}, \mathbf{p}, t) + \frac{\partial F_2}{\partial t}.$$

Example The identity transformation can be generated by $F_2(\mathbf{q}, \mathbf{P}) = \mathbf{P} \cdot \mathbf{q}$.

$$\text{If } F_2(\mathbf{q}, \mathbf{P}) = \sum_{j=1}^n P_j q_j \Rightarrow p_j = \frac{\partial F_2}{\partial q_j} = P_j, \quad Q_j = \frac{\partial F_2}{\partial P_j} = q_j.$$

Near identity transformations are also generated by F_2 generating functions:

$$F_2(\mathbf{q}, \mathbf{P}, t) = \mathbf{P} \cdot \mathbf{q} + \epsilon G(\mathbf{q}, \mathbf{P}, t) \quad \text{where } \epsilon \text{ is assumed to be small.}$$

Example The example we looked at before

$$H(q_1, q_2, p_1, p_2) = \frac{p_1^2}{2} + \frac{p_2^2}{2} + \cos(2q_1 + q_2)$$

can also be generated by an F_2 generating function.

$$\text{We chose } Q_1 = (2q_1 + q_2) \quad \text{and} \quad Q_2 = q_2$$

So that

$$\frac{\partial F_2}{\partial P_1} = (2q_1 + q_2) \quad \text{and} \quad \frac{\partial F_2}{\partial P_2} = q_2 \Rightarrow F_2 = (2q_1 + q_2)P_1 + q_2P_2$$

So that

$$p_1 = \frac{\partial F_2}{\partial q_1} = 2P_1 \quad \text{and} \quad p_2 = \frac{\partial F_2}{\partial q_2} = P_1 + P_2 \Rightarrow P_1 = \frac{p_1}{2}, P_2 = p_2 - \frac{p_1}{2}$$

as before.

Example The two body problem.

Consider the motion of two masses m_1 and m_2 , subject only to a mutual gravitational attraction described by the potential $V(r)$, where r is the distance between the particles. Let \mathbf{x}_1 and \mathbf{x}_2 be the coordinates of the two masses and \mathbf{p}_1 and \mathbf{p}_2 their conjugate momenta. Then if $r = \|\mathbf{x}_1 - \mathbf{x}_2\|$ and

$$H(\mathbf{x}_1, \mathbf{x}_2, \mathbf{p}_1, \mathbf{p}_2) = \frac{\mathbf{p}_1 \cdot \mathbf{p}_1}{2m_1} + \frac{\mathbf{p}_2 \cdot \mathbf{p}_2}{2m_2} + V(r)$$

Now consider new variables

$$\mathbf{x} = \mathbf{x}_2 - \mathbf{x}_1 \quad \text{and} \quad \mathbf{X} = a\mathbf{x}_1 + b\mathbf{x}_2 \quad \text{for some } a \text{ and } b$$

Now choose an F_2 generating function:

$$F_2(\mathbf{x}_1, \mathbf{x}_2, \mathbf{P}_1, \mathbf{P}_2) : \quad \mathbf{x} = \text{grad}_{\mathbf{P}_1} F_2 \quad \text{and} \quad \mathbf{X} = \text{grad}_{\mathbf{P}_2} F_2$$

$$\Rightarrow F_2 = \mathbf{P}_1 \cdot (\mathbf{x}_2 - \mathbf{x}_1) + \mathbf{P}_2 \cdot (a\mathbf{x}_1 + b\mathbf{x}_2)$$

$$\text{so that } \mathbf{p}_1 = -\mathbf{P}_1 + a\mathbf{P}_2 \quad \text{and} \quad \mathbf{p}_2 = \mathbf{P}_1 + b\mathbf{P}_2 \quad \Rightarrow \quad \mathbf{P}_1 = \frac{a\mathbf{p}_2 - b\mathbf{p}_1}{a+b}, \quad \mathbf{P}_2 = \frac{\mathbf{p}_1 + \mathbf{p}_2}{a+b}$$

This means that

$$\begin{aligned} H(\mathbf{x}, \mathbf{X}, \mathbf{P}_1, \mathbf{P}_2) &= \frac{|-\mathbf{P}_1 + a\mathbf{P}_2|^2}{2m_1} + \frac{|\mathbf{P}_1 + b\mathbf{P}_2|^2}{2m_2} + V(\|\mathbf{x}\|) \\ &= \frac{|\mathbf{P}_1|^2}{2\mu} + \frac{|\mathbf{P}_2|^2}{2M} + \left(\frac{b}{m_2} - \frac{a}{m_1} \right) \mathbf{P}_1 \cdot \mathbf{P}_2 \end{aligned}$$

where $\mu = \frac{1}{m_1} + \frac{1}{m_2}$ is called the reduced mass, and $\frac{1}{M} = \frac{a^2}{m_1} + \frac{b^2}{m_2}$. If we choose a and b to remove the $\mathbf{P}_1 \cdot \mathbf{P}_2$ term then since \mathbf{P}_2 is a constant of the motion which is uncoupled from \mathbf{P}_1 and since the only position variable is $r = \|\mathbf{x}\|$ the system is, as given earlier, effectively a one degree of freedom system

$$H(r, p_r, p_\theta) = \frac{p_r^2 + p_\theta^2/r^2}{2\mu} + V(r) + \text{constants of the motion.}$$

Rotating Coordinates Suppose we have a one degree of freedom time dependent Hamiltonian, where the time and position variable only appear as $q - \omega t$.

$$H(q, p, t) = \frac{p^2}{2} + V(q - \omega t)$$

Then the time dependence can be 'removed' by moving to new canonical variables via an F_2 generating function.

$$\text{Let } Q = q - \omega t, \quad \Rightarrow \quad p = \frac{\partial F_2}{\partial q}, \quad Q = \frac{\partial F_2}{\partial P} \quad \Rightarrow \quad F_2 = P(q - \omega t).$$

In fact p is unchanged as $\frac{\partial F_2}{\partial q} = P$. But the Hamiltonian is changed. The new Hamiltonian $K(Q, P)$ is

$$K(Q, P) = H(Q + \omega t, P, t) + \frac{\partial F_2}{\partial t} = \frac{P^2}{2} + V(Q) - \omega P = \frac{(P - \omega)^2}{2} + V(Q) - \frac{\omega^2}{2}$$

The resulting system is integrable as $K(Q, P)$ is independent of time.

CHAPTER 6

Attractors

6.1 Chaos

"Arguably the most broad based revolution in the worldview of science in the twentieth century will be associated with chaotic dynamics. Yes, I know about Quantum Mechanics and Relativity, and for physicists and philosophers these theories must rank above Chaos for their impact on the way we view the world. My assertion, however, refers to science in general, not just to physics. Leaving improved diagnostic instrumentation aside, it is not clear that Quantum Mechanics or Relativity have had any appreciable effect whatever on medicine, biology, or geology. Yet chaotic dynamics is having an important impact in all these fields, as well as many others, including chemistry and physics."

Surely part of the reason for this broad application is that chaotic dynamics is not something that is part of a specific physical model, limited in its application to one small area of science. But rather chaotic dynamics is a consequence of mathematics itself and hence appears in a broad range of physical systems. Thus, although the mathematical representations of these physical systems can be very different, they often share common properties."

—S. Neil Rasband, *Chaotic Dynamics of Nonlinear Systems*, Wiley, 1990.

6.1.1 Defining "chaos"

The concept of chaos can be quite hard to define. For our purposes, the best definition is that a dynamical system is chaotic if it displays dynamics that are *highly sensitive to initial conditions*. It is important to note that there is no probability or chance involved: *chaotic dynamics are deterministic*. However, due to the sensitivity to initial conditions, after a certain time it may appear that the results are totally unrelated to one another.

6.1.2 Lyapunov exponent

Viewed in phase space, sensitivity to initial conditions can be defined in terms of paths in phase space: paths beginning at nearby points in phase space rapidly diverge. This divergence is parameterised by the *Lyapunov exponent* λ , probably the most popular measure of chaotic behaviour.

For Consider a one-dimensional system with initial states x and $x + \epsilon$, where $\epsilon \ll 1$ is a small parameter. After time t , their divergency $\epsilon(t)$ may be approxi-

mated as

$$\epsilon(t) \approx \epsilon e^{\lambda t}. \quad (6.1.1)$$

Thus the Lyapunov exponent gives the average rate of divergence. More precisely it can be defined as

$$\lambda(\epsilon) = \lim_{t \rightarrow +\infty} \frac{1}{t} \ln \frac{\epsilon(t)}{\epsilon} \quad (6.1.2)$$

Roughly, If $\lambda < 0$ then separate trajectories converge and the system is not chaotic. However, if $\lambda > 0$ then separate trajectories diverge and the system is chaotic.

Since we have a $2n$ dimensional phase space for n degrees of freedom, we can extend this definition to higher-dimensional systems as

$$|\epsilon(t)| \approx |\epsilon| e^{\lambda t} \quad (6.1.3)$$

where $|\epsilon(t)| = [\sum(\Delta q_i^2(t) + \Delta p_i^2(t))]^{1/2}$. This assumes that $|\epsilon|$ is small enough for the divergence to be treated within a linearised approximation. This can be ensured by taking the limit $|\epsilon| \rightarrow 0$. Then one can define the Lyapunov exponent as

$$\lambda = \lim_{t \rightarrow +\infty} \lim_{|\epsilon| \rightarrow 0^+} \frac{1}{t} \ln \frac{|\epsilon(t)|}{|\epsilon|} \quad (6.1.4)$$

The previous definition is dependent upon the position of the initial condition and the direction of the displacement vector with modulo $|\epsilon|$. This leads to a spectrum of Lyapunov exponents and one can define the Lyapunov exponent as the maximum one. However, we will neglect these (important) details unless necessary and simply underline that the Lyapunov exponent is one of the important tools to indicate whether a system is in a chaotic phase.

In most of the course we have focused on conservative Hamiltonian systems with one degree of freedom. It turns out that such systems do not display chaotic dynamics. These are the simplest example of an integrable system for which we know that the dynamics is equivalent of paths of straight lines which clearly remain parallel to each other as time evolves. This understanding in terms of action-angle variables translate to every canonical system of coordinates. For example, we can obtain some insight into this by considering the relationship between paths in phase space and the Hamiltonian: the paths in phase space are contours of the Hamiltonian. In this case, as we take the limit $|\epsilon| \rightarrow 0$, we find $\lambda = 0$. That is, the paths neither converge nor diverge in this limit.

More generally, the paths are confined to a 2D phase space, and in a conservative system, the paths cannot cross or meet except at special points; the contours can only meet at saddle points of the 2D Hamiltonian surface $H(q, p)$. Each path is confined by neighbouring paths, and rapid divergence is not possible.

Therefore, if we want a chaotic system, we must look at non-conservative systems or (non-linear) systems with more than 1 degree of freedom. Both of these have the effect of giving the paths in phase space more than two dimensions to move in, and paths are no longer constrained by neighbouring paths. Liouville's theorem still constraints the dynamics of the volumes in phase space for systems with more than one degrees of freedoms, and this translates in constraints in the spectrum of Lyapunov's exponents. However, trajectories can distort enough

that these constraints still allow for the system to be highly sensible to initial conditions and non-trivial chaotic behaviour to emerge. Still, conservative systems do not (normally) develop attractors and, as we will see in examples later in the lectures, chaos arise in different ways.

To conclude we make a useful observation. It is simple to find an example where a positive Lyapunov exponent does not necessarily mean chaotic behaviour. Think about the dynamics of the 2D linear ODE associated to an unstable repulsive “star” fixed point. As we have seen in chapter 3 the time evolution of an unstable repulsive star is given by

$$\mathbf{u}(t) = \mathbf{u}_0 e^{\lambda t}, \quad \lambda > 0$$

with \mathbf{u}_0 the vector of initial conditions. This implies that

$$\lambda = \frac{1}{t} \ln \frac{|\Delta \mathbf{u}(t)|}{|\Delta \mathbf{u}_0|} = \lim_{t \rightarrow +\infty} \lim_{|\Delta \mathbf{u}_0| \rightarrow 0^+} \frac{1}{t} \ln \frac{|\Delta \mathbf{u}(t)|}{|\Delta \mathbf{u}_0|}$$

The Lyapunov exponent is positive and indeed trajectories diverge exponentially from each other. But the system is certainly not Chaotic. This indicates that positive Lyapunov exponent is not sufficient to lead to Chaos. In general it is a necessary condition while it becomes also sufficient if used in a bounded region of orbits. In this case one can intuitively imagine that if orbits are bounded but still exponentially diverge from each other then Chaos will emerge. These are the cases of strange attractors that we will show at the end of this chapter.

6.2 Attractors

An *attractor* is a set of points in phase space which a dynamical system evolves towards over time. Trajectories that get close to the attractor will remain close, even if they are perturbed slightly. Geometrically, the attractor can be anything from a single point, to a curve, a higher dimensional manifold, or something more complicated: a *strange attractor* with a fractal structure and a (potentially) non-integer dimension.

Mathematically, an attractor is a subset A of the phase space, that satisfies:

- A is a fixed set under the evolution. For each $\mathbf{x}_0 \in A$, then $\mathbf{x}(t)$ is also in A , for all $t > 0$.
- There exists a neighbourhood of A called the *basin of attraction*, B , with the property that all points $\mathbf{x}_0 \in B$ enter the attractor in the limit $t \rightarrow \infty$. (More precisely, for any ϵ , no matter how small, there is some finite time t such that $\mathbf{x}(t)$ is within a distance ϵ of the attractor A .)
- There is no proper subset of A with the first two properties.

Not all dynamical systems have attractors. In particular, to have an attractor a system must be non-conservative, because in order for a range of different trajectories to all reach the same attracting set they must be able to gain or lose energy throughout the motion. Thus, conservative Hamiltonian systems (ie, time-independent Hamiltonians) do not have attractors.

6.3 Types of attractors

Let us mention a few examples of attractors in dynamical systems.

6.3.1 Fixed point attractor

A *fixed point attractor* is a single point in phase space. We have already seen examples in the previous chapters such as attractive stars and spirals for 2D linear ODEs. This typically occurs when there is dissipation in the system whereby the system comes to rest with zero velocity. For example, the damped pendulum,

$$\ddot{\theta} = -\frac{g}{a} \sin \theta - \alpha \dot{\theta}. \quad (6.3.5)$$

For any $\alpha > 0$, the system eventually comes to rest at the fixed point at $\dot{\theta} = \theta = 0$ through attractive spirals. Another example is the attractive star for the linear 2D ODE which clearly have a negative Lyapunov exponent. A feature of orbits close to attractors is to have negative Lyapunov exponent.

6.3.2 Limit cycle attractors

A *limit cycle attractor* is a closed curve in phase space. This implies that the motion of the system is periodic, with some fixed frequency ω . Many engineered devices exhibit limit cycles, for example a pendulum clock (driven, damped oscillator), and many types of electrical circuit. Note that an undamped pendulum is an oscillator but does not have a limit cycle, because a perturbation applied to the system simply shifts the trajectory to a different orbit in phase space without returning to an attractor.

A typical example of a limit cycle is shown in Fig. 6.1 and 6.2, for the van der Pol oscillator,

$$\ddot{x} - \mu(1 - x^2)\dot{x} + x = 0 \quad (6.3.6)$$

which was introduced by the Dutch physicist Balthasar van der Pol, in order to explain oscillations in vacuum tube circuits. (If an additional periodic driving force is added, then it is possible that the motion becomes chaotic and the limit cycle attractor is replaced with a strange attractor.) The use of devices that have dynamics possessing a limit cycle is the core of constructions of clocks.

6.3.3 A limit torus attractor

A *limit torus* occurs if there is more than one frequency in the periodic trajectory through a limit cycle. If two of these frequencies are incommensurate (ie, ω_1/ω_2 is an irrational number), then the trajectory is not closed and the limit cycle becomes a limit torus.

6.4 Defining chaos revisited

An attractor is called a *strange attractor* if it has infinite degree of complexity (we'll see this to be related to fractals in a couple of chapters) and (often) a non-integer dimension and/or if the motion on the attractor is chaotic. Essentially a strange attractor is a bounded region in phase space that has all the properties of an attractor but whose orbits are highly sensible to initial conditions making the dynamics essentially unpredictable.

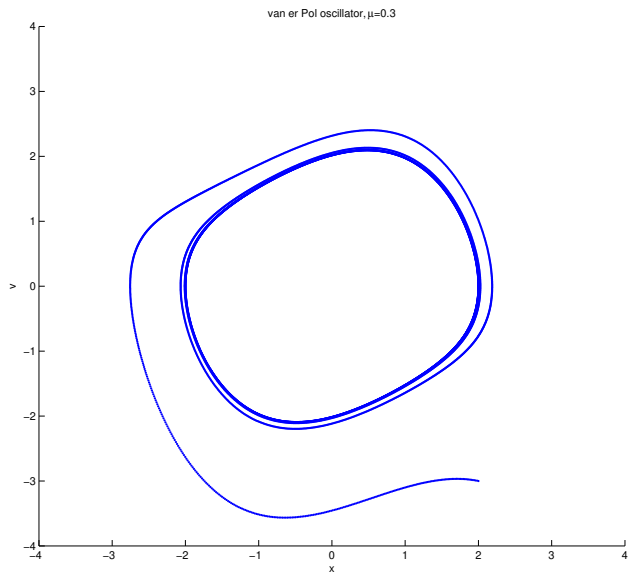


Figure 6.1: Evolution of a trajectory of the van der Pol oscillator with initial point $(2, -3)$. For any initial condition, the trajectory quickly approaches the limit cycle attractor.

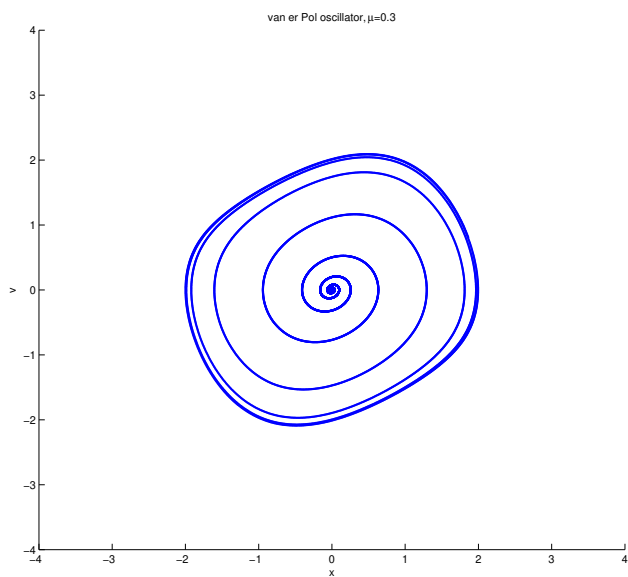


Figure 6.2: Evolution of a trajectory of the van der Pol oscillator with initial point $(0.01, 0.01)$, approaching the limit cycle from the inside.

If a strange attractor is chaotic, paths on the attractor are sensitive to the initial conditions. Although paths remain on the attractor, if they start from any two arbitrarily close points on the attractor, after some time, they will be arbitrarily far apart, subject to the confines of the attractor (and after some further time, they can be arbitrarily close together again). Thus a dynamical system with a chaotic attractor is locally unstable yet globally stable: once some sequences have entered the attractor, nearby points diverge from one another but never depart from the attractor.

An important property to keep in mind is that regular orbits converging to the non-chaotic attractors will have negative Lyapunov exponents. They all converge exponentially to the non-chaotic attractor. The attractive fixed points and cycles are good examples of this behaviour. Strange attractors will have negative Lyapunov exponent in regions where the orbits move towards the attractors. On the strange attractor, Lyapunov exponents have positive value (or fluctuate depending on the complexity of the structure). The same holds for orbits already exponentially close to the strange attractors.

6.4.1 Lorenz System

In the early 1960's, a metereologist named Edward Lorenz experimented with modelling weather systems. He was surprised that he couldn't find solutions to the equations, even for a dramatically simplified problem with 3 variables,

$$\begin{aligned}\dot{x} &= \sigma(y - x) \\ \dot{y} &= x(\rho - z) - y \\ \dot{z} &= xy - \beta z\end{aligned}\tag{6.4.7}$$

which is known as the *Lorenz system*. In general, all of $\sigma, \rho, \beta > 0$, but it is usual to fix $\sigma = 10$, $\beta = 8/3$, and modify ρ , called the Rayleigh number.

The Lorenz attractor—the attractor of this system—is a classic example of a chaotic strange attractor. The detailed analysis of the structure of the Lorenz attractor goes beyond the scope of this course but it is worth mentioning that the set proves to be a fractal of dimension higher than two with high complexity. We will discuss fractals in chapter 8 and now turn to other simpler chaotic systems described by 1D maps.

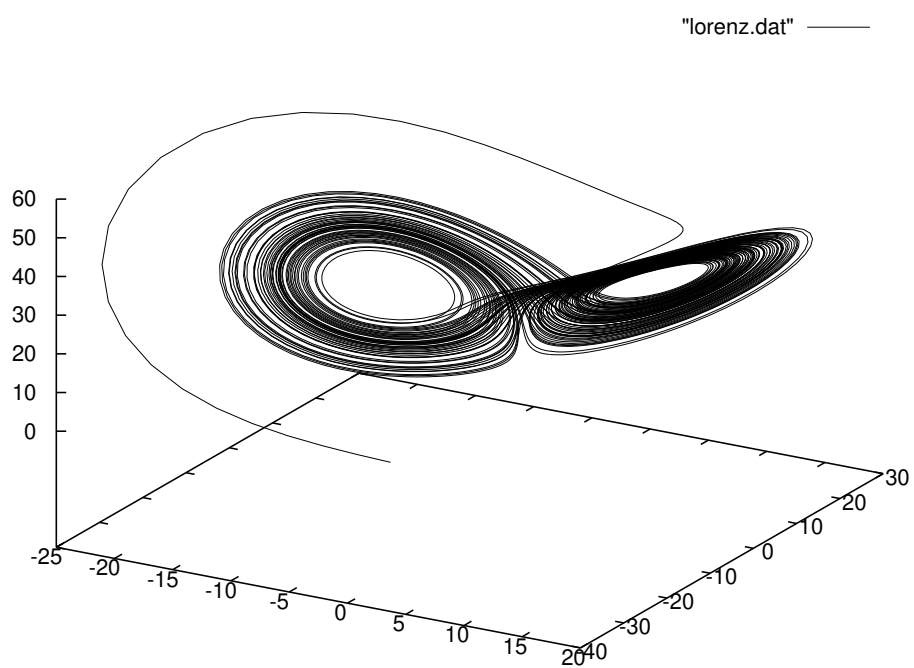


Figure 6.3: Trajectory of the Lorenz system, with $\sigma = 10$, $\beta = 8/3$, $\rho = 28$. The initial point was chosen to be well away from the attracting set.

The logistic map

While visualisation of the dynamics of conservative Hamiltonian systems with one degree of freedom is straightforward, and the phase portraits of such systems are easy to interpret, such systems do not display chaotic dynamics. To observe chaos, we require the system to be non-conservative or to have 2 or more degrees of freedom. However, the visualisation of the dynamics of such systems is more difficult, and it is worthwhile to first look at simpler systems exhibiting chaos (thus, an example outside Hamiltonian dynamics).

To begin our introduction to chaotic dynamics, we will look at one-dimensional nonlinear maps which display many of the important features of chaos in a very simple system. They also represent limits or simplified reductions of systems of differential equations which exhibit chaotic behaviour. We will see how for instance sequences of maps naturally arise by making appropriate visualisations of slices of phase spaces for systems of ODEs. They are also occurring as models of natural phenomena (inc. economics and finance!).

7.1 One-dimensional maps

One dimensional maps are extremely simple: they are of the form

$$x_{n+1} = f(x_n) \tag{7.1.1}$$

i.e. they take a value of x and transform it to another value of x . They are maps of the real line in the real line but often, and always in our case, one restricts to a unit line segment

$$0 \leq x_n \leq 1.$$

Essentially the sequence x_n is generated by composing n -times the map given by the function $x \rightarrow f(x)$. In fact it holds

$$x_0 = x, \tag{7.1.2}$$

$$x_1 = f(x), \tag{7.1.3}$$

$$x_2 = f(f(x)) := f^2(x), \tag{7.1.4}$$

$$x_3 = f(f(f(x))) := f^3(x) \tag{7.1.5}$$

$$\dots \tag{7.1.6}$$

$$x_n = f(f(f(\dots f(x)\dots))) \tag{7.1.7}$$

In this context be careful to not confuse $f^N(x)$ with $(f(x))^N$.

Linear maps are of the form

$$x_{n+1} = ax_n + b, \quad (7.1.8)$$

for some constants a, b . Such maps are one-to-one, and they cannot display chaotic behaviour. However, nonlinear maps are many-to-one, and can display chaos. We will not enter in the general study of 1D maps. We are going to focus immediately on the case we are mostly interested in which displays chaotic features that prove to be universal. Note that maps are capable of much wilder behaviour than differential equations because the points x_n hop discontinuously along their orbits rather than flow continuously.

7.2 The logistic map and relation to population dynamics

A very studied example of a 1D nonlinear map is the *logistic map*

$$f(x) = rx(1 - x), \quad 0 \leq x \leq 1. \quad (7.2.9)$$

It is easy to show that for $f(x)$ to be bounded by zero and one, that we must have $0 \leq r \leq 4$. The constant parameter r dramatically affects the behaviour of the map, as we will see soon.

The logistic map is a discretisation of the ODE given by the *logistic equation*

$$\dot{x} = bx - cx^2. \quad (7.2.10)$$

This is a very simple model of the dynamics of a biological population x . The populations of insects, birds, fish, and mammals are increased by births and decreased by deaths, the rates of which depend on a very complicated interplay of huge range of influences. The simplest model you can come up with is that the rate equation for the population can be written as

$$\dot{x} = [B(x) - D(x)]x, \quad (7.2.11)$$

where we have assumed that the birth rate $B(x)$ and the death rate $D(x)$ may depend on the current population, but not on space, time, or any other factors. Of course we must have that $B(x), D(x) \geq 0$, and also there is a natural boundary of $x \geq 0$.

The simplest assumption is that the birth and death rate are constants independent of the population, so that

$$\dot{x} = [B - D]x. \quad (7.2.12)$$

The solution to this equation is exponential growth for $B > D$, or exponential decay for $B < D$ with a growth/decay factor given by $(B - D)$.

However, in practice a population in a confined region of space cannot increase without bound forever, as there will be limiting factors such as competition for food and other resources. The next simplest assumption is to suppose that such factors leave the birth rate unchanged, but give a death rate per individual proportional to the population, so that

$$B(x) = b, \quad D(x) = cx, \quad (7.2.13)$$

which gives the logistic equation (7.2.10). It turns out that some actual populations closely follow the dynamics predicted by the logistic equation.

However, the situation is rarely so simple. In particular, often one species preys on another, and so their population equations are coupled together leading to more complicated systems.

Another possible feature is that often individual species have a definite reproductive season, so that the change in population is not represented by a differential equation, but instead by a difference equation or map. By discretising and scaling Eq. (7.2.10) to introduce the dimensionless variable $\tilde{x} = x/x_0$ we can write

$$\Delta\tilde{x}x_0 = b\tilde{x}x_0\Delta t - c(\tilde{x}x_0)^2\Delta t, \quad (7.2.14)$$

$$\Delta\tilde{x} = (b\Delta t)\tilde{x} - (cx_0\Delta t)\tilde{x}^2, \quad (7.2.15)$$

$$\Rightarrow \tilde{x} + \Delta\tilde{x} = (b\Delta t + 1)\tilde{x} - (cx_0\Delta t)\tilde{x}^2. \quad (7.2.16)$$

By identifying $r = b\Delta t + 1$ and choosing $x_0 = r/c\Delta t$, then (dropping tildes) we have derived the logistic map

$$x_{n+1} = rx_n(1 - x_n). \quad (7.2.17)$$

This can cause completely new phenomena to appear in the time dependence of the population as compared to the logistic equation.

7.3 Geometrical representation of logistic map

Let's take a particular example, with $r = 0.8$ and $x_0 = 0.7$ (in the pictures μ is our r in the equations). Then we find that

$$x_0, x_1, x_2, x_3, \dots = 0.7, 0.1680, 0.1118, 0.0795, 0.0585, \dots, 0, 0, \dots$$

which eventually converges to the fixed value 0. The mapping can be represented geometrically as in Fig 7.1 and described in the caption. These graphs are sometimes called cobwebs. You might have had the opportunity to investigate the logistic map numerically in a computer lab. What you would have found is that for $r < 1$, then the mapping eventually converges to 0. Then up until $r = 3$, the mapping converges to a finite value of x . For $r > 3$, sometimes the mapping settles down to a regular pattern, but other times it doesn't. So it is obvious that some stable fixed points exist in the mapping. The behaviour for particular selections with iteration number n are show in Fig. 7.2. A so called "bifurcation diagram" that attempts to plot the fixed points for the interesting range of values of r is shown in Fig. 7.3

7.4 Fixed points

The fixed points of a 1D map x_f are found by setting

$$x_f = f(x_f). \quad (7.4.18)$$

For the logistic map this is

$$x_f = rx_f(1 - x_f), \quad \Rightarrow \quad x_f(r - 1 - rx_f) = 0. \quad (7.4.19)$$

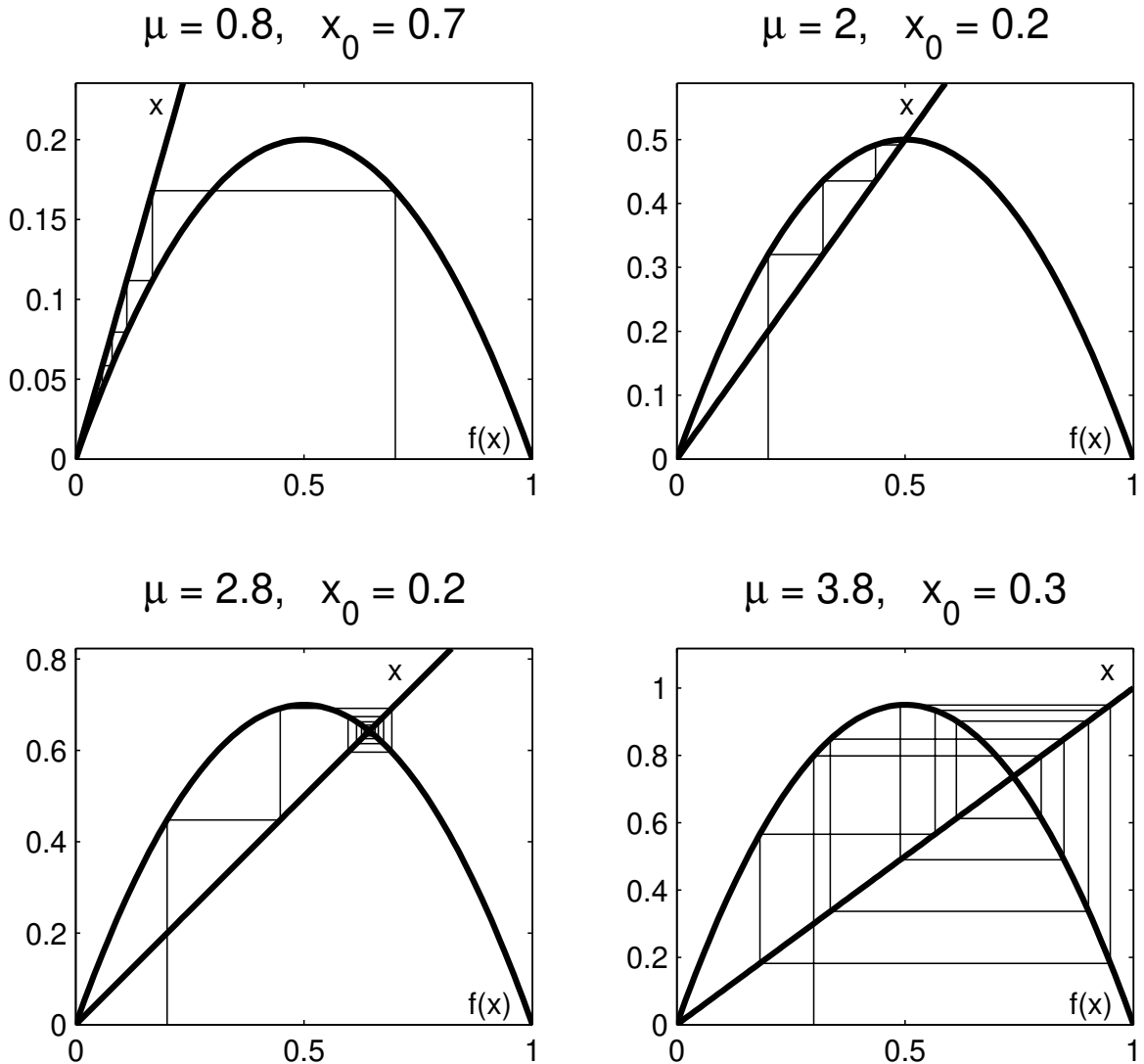


Figure 7.1: Geometrical representation of the logistic map for a number of combinations of r and x_0 for ten iterations. We begin at x_0 on the horizontal axis, and move vertically until we hit $x_1 = f(x_0)$. This is mapped back to an initial condition by moving horizontally we hit the curve x . Then move vertically to give $x_2 = f(x_1)$, and so on.

So the fixed points are

$$x_f = 0, \quad 1 - \frac{1}{r}. \quad (7.4.20)$$

These are just the intercepts of the two curves in Fig. 7.1. As we have $0 \leq x \leq 1$, then the second fixed point can only exist for $r \geq 1$.

Lets consider the stability of the fixed points. We define the distance of x_n from the fixed point at x_f by

$$\delta_n = x_n - x_f, \quad (7.4.21)$$

and we consider this quantity in a small neighborhood of the fixed point x_f . We

have

$$|\delta_{n+1}| = |x_{n+1} - x_f| = |f(x_n) - x_f| = |f(x_f + \delta_n) - x_f|, \quad (7.4.22)$$

$$= \left| f(x_f) + \delta_n f'(x_f) - x_f \right| = \left| f'(x_f) \right| |\delta_n|, \quad (7.4.23)$$

where we have made a first order Taylor series expansion of $f(x)$ about the fixed point. We have that $|\delta_{n+1}| < |\delta_n|$ and the fixed point is stable if and only if $|\lambda| < 1$, where

$$\lambda = \left. \frac{df}{dx} \right|_{x=x_f}, \quad (7.4.24)$$

which is called the *stability coefficient*. For the logistic map

$$\frac{df}{dx} = r(1 - 2x), \quad (7.4.25)$$

and the two fixed points are $x_f = 0$ and $x_f = 1 - 1/r$. Hence the stability coefficient of the period-1 orbit is

$$\lambda_1 = \begin{cases} r & \text{for } x_f = 0 \\ 2 - r & \text{for } x_f = 1 - 1/r \end{cases} \quad (7.4.26)$$

So the fixed point at $x_f = 0$ is stable for $r < 1$, and the fixed point at $x_f = 1 - 1/r$ is stable for $|2 - r| < 1 \implies 1 < r < 3$. Neither of the fixed points are stable for $3 \leq r \leq 4$.

When the stability coefficient vanishes, $\lambda = 0$, this is the 'most stable' point of the map, in the sense that small perturbations vanish very quickly. This is referred to as the *superstable* orbit. For the period 1 orbit of the Logistic map, the superstable orbit occurs at $r = 2$.

For $|\lambda| > 1$ the fixed point is unstable. On the other hand, for $|\lambda| = 1$ one needs to consider the next order in the Taylor expansion to determine the nature of the fixed point.

As another examples consider

$$x_{n+1} = (x_n)^2$$

there are two fixed points:

$$\bar{x} = \bar{x}^2, \quad \implies \quad \bar{x} = 0, 1.$$

It holds $\lambda_0 = 0$ and then $\bar{x} = 0$ is stable while, $\lambda_1 = 2$ and $\bar{x} = 1$ is unstable. Another example is the cosine map

$$x_{n+1} = \cos x_n$$

An example of its map is given in Figure 7.4. Without finding explicitly the value of the fixed point solving $\bar{x} = \cos \bar{x}$ we are sure that this is a stable fixed point since the first derivative between 0 and $\pi/2$ is always with modulus lower than one.

7.5 Unstable fixed points and n -cycles

Let us consider the case for $r \geq 3$. From Fig. 7.2 we can see that for some values of r it looks like the map settles down to some sort of periodic behaviour, but for others it seems there is no pattern at all. This is confirmed in the bifurcation diagram Fig. 7.3.

For the regime $3 < r < 3.44$ it appears that rather than having a single fixed point, the map oscillates about two values of x , such that $x_{n+2} = x_n$. As the number of steps between identical values of x_n is now two rather than one, the period is said to have *doubled*. The map has developed an attractive limit periodic 2-cycle.

Given a positive integer p , a periodic p -cycle of a 1D map is defined by a sequence x_1, x_2, \dots, x_p , such that $f(x_i) = x_{i+1}$ with $i = 1, 2, \dots, p-1$, and $f(x_p) = x_1$. This implies that $x_{i+p} = x_i$ whenever x_i is one of the elements of the sequence x_1, x_2, \dots, x_p that defines the p -cycle. Therefore, each of these points, x_i with $i = 0, \dots, p$, are fixed points for the map $f^p(x) = f(f(f(\dots f(x))))$ which is the p -th iteration of the map f (for example $f^2(x) = f(f(x))$, $f^3(x) = f(f(f(x)))$, etc): $f^p(x_i) = x_i$, $\forall i = 0, \dots, p$. The integer p identifies the period of the p -cycle. In a tutorial it will be proven that the stability coefficient for a p -cycle is

$$\lambda = \prod_{i=1}^p f'(x_i)$$

It is important to stress that in the previous definition we are not requiring x_1, x_2, \dots, x_p to be all different from each other, $x_1 \neq x_2 \neq \dots \neq x_p$. This for instance implies that a 1-cycle, defined by a fixed point \bar{x} for the map $f(x)$, is also a p -cycle for every p : $f(\bar{x}) = \bar{x} \implies f^p(\bar{x}) = \bar{x}$. We will use this property soon to simplify the problem of searching for all 2-cycles of the logistic map.

In the logistic map, as r is further increased, we can see that around $r = 3.45$ then there are four stable values of x , and we have $x_{n+4} = x_n$. So the period has doubled again. As r is further increased the period doubling mechanism continues until the system is chaotic. The points at which the splits occur in Fig. 7.3 are known as *pitchfork bifurcations*. The structure of the appearance of n -cycles can be studied both by computer experiments but also direct analytic investigations. Let's consider for instance 2-cycles.

To analyse the period 2 orbit, called also 2-cycles, we consider the map $f^2(x) = f(f(x))$. Fixed points of this map will occur in pairs, $f^2(x_1) = x_1$, and $f^2(x_2) = x_2$, (but, once more, we don't forbid $x_1 = x_2$!) such that

$$x_2 = f(x_1) \tag{7.5.27}$$

$$x_1 = f(x_2) \tag{7.5.28}$$

We can solve these equations:

$$\begin{aligned} x_1 &= f(f(x_1)) \\ &= r^2 x_1 (1 - x_1) (1 - rx_1(1 - x_1)) \end{aligned} \tag{7.5.29}$$

or,

$$x_1 [r^2 (1 - x_1) (1 - rx_1 + rx_1^2) - 1] = 0. \tag{7.5.30}$$

The two period 1 orbits at $x = 0$ and $x = 1 - 1/r$ must be solutions also of the period 2 orbits (with $x_1 = x_2$), hence we can factor out a term $x(x - (1 - 1/r))$, which must leave a quadratic part. Substituting

$$x_1[r^2(1 - x_1)(1 - rx_1 + rx_1^2) - 1] = x_1(x_1 - (1 - 1/r))(ax_1^2 + bx_1 + c) \quad (7.5.31)$$

we can solve for the coefficients a, b, c

$$a = -r^3 \quad (7.5.32)$$

$$b = r^3 + r^2 \quad (7.5.33)$$

$$c = -r^2 - r \quad (7.5.34)$$

As an assignment you will work through the algebra of these results. Hence the two solutions are at $ax^2 + bx + c = 0$, which gives

$$x_{1,2} = \frac{1}{2}[(1 + 1/r) \pm (1/r)\sqrt{(r - 3)(r + 1)}]. \quad (7.5.35)$$

It is clear that 2-cycles only occur for $3 \leq r \leq 4$. The stability coefficient of f^2 is

$$\lambda_2 = (f^2)'(x_1) = f'(x_2)f'(x_1). \quad (7.5.36)$$

As an assignment you will solve these equations to determine the nature of stability of the 2-cycles and the position of the superstable point $\lambda_2 = 0$, which proves to occur at

$$r = 1 + \sqrt{5} = 3.2360... \quad (7.5.37)$$

Note that a similar analysis cannot be performed analytically for every higher n -cycle. You can imagine that solving for the position of fixed n -cycles will be an algebraic problem of finding zeros of increasingly high degrees polynomials. In this analysis knowing the positions of n -cycles up to a certain n helps thanks to the fact, already employed, that: fixed points are n -cycles for every n ; that 2-cycles are also $2p$ -cycles for every p ; etc. However, in general, one has to rely on numerical techniques up to exceptions. For example it is possible to prove that non-trivial 3-cycles start to occur at

$$r = 1 + \sqrt{8} = 3.828427...$$

Remarkably the appearance of this point for such a value of r coincide with a value where the map $f^3(x)$ intersect tangentially the line $f(x) = x$ in two points, that are degenerate double zeros of a degree 8 polynomial.

7.6 More on period doubling

The period doubling mechanism is a typical route to chaotic dynamics, and can be characterised by certain numbers that in general do not depend on the nature of the map. For example, the ratio of the spacings between consecutive values of r at the bifurcation points approaches a universal constant called the Feigenbaum constant, that was only discovered in 1980

$$\delta = \lim_{k \rightarrow \infty} \left(\frac{r_k - r_{k-1}}{r_{k+1} - r_k} \right) = 4.669201609.... \quad (7.6.38)$$

This proves to be the same for every chaotic unimodal maps (1D maps from length one interval to length one interval, as the logistic map).

For the logistic map the values of r for which bifurcations occur for the logistic map are found to be

$$\begin{array}{ll} r_1 = 3 & r_2 = 3.449490\dots \\ r_3 = 3.544090\dots & r_4 = 3.564407\dots \\ r_5 = 3.568759\dots & r_6 = 3.569692\dots \\ r_7 = 3.569891\dots & r_8 = 3.569934\dots \end{array}$$

Extrapolating we can see that we have $r_\infty = 3.5699456\dots$

However, beyond this value it is obvious from Fig. 7.3 that there are still values of r for which there are stable periodic cycles, the biggest being around $r = 3.828427\dots$ where there is a stable period-3 cycle. Outside these windows, the map appears chaotic though chaos comes together with windows of ordered dynamics (the biggest of which is the window associated to the stable 3-cycle).

It is remarkable to see how this behaviour is generic. Compare for example the bifurcation diagram of the sine map, $x_{n+1} = \sin x_n$, with the one of the logistic map as shown in Figure 7.7. The equivalence of the two maps is a strong indication that these structures are universal.

7.6.1 Lyapunov exponent

It would be of use to be able to define parameters that can be used to characterise chaos. Remember that we defined chaos as being the rapid divergence of nearby points in phase space. This divergence has been parameterised by the *Lyapunov exponent* λ , probably the most popular measure of chaotic behaviour.

Consider a one-dimensional system with initial states x and $x + \epsilon$, where $\epsilon \ll 1$ is a small parameter. After n iterations their divergency $\epsilon(n)$ may be approximated as

$$\epsilon(n) \approx \epsilon e^{n\lambda}. \quad (7.6.39)$$

Thus the Lyapunov exponent gives the average rate of divergence. If $\lambda < 0$ then separate trajectories converge and the system is not chaotic. However, if $\lambda > 0$ then separate trajectories diverge and the system is chaotic.

For a 1D map

$$x_{n+1} = f(x_n). \quad (7.6.40)$$

So in going from the initial value x_0 to x_{n+1} the map f has been applied n times

$$x_{n+1} = f^n(x_0). \quad (7.6.41)$$

The difference in the “state” of the system after n steps is

$$f^n(x_0 + \epsilon) - f^n(x_0) \approx \epsilon e^{n\lambda}, \quad (7.6.42)$$

and so

$$\lambda \approx \frac{1}{n} \ln \left[\frac{f^n(x_0 + \epsilon) - f^n(x_0)}{\epsilon} \right]. \quad (7.6.43)$$

In the limit that $\epsilon \rightarrow 0$ then we have

$$\lambda = \frac{1}{n} \ln \left[\left. \frac{df^n(x)}{dx} \right|_{x=x_0} \right]. \quad (7.6.44)$$

Using the chain rule and $\ln ab = \ln a + \ln b$ one can show (we suggest to show the following as an instructive exercise)

$$\lambda = \lim_{n \rightarrow \infty} \frac{1}{n} \sum_{i=0}^{n-1} \ln |f'(x_i)|. \quad (7.6.45)$$

The Lyapunov exponent for the logistic map is shown in Fig. 7.8.

It turns out that, similarly to the Lorentz attractor, also the logistic map possesses a strange attractor with a non-integer “dimension” different than zero in the region of r exhibiting chaotic behaviour. Sets having a non-integer dimension are so-called fractal sets and consistently appear in systems exhibiting chaotic behaviour. Let us turn in the next chapter to discuss what a fractal is and provide some examples and ways to characterise them.

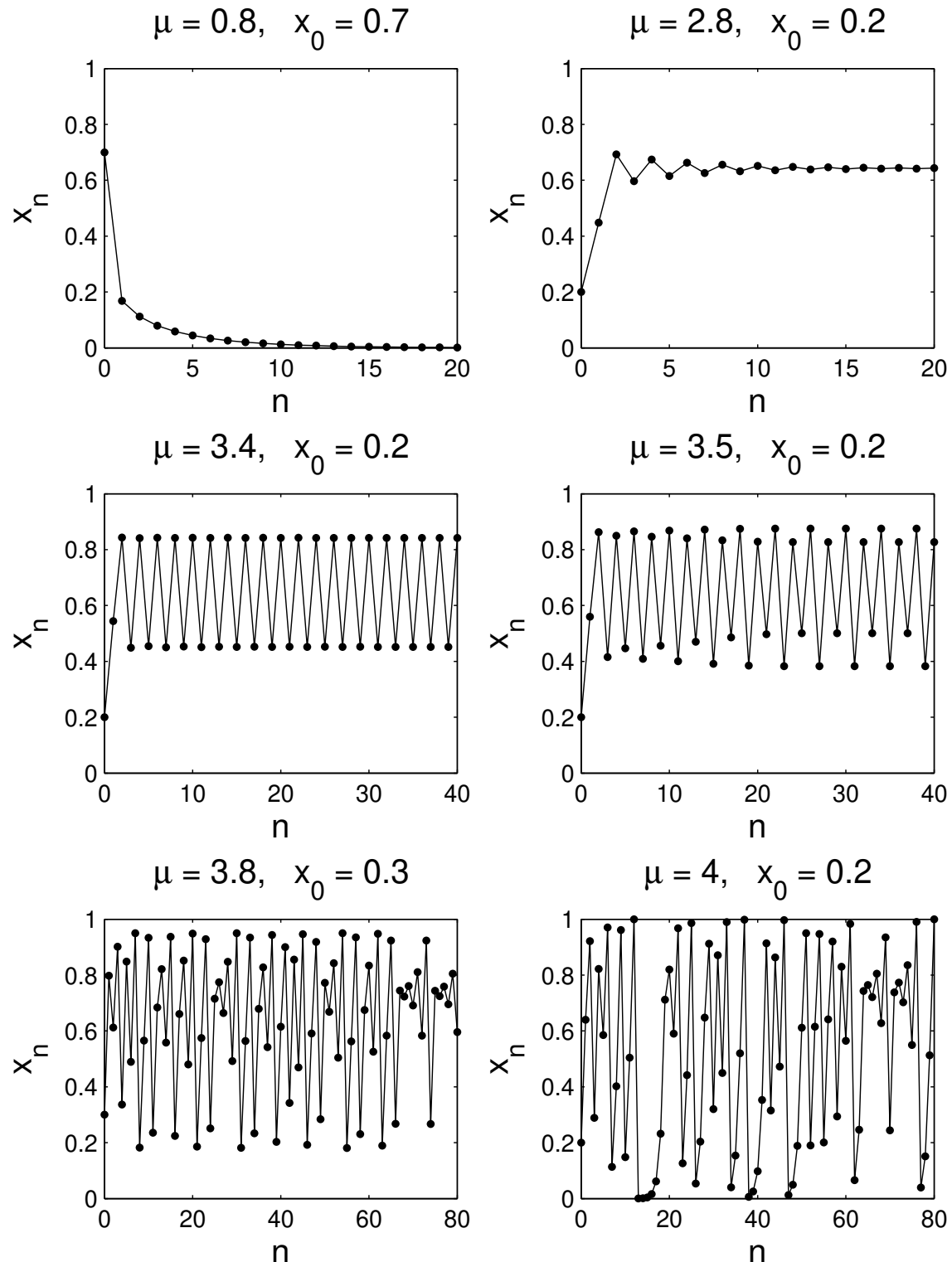


Figure 7.2: Evolution of the logistic map with iteration number n for some particular values of x_0 and r .

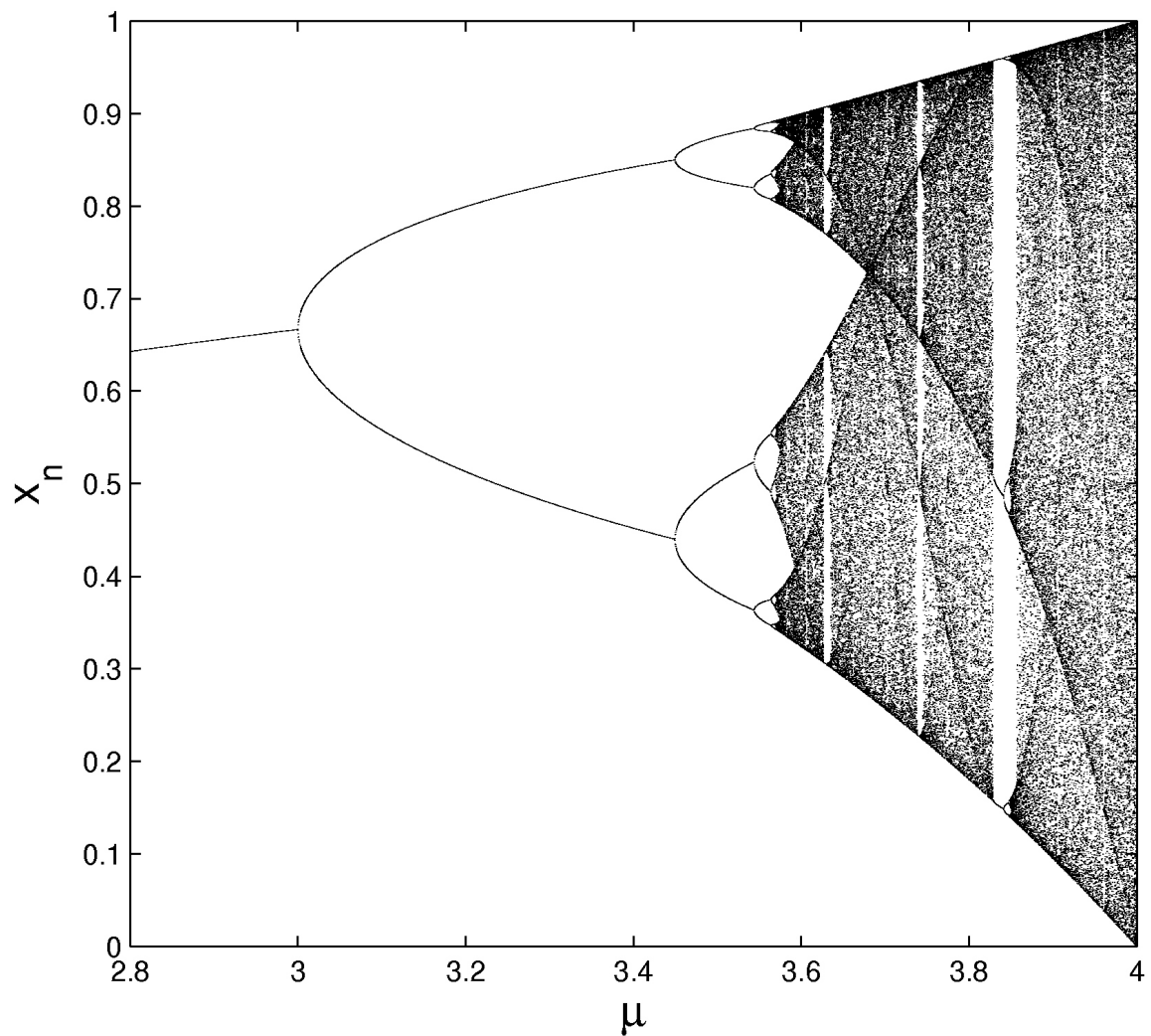


Figure 7.3: Bifurcation diagram for the logistic map for the region $2.8 \leq r \leq 4$.

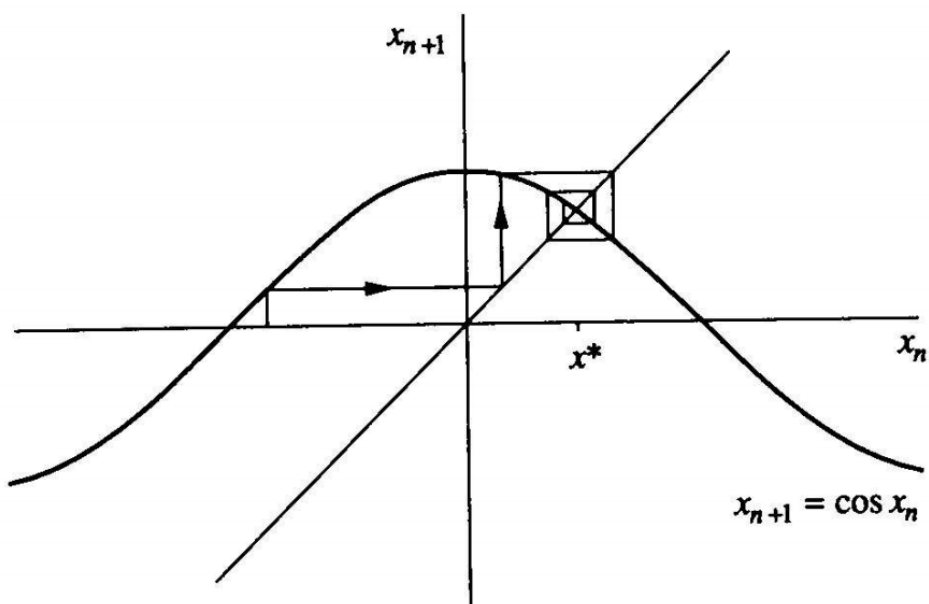


Figure 7.4: Cosine map

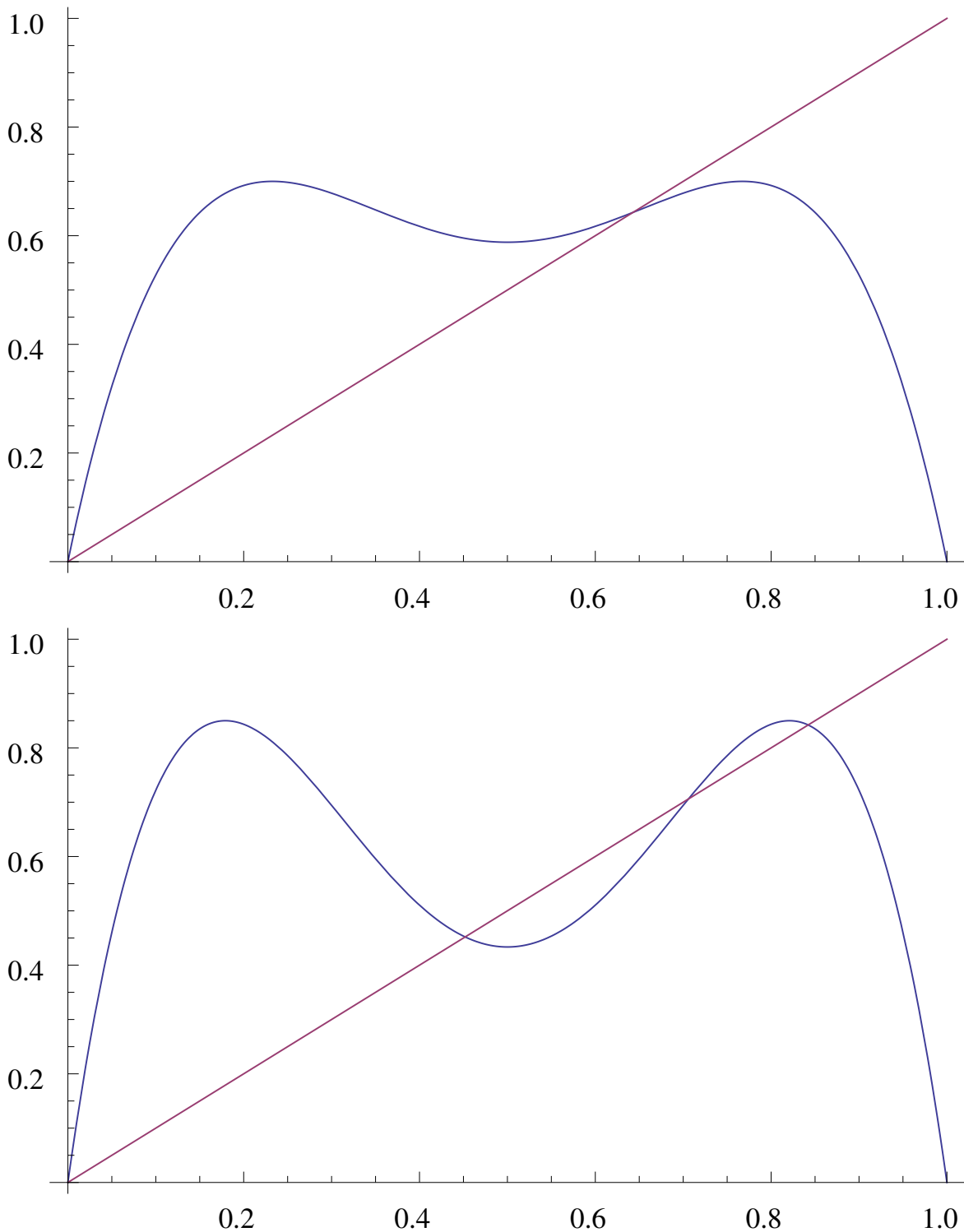


Figure 7.5: $f^2(x)$ versus x for (a) $r < 3$ and (b) $r > 3$.

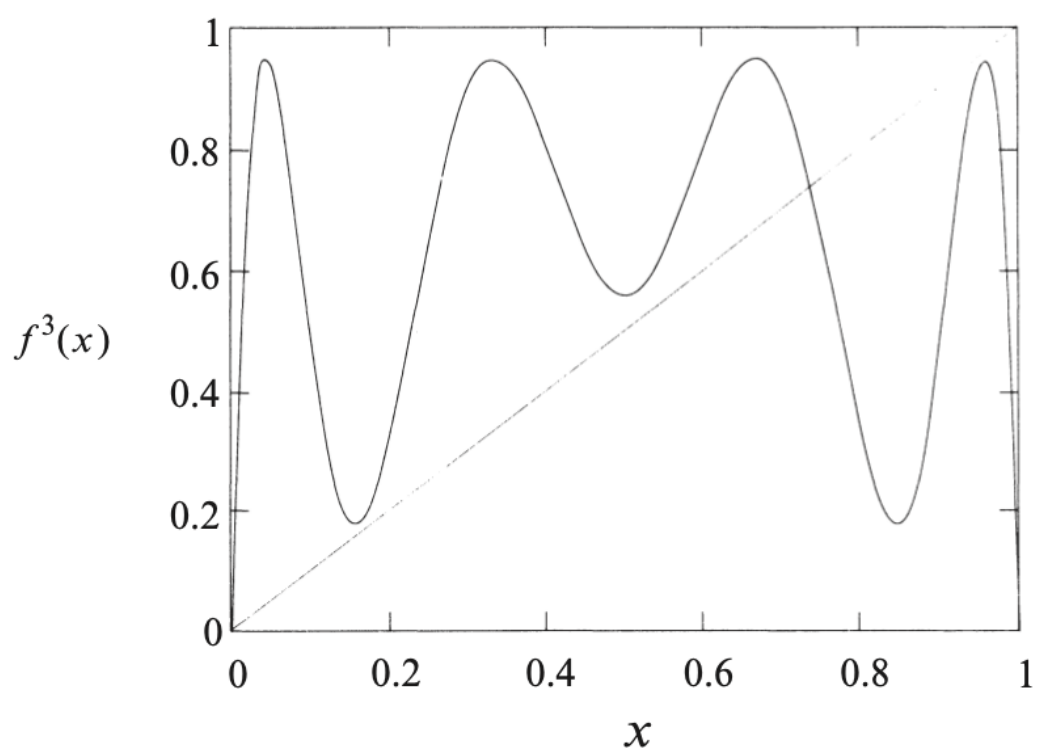


Figure 7.6: Behaviour of $f^3(x)$ close to developing the 3-cycles.

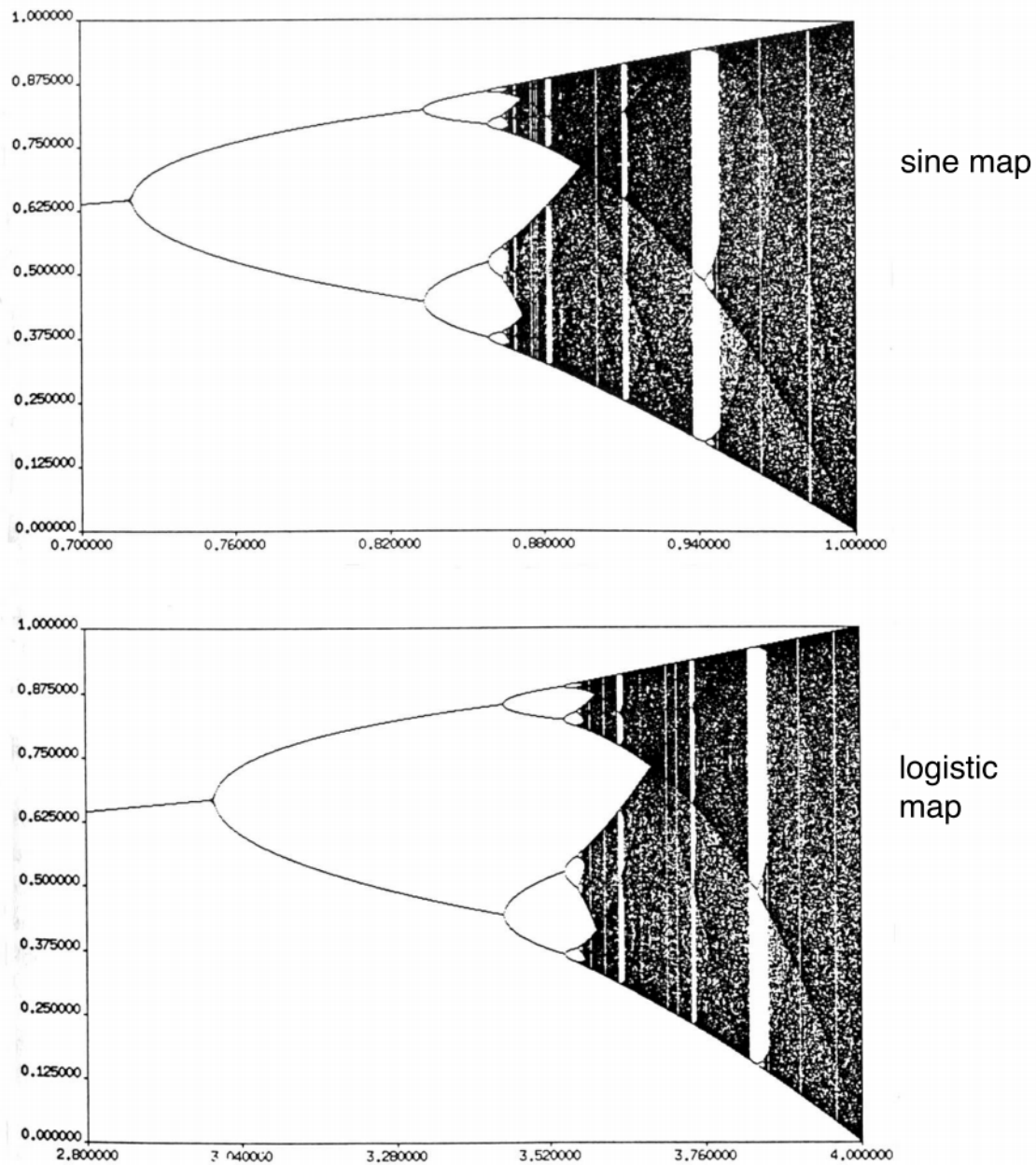


Figure 7.7: Sine vs Logistic bifurcation.

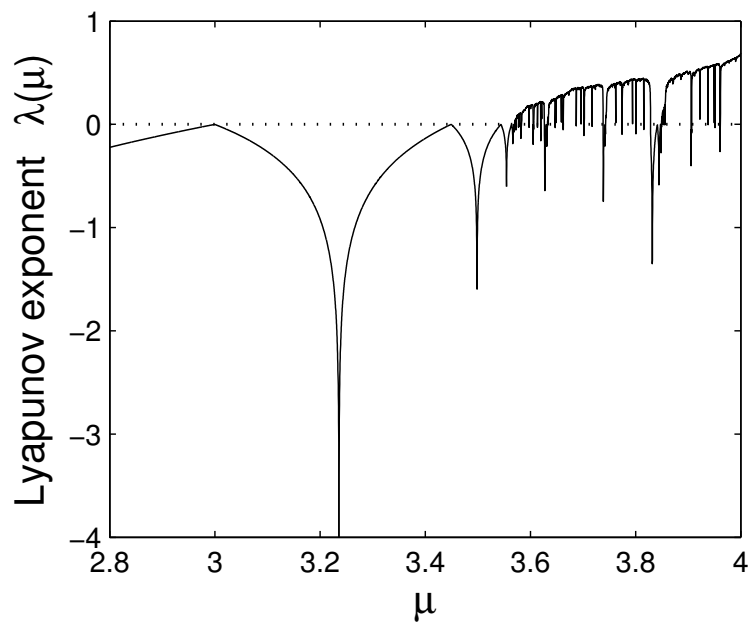


Figure 7.8: Lyapunov exponent for the logistic map for the region $2.8 \leq r \leq 4$.

CHAPTER 8

Fractals

A *fractal* is a geometrical shape that has fine structure at arbitrarily small scales, that is, it shows *self-similarity*. This can take several forms, such as an *exact self similarity*, meaning that a zoomed in picture of the object looks exactly the same as the original view, or *statistical self-similarity*, meaning that the zoomed in picture has similar properties but isn't exactly identical. There are various versions of definitions of fractals. A feature is that fractals have some types of self similarity at different scales one look at them. They can also possess non-integer dimension, or box counting as we will see.

To see how this works, let's first consider an example, the *Cantor set*.

8.1 Cantor Set

The Cantor set is a subset of the unit interval (i.e., the line $[0, 1]$) which has some very interesting properties and have played fundamental roles in mathematics (set theory, measure theory, dynamics...), physics (chaotic systems) and other dynamical systems exhibiting chaotic behaviour. Strange attractors in dynamical systems have properties completely analogue of the cantor set, in fact in some cases they are equivalent. To construct the set, we are going to iteratively remove the open middle third from the line segment, starting from the unit interval.



Figure 8.1: The first seven iterations of the Cantor set

The resulting set of points gets smaller at each iteration.

$$n = 0$$

$$[0,1]$$

$$n = 1$$

$$[0,1/3]$$

$$[2/3,1]$$

$$n = 2$$

$$[0,1/9] \quad [2/9,1/3]$$

$$[2/3,7/9] \quad [8/9,1]$$

What is the length of the set that remains? We can calculate this, because at each iteration we subdivide each set into three parts and we keep two of those parts. So the length of the set that we *remove* is the limit of a geometric series,

$$x = \frac{1}{3} + \frac{2}{9} + \frac{4}{27} + \cdots = \frac{1}{3} \sum_{n=0}^{\infty} \left(\frac{2}{3}\right)^n \quad (8.1.1)$$

The sum of this geometric series is $(1/3)/(1 - 2/3) = 1$. Hence the length of the set that remains is $1 - 1 = 0$. So, the Cantor set doesn't contain any intervals, only points of zero length. Indeed, it may seem surprising that the Cantor set contains *any* points, but we can easily see that it does: the end points of each interval are in the set, so for example the points $0, 1, 1/3, 2/3, 1/9, 2/9, 7/9, 8/9, \dots$ are in the set. Interestingly, there are points in the Cantor set that are not end points of any interval. For example, the point $1/4$ is inside the lower third at the first iteration, and then the upper third at the second iteration, then the lower third again, ad infinitum. Since it is never in one of the middle thirds, it is never removed hence it is part of the Cantor set, although it is not an endpoint. It will result clearer this fact from results in the next section

8.1.1 Cardinality

It can be shown that there are an uncountably infinite number of points in the Cantor set. To see this, we notice that we can generalize our discussion above for the number $1/4$ and describe *any* point in the Cantor set by whether it is in the upper or the lower kept third at each iteration. If we call the lower third '0' and the upper third '1', we can ascribe a repeated decimal expansion to each number in the set. For example, the end point $1/3$ would be described as $.01111111\dots$, since it is in the lower ('0') third at the first iteration, and thereafter it is always in the upper ('1') third. The number $1/4$ is located at $.010101010101\dots$. Hence the number of points in the Cantor set is equal to the number of distinct binary numbers in the range $[0, 1]$, and this is just equal to the number of points in the unit interval!¹ So, we have a subset of the unit interval, that contains the same number of points as the unit interval, but it has zero length. Numbers in the cantor set can also be efficiently described as all possible real numbers in the $[0, 1]$ interval described in a basis 3 where constrained to have entries $a_n = 0, 2$ (not 3) in the sequence:

$$x = \sum_{n=1}^{+\infty} \frac{a_n}{3^n} = 0.a_1a_2\dots a_i\dots$$

From this it is clear that the cardinality of Cantor's set is the same as the real numbers.

There are many different Cantor-like sets that mathematicians have abstracted their essence in the following definition. A closed set S is called a topological Cantor set if it satisfies the following properties:

1. S is “totally disconnected.” This means that S contains no connected subsets (S is described only by points not segments in the real line). In this

¹The proof of this is called the *diagonal slash*, which was introduced by Cantor as a proof that there exist sets with an uncountably large number of elements. The Cantor set itself an example of this.

sense, all points in S are separated from each other. For the middle-thirds Cantor set and other subsets of the real line, this condition simply says that S contains no intervals.

2. On the other hand, S contains no “isolated points.” This means that every point in S has a neighbor arbitrarily close by—given any point $p \in S$ and any small distance $\epsilon > 0$ there is some other point $q \in S$ within a distance ϵ of p .

The paradoxical aspects of Cantor sets arise because the first property says that points in S are spread apart, whereas the second property says they’re packed together. This type of property is shared by strange attractors and other types of fractals.

8.1.2 Self-similarity

The Cantor set shows self-similarity, in the sense that if you take a microscope and zoom in closely on a small part of the Cantor set, it looks exactly the same as it does on a larger scale. This is an example of exact self-similarity.

8.2 Dimensions

One of the most basic properties of any set is its dimension. Physically, the dimension gives important information about the characteristics of the set. For example, if the set is a trajectory of some dynamical system, then the dimension of the trajectory tells us how many parameters are needed in order to write down a model of the dynamics.

There are many ways of defining the dimension of an object, and for simple objects (i.e., non-fractals) these definitions generally turn out to be equivalent. A point has dimension zero, a line has dimension 1, a plane has dimension 2, and a solid object has dimension 3, and so on.

From a physical point of view, what do we mean by *dimension*? One way of viewing this that is particularly appealing is that the dimension describes the relationship between the size of an object and the physical length scale that we are using. As we change the length scale, how does the measurement of the size of the set change. For example, if we double the scale of a piece of string, then the length doubles. But if we double the scale of a piece of paper, then the surface area is increased by a factor $2^2 = 4$. And if we double the scale of balloon, the volume is increased by a factor $2^3 = 8$. These notions can be put in a concrete form by considering the box counting dimension.

Assume that we have a set that lies in an N -dimensional Cartesian space. We can then imagine covering the space by a grid of N -dimensional cubes, of edge length ϵ . We then count the number of cubes $\tilde{N}(\epsilon)$ needed to cover the set. If we do this for successively smaller values of ϵ , then we can obtain the box-counting dimension (assuming this limit exists)

$$D_0 = \lim_{\epsilon \rightarrow 0} \frac{\ln \tilde{N}(\epsilon)}{\ln(1/\epsilon)}. \quad (8.2.2)$$

Note that the count of the number of boxes $\tilde{N}(\epsilon)$ need not be precise, and a rough estimate will do. If we can estimate the number of boxes up to some uncertainty

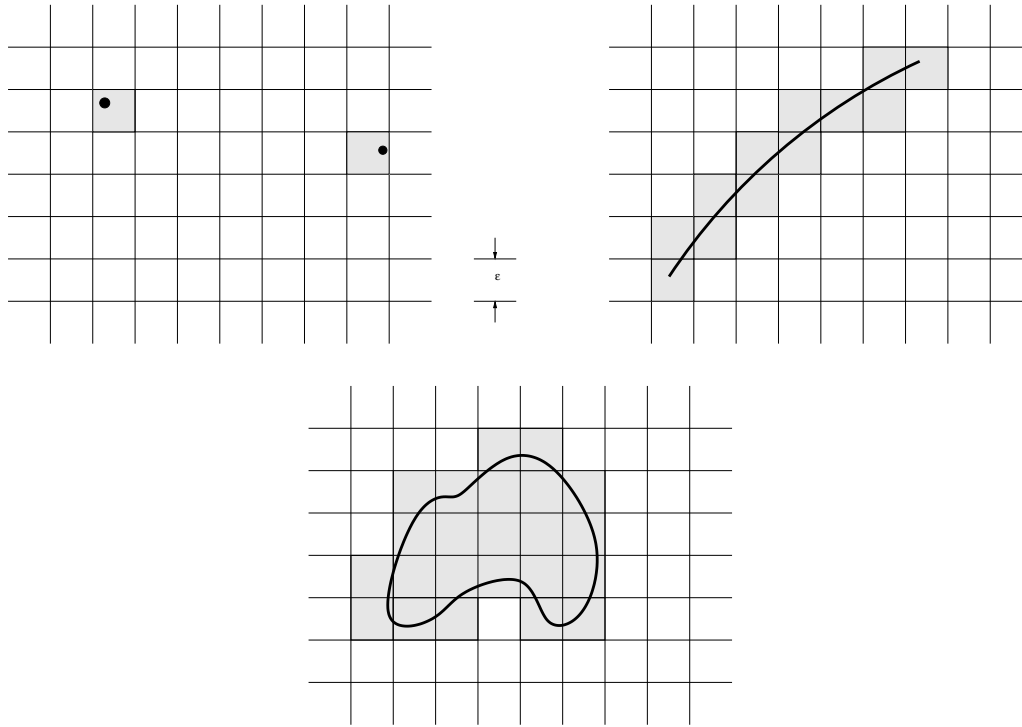


Figure 8.2: The calculation of $\tilde{N}(\epsilon)$ for various sets; two points, a curve segment, and the area inside a closed curve.

factor K , then this makes no difference to the box counting dimension. Due to the logarithm, the important factor is how the number of boxes scale with the factor of ϵ . If the number of boxes is

$$\tilde{N}(\epsilon) \simeq K \left(\frac{1}{\epsilon} \right)^d$$

then the box counting dimension is $D_0 = d$.

Note also that it is simple to show that the box counting dimension for a fractal is bounded by the topological dimension of the Euclidean space it is embedded in (for fractals that are not defined as sets embedded in an Euclidean space the situation is more complicated but we certainly avoid those cases). For simplicity, consider a fractal defined as a set on the plane \mathbb{R}^2 . For simplicity we also think that the set is bounded, which means that there exist at least one box of length L that contains the fractal. We call this box B_0 . We can then certainly compute the box counting by using a sequence where we slice B_0 in 4^n boxes, all of length $\epsilon_n = \frac{L}{2^n}$. Since the number of boxes covering the fractal is certainly lower or equal to the number of boxes we are dividing B_0 , it has to hold $\tilde{N}(\epsilon_n) \leq 4^n$. Then it holds

$$0 \leq \frac{\ln \tilde{N}(\epsilon_n)}{\ln(1/\epsilon_n)} \leq \frac{\ln 4^n}{\ln(1/\epsilon)_n} = \frac{2n \ln 2}{n \ln 2 + \ln L}.$$

and taking the limit $n \rightarrow \infty$ one gets

$$0 \leq D_0 \leq 2.$$

The same result holds for fractals that are defined as subsets of the Euclidean p -dimensional real space \mathbb{R}^p (with p clearly integer). In this case one has the bound

$$0 \leq D_0 \leq p.$$

There are interesting examples of fractals that still have integer dimensions. A famous example, which we will not discuss in detail, is the Hilbert curve which is an example of a space-filling fractal. Let us come to some famous examples of fractals which have non-integer box counting dimension.

8.2.1 Box counting dimension of the Cantor set

To calculate the box counting dimension for a specific set, we need to decide how to choose the scale ϵ . For the Cantor set, it is convenient to choose this to be decreasing by $1/3$ per iteration, since we are dividing intervals into three sections each time. Thus we have $\epsilon = (1/3)^n$. By the construction of the Cantor set, at each iteration the number of boxes we need is 2^n . Thus

$$D_0 = \lim_{n \rightarrow \infty} \frac{\ln 2^n}{\ln 3^n} = \frac{\ln 2}{\ln 3} = 0.630929\dots$$

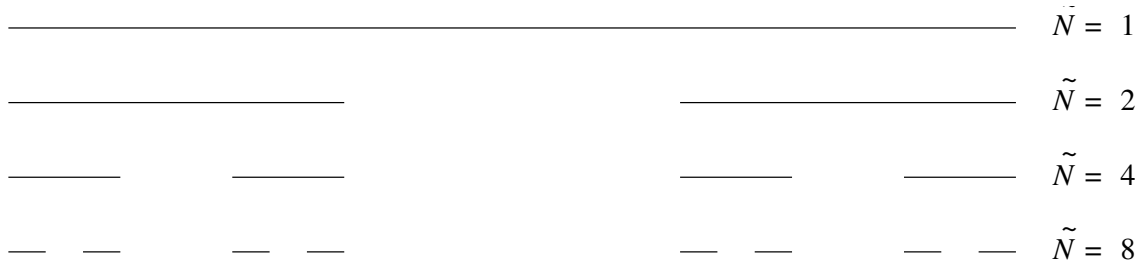


Figure 8.3: Box counting dimension of the Cantor set. The distance scale changes by a factor $1/3$ each iteration, while the number of boxes doubles.

8.2.2 Koch curve

There are many ways of constructing fractal shapes in a similar way to the Cantor set. Another famous example is the *Koch curve*, also known as the Koch snowflake. In this construction, we start with a line, and at each iteration we replace the middle third of each segment with two segments of the same length, making two sides of an equilateral triangle. The first 4 iterations of this procedure are shown in Figure 8.4. Although the Koch curve fits into a fixed area, at each iteration the length of the line increases by a factor $4/3$. Thus the curve gets very long after a few iterations. For example, if we started with a line 1m long, at the first iteration it would become $1.333\dots$ m long, after 10 iterations it will be $17.757\dots$ m long, and after 100 iterations it will be over 3×10^{12} m long!

We can calculate the box counting dimension D_0 of this curve in a similar way to the Cantor set. Remembering that we don't need to be rigorous in how we divide up our area into boxes, as long as they have approximately the same size. Choosing a length scale to be $(1/3)^n$ at the n^{th} iteration, the number of boxes we need is proportional to the number of distinct line segments we have, which is 4^n . Note that this indicates that the number of boxes is proportional to the length of the curve (perimeter) over the inverse of the (small) scale length of the boxes we are using to cover the curve. Hence the box counting dimension is

$$D_0 = \lim_{n \rightarrow \infty} \frac{\ln 4^n}{\ln 3^n} = \frac{\ln 4}{\ln 3} = 1.2618595\dots$$

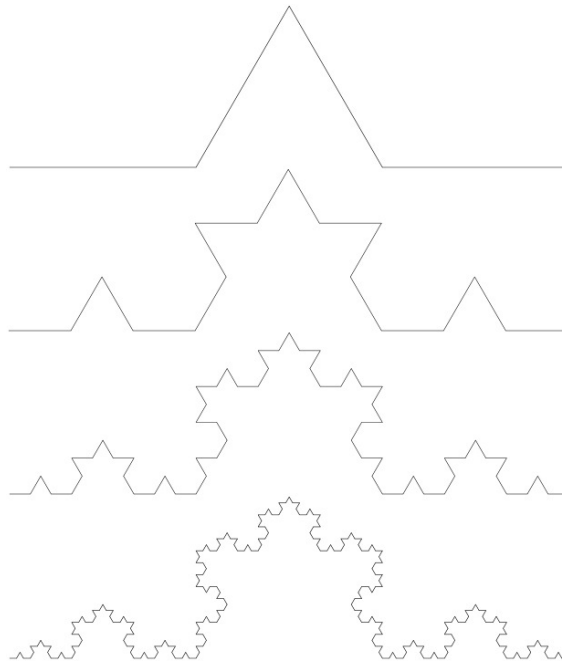


Figure 8.4: First 4 iterations of the Koch curve.

8.2.3 Box counting dimension of Logistic map

The attracting set of the logistic map is sometimes a stable periodic orbit and sometimes it is a strange attractor. Note also that it is possible to show a relationship between strange attractors and cantor sets. To investigate the strange attractor of the logistic map further, we could attempt to determine the box counting dimension. The transition to chaos at the end point of the period doubling bifurcation is at $r = 3.5699457\dots$. At a point just above this value, at above the transition to chaos, $r = 3.5699457\dots$, choose a box size of $\epsilon = 2^{-n}$, for $n = 11$ up to 25. For a small size box, $\epsilon = 1/2^{25}$, we can see in Figure 8.5 a histogram of the number of times the trajectory visited each box, in the course of around 2^{30} iterations of the map. Although the motion is *not* periodic and no point in the trajectory is ever visited twice, we can see that a clear characteristic of the attracting set is that there are many regions that are not visited at all. This structure is repeated on all length scales, as Figure 8.5 also shows what happens when we zoom in on a small section of the histogram (this also has a smaller length scale ϵ , so that the counts are not identical to the zoomed out view).

To calculate the box counting dimension, we can plot $\tilde{N}(\epsilon)$ as a function of ϵ on a log-log plot, and the slope of the line will determine the box counting dimension D_0 . This is shown in Figure 8.6.

8.2.4 Box counting dimension of the Lorenz attractor

The Lorenz attractor is an outstanding example of a fractal with non-integer dimension. Numerical results have given

$$2.06 \pm 0.01$$

as the dimension of the Lorenz attractor.

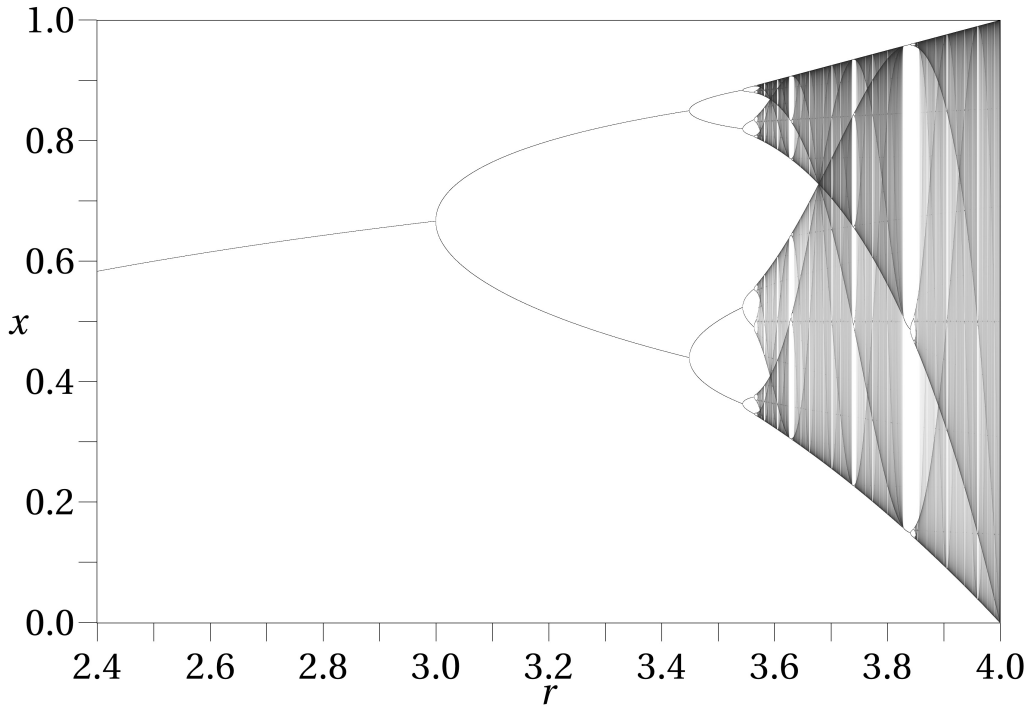


Figure 8.5: A histogram of how often the logistic map visits a box of size ϵ . The zoomed in views show that the fine structure exists on all length scales.

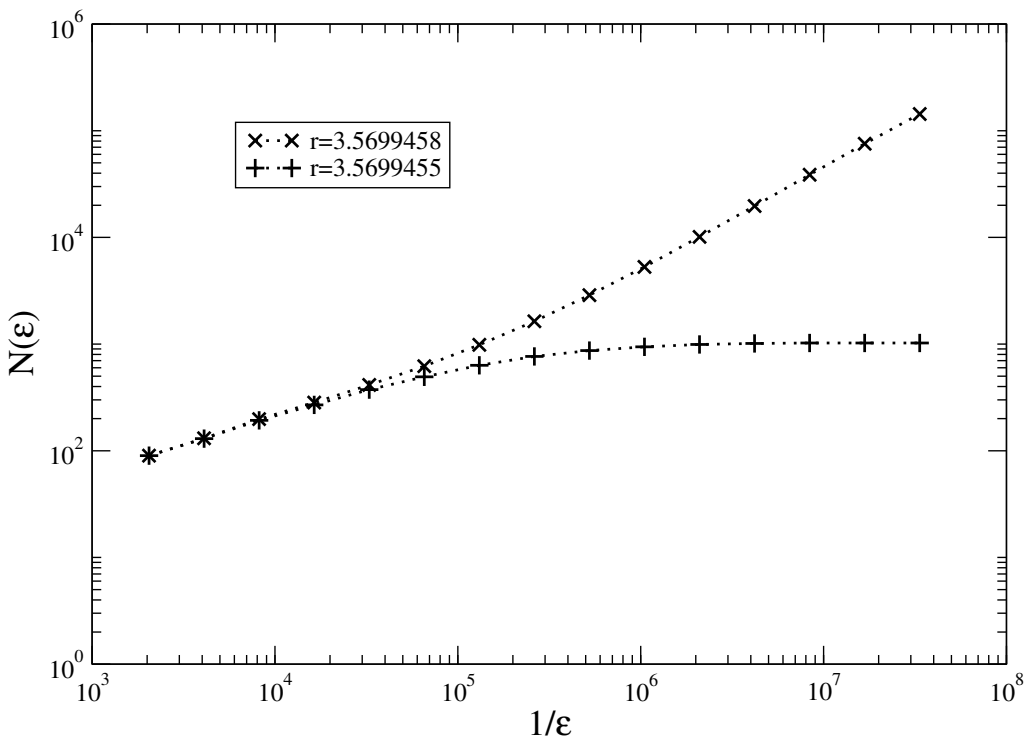


Figure 8.6: The box-counting dimension of the Logistic map for two values of r above and below the chaotic transition. Below the chaotic transition, the orbit is periodic, and here the count $\tilde{N}(\epsilon)$ saturates near 1024, indicating that this is a period- 2^{10} orbit. Above the chaotic transition, the slope of the line is approximately 0.55, which is the box counting dimension for the attracting set.

The driven pendulum, Recurrence plots and Poincaré sections

Having studied the appearance of chaos in the logistic map, we now move on to look at how chaos arises in Hamiltonian systems.

So far the Hamiltonian systems that we have considered have had one degree of freedom and have also been conservative: the energy has been a constant of the motion. Together these two facts mean that the systems have been *integrable*. Basically, this means that there are as many conserved quantities as there are degrees of freedom. Integrable systems do not display chaotic behaviour. Their dynamics is equivalent to straight lines in phase space, as we have already seen before.

So in order to study chaos in a Hamiltonian system, we either need to move to a system with (at least) two degrees of freedom, or introduce time-dependence into the Hamiltonian for a system with one degree of freedom. The second route is somewhat simpler: we can introduce a time-dependent potential that means energy is no longer conserved. We will look at the second option in the next chapter.

The particular example we will consider is the *vertically driven pendulum*. By controlling the amplitude of the driving we can influence the chaotic behaviour, leaving all other parameters fixed.

9.1 Hamiltonian for the driven pendulum

We consider a pendulum with a pivot that is driven vertically by a function $\gamma(t)$. The coordinates of the system are

$$x = a \sin \phi, \quad y = -a \cos \phi - \gamma(t), \quad (9.1.1)$$

where a is the length of the pendulum. Thus the kinetic energy is

$$T = \frac{m}{2}(\dot{x}^2 + \dot{y}^2) = \frac{m}{2}(a^2\dot{\phi}^2 - 2a\dot{\phi}\dot{\gamma}\sin\phi - \dot{\gamma}^2), \quad (9.1.2)$$

and the potential energy is

$$V = mgy = -mga \cos \phi - mg\gamma, \quad (9.1.3)$$

and is a function of time. Thus the Lagrangian is

$$\mathcal{L} = T - V = \frac{m}{2}a^2\dot{\phi}^2 - ma\dot{\phi}\dot{\gamma}\sin\phi + mga \cos \phi + h(t), \quad (9.1.4)$$

where $h(t) = m\dot{\gamma}^2 + mg\gamma$ is a function of time only, and hence may be ignored. (It is easy to show that it does not contribute to the equations of motion.)

The momentum conjugate to ϕ for this Lagrangian is

$$p = \frac{\partial \mathcal{L}}{\partial \dot{\phi}} = m(a^2\dot{\phi} - a\dot{\gamma} \sin \phi), \quad (9.1.5)$$

which leads to the Hamiltonian

$$H(\phi, p, t) = \frac{(p + ma\dot{\gamma} \sin \phi)^2}{2ma^2} - mga \cos \phi. \quad (9.1.6)$$

However, a more convenient Hamiltonian can be obtained by making use of the property that two Lagrangians related by

$$\bar{\mathcal{L}}(q, \dot{q}, t) = \mathcal{L}(q, \dot{q}, t) + \frac{d}{dt}f(q, t) \quad (9.1.7)$$

describe the same motion. If we choose $f(q, t) = \dot{\gamma} \cos \phi$ and add its time derivative

$$-ma \frac{d}{dt}(\dot{\gamma} \cos \phi) = -ma\ddot{\gamma} \cos \phi + ma\dot{\gamma}\dot{\phi} \sin \phi \quad (9.1.8)$$

to Eq. (9.1.4) we get a new Lagrangian

$$\bar{\mathcal{L}} = \frac{m}{2}a^2\dot{\phi}^2 + ma(g - \ddot{\gamma}) \cos \phi, \quad (9.1.9)$$

which shows that vertical acceleration has the same effect as a time-varying gravitational field. The conjugate momentum is now the angular momentum

$$\ell = \frac{\partial \bar{\mathcal{L}}}{\partial \dot{\phi}} = ma^2\dot{\phi} = J\dot{\phi}, \quad (9.1.10)$$

where $J = ma^2$ is the moment of inertia of the pendulum. The Hamiltonian is then

$$H'(\phi, \ell, t) = \frac{\ell^2}{2J} - J\omega_0^2 \left(1 - \frac{\ddot{\gamma}}{g}\right) \cos \phi, \quad (9.1.11)$$

where $\omega_0^2 = g/a$ is the SHO frequency of small oscillations of the free pendulum.

9.2 Equations of motion

Hamilton's equations for the system are

$$\dot{\phi} = \frac{\partial H'}{\partial \ell} = \frac{\ell}{J}, \quad \dot{\ell} = -\frac{\partial H'}{\partial \phi} = -J\omega_0^2 \sin \phi \left(1 - \frac{\ddot{\gamma}}{g}\right), \quad (9.2.12)$$

which can be combined to give a single second-order differential equation

$$\ddot{\phi} = -\omega_0^2 \sin \phi \left(1 - \frac{\ddot{\gamma}}{g}\right). \quad (9.2.13)$$

We now assume a periodic driving function

$$\gamma(t) = \gamma_0 \cos(\omega_D t) \quad \Rightarrow \quad \ddot{\gamma} = -\gamma_0 \omega_D^2 \cos(\omega_D t), \quad (9.2.14)$$

where ω_D is the driving frequency and γ_0 is the amplitude of the driving. By introducing the dimensionless parameters

$$\kappa = \left(\frac{\omega_0}{\omega_D} \right)^2, \quad \epsilon = \omega_D^2 \frac{\gamma_0}{g} = \frac{\gamma_0 \omega_0^2}{g \kappa}, \quad \tau = \omega_D t, \quad (9.2.15)$$

the equation of motion for the driven pendulum becomes

$$\ddot{\phi} = -\kappa \sin \phi (1 - \epsilon \cos \tau). \quad (9.2.16)$$

This vertically-driven pendulum is an interesting and complex chaotic system. In particular, note that the driving force is a function of position as well as a function of time. While this results in much interesting behaviour, it also makes this system more difficult to study as a first example. Therefore, we will return to this system later in this chapter (and the impatient might wish to read M. V. Bartuccelli, G. Gentile and K. V. Georgiou, "On the dynamics of a vertically driven damped planar pendulum", *Proc. R. Soc. Lond. A* 2001 **457**, 3007–3022), and look first at a simpler system, where the driving force is a function of time, but not position.

If, instead of a vertical force, we apply a force at right angles to the pendulum, we obtain an equation of motion

$$\ddot{\phi} = -\kappa \sin \phi + \epsilon \cos \tau. \quad (9.2.17)$$

A key advantage of first studying this simpler system is that it is easy to compare with the driven SHO, which has equation of motion

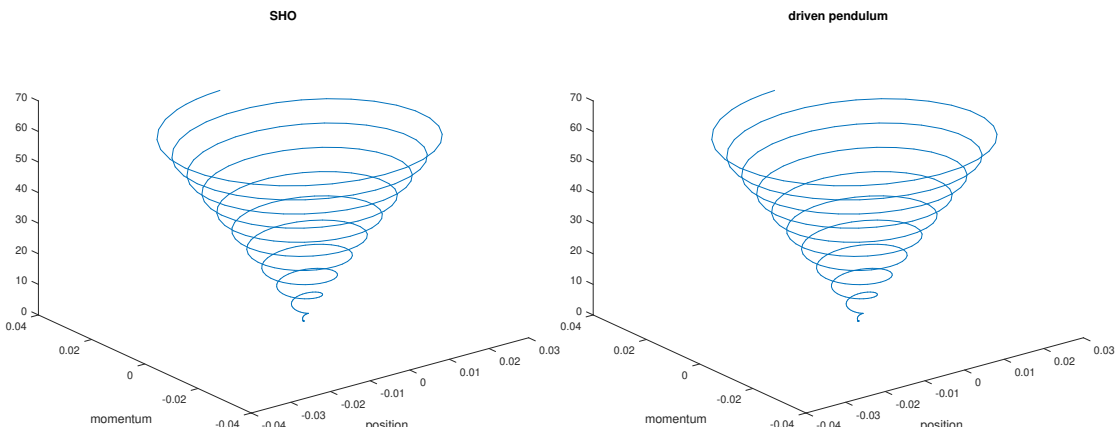
$$\ddot{\phi} = -\kappa \phi + \epsilon \cos \tau \quad (9.2.18)$$

whose solutions can be found exactly (and you have most likely seen before in your physics and maths studies).

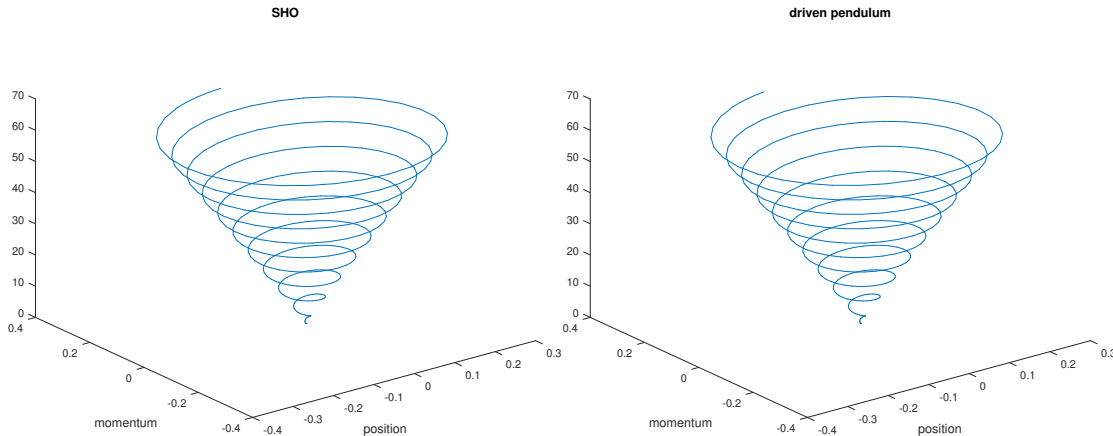
9.3 Behaviour of the driven pendulum

For convenience, we can choose $\kappa = 1$. Noting that for small oscillations, the frequency of the undriven pendulum is $\omega_0 = \sqrt{g/a}$, we can use this to choose the driving frequency ω_D . Let us begin with $\omega_D = \omega_0$.

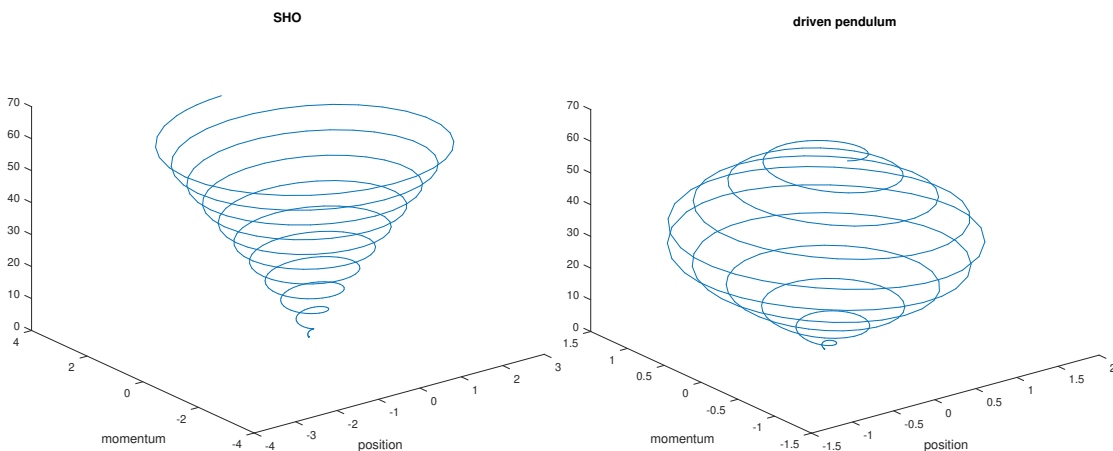
For a short time (10 periods) and weak driving ($\epsilon = 0.001$), we obtain very similar trajectories in our 3D phase space:



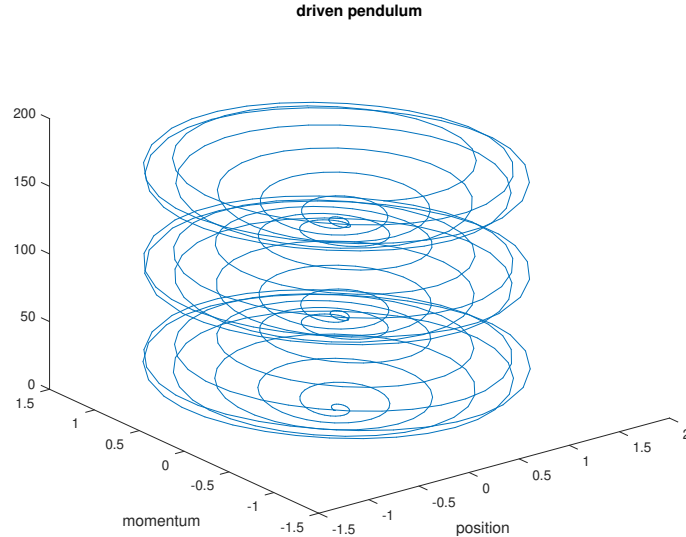
In both cases, we are adding energy to the system (which begins at $(0, 0)$), and the amplitude of the oscillation increases. Increasing the driving force to $\epsilon = 0.01$, we still obtain very similar results:



However, with a further increase to $\epsilon = 0.1$, we see a clear difference between the SHO and the pendulum:

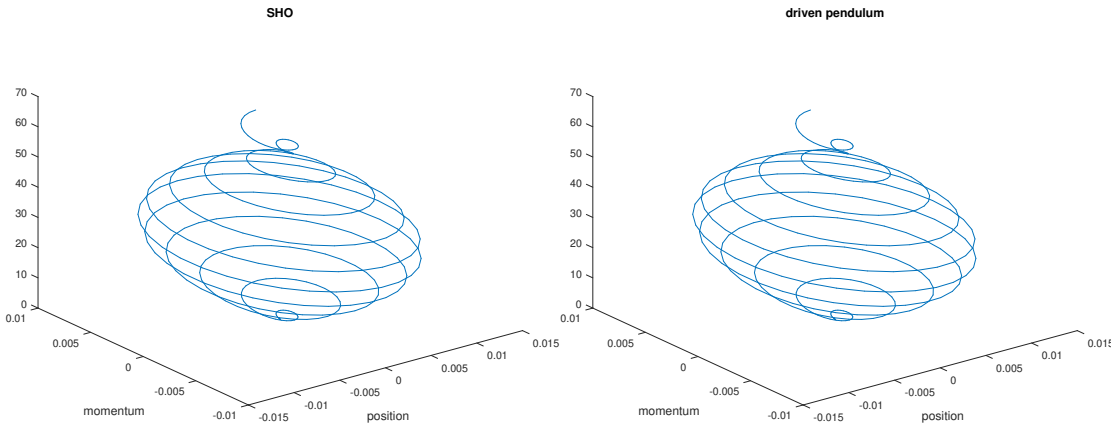


What has happened? This is a result of the non-linearity of the pendulum (and the linearity of the SHO). Since we chose $\omega_D = \omega_0$, the driving force was at the resonant frequency of the SHO, and for the pendulum at small amplitudes. However, since the oscillation frequency of the pendulum changes as the amplitude increases, the relative phase of the oscillation compared to the driving force changes once the amplitude becomes large, and the driving force will soon be out of phase with the oscillation, and will remove energy from the system rather than adding energy to the system. If we plot the path for a longer time (30 periods),

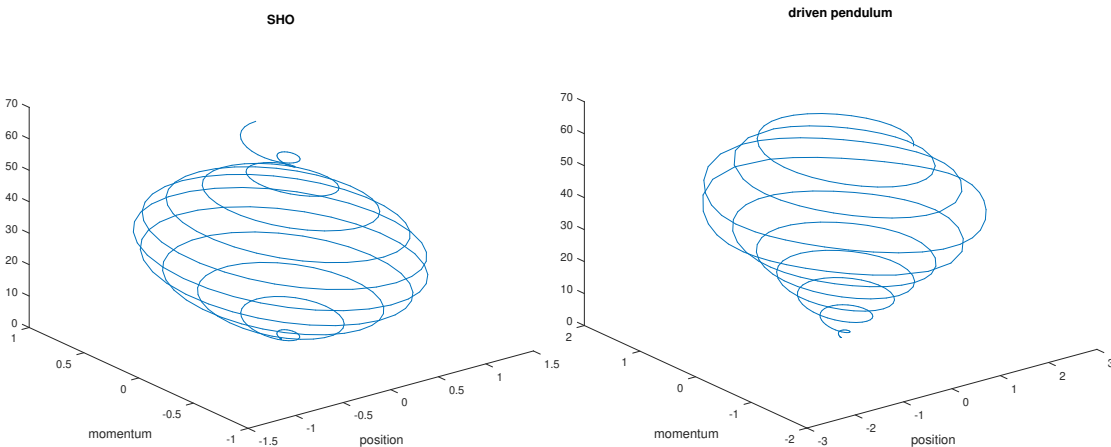


we can see that we cycle through adding and subtracting energy. Since the SHO is always resonantly driven when $\omega_D = \omega_0$, regardless of amplitude, we don't see this here.

Returning to $\epsilon = 0.001$, but with $\omega_D = 0.9\omega_0$, we can expect to see similar patterns of adding and subtracting energy in both the SHO and pendulum:

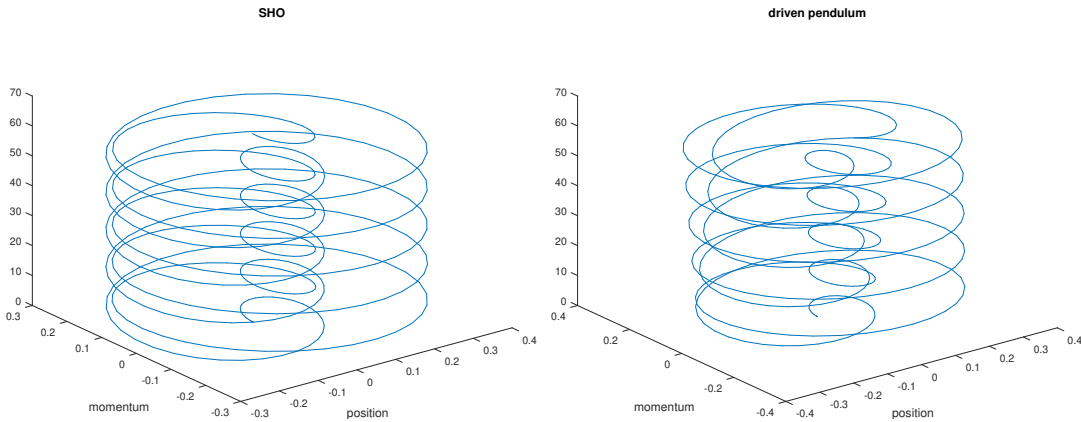


As long as the amplitude of oscillation remains small, the pendulum is very similar to the SHO. With $\epsilon = 0.1$ and $\omega_D = 0.9\omega_0$, we see differences in detail, but the overall behaviours are similar:

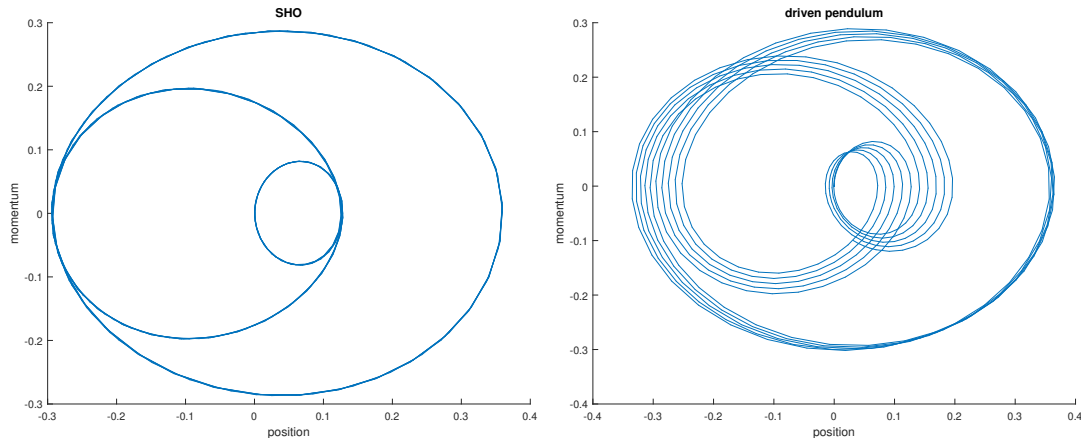


Moving further off resonance, to $\omega_D = (2/3)\omega_0$, with $\epsilon = 0.1$, we see similar

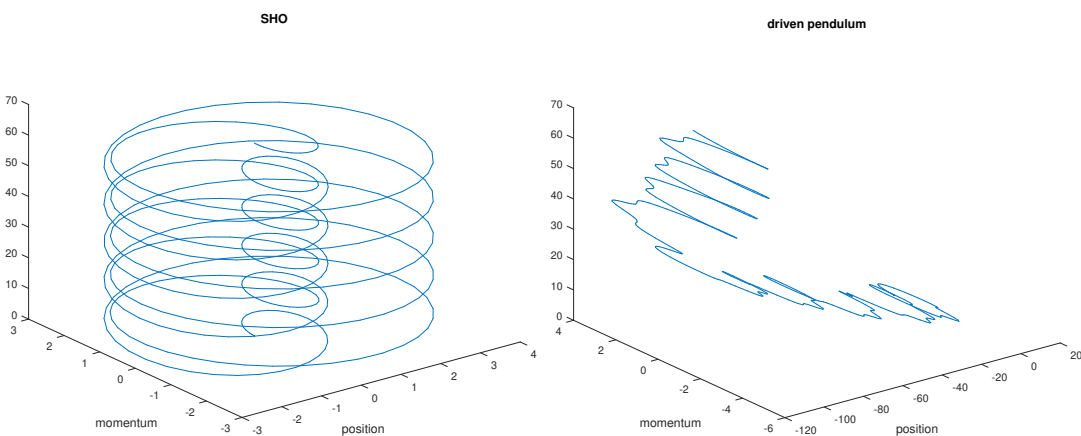
paths in 3D:



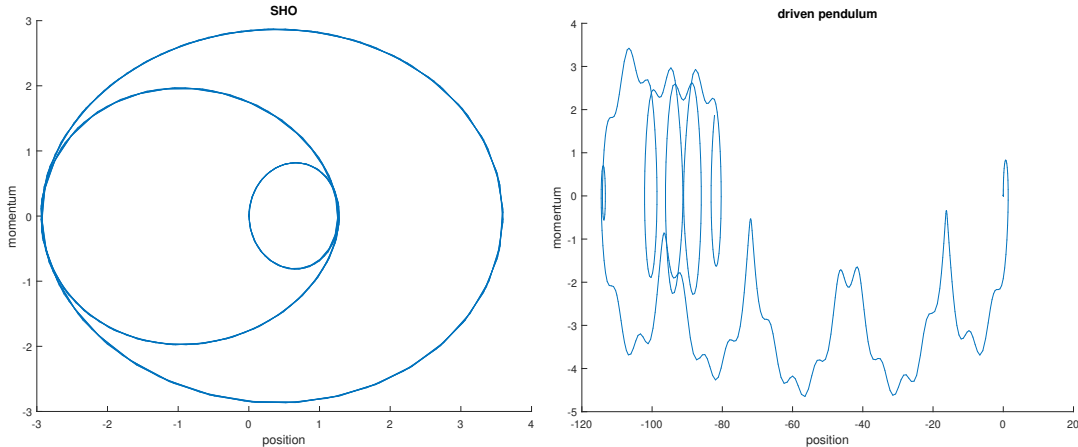
though if we project these onto our 2D position–momentum space, we see quite different behaviour. For the SHO, we have motion that appears to have period $3T$, as we expect (why?), but while the motion of the pendulum is almost periodic, it isn't periodic:



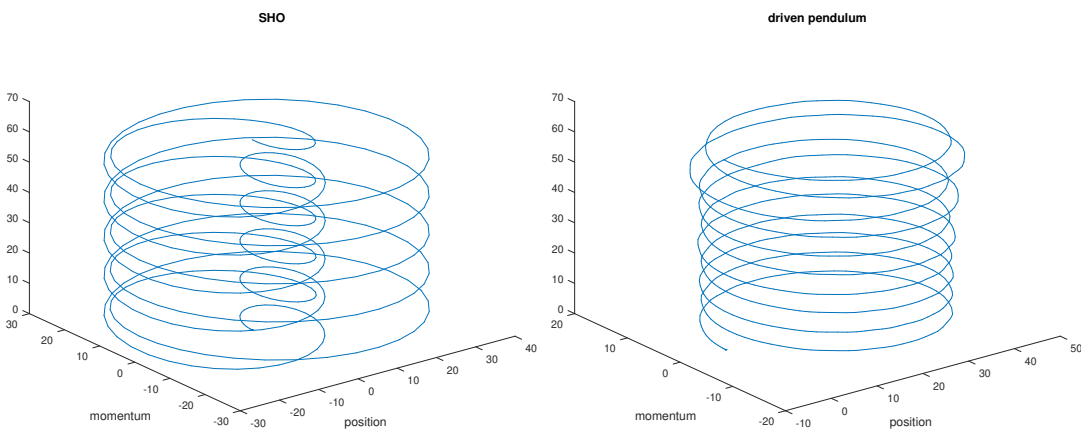
This is just the kind of thing we might look for when trying to find chaotic behaviour. Encouraged by this, let us try stronger driving, and set $\epsilon = 1$:



and projecting into our 2D space:



and we appear to have found chaotic behaviour. What if we increase the driving still further, to $\epsilon = 10$?



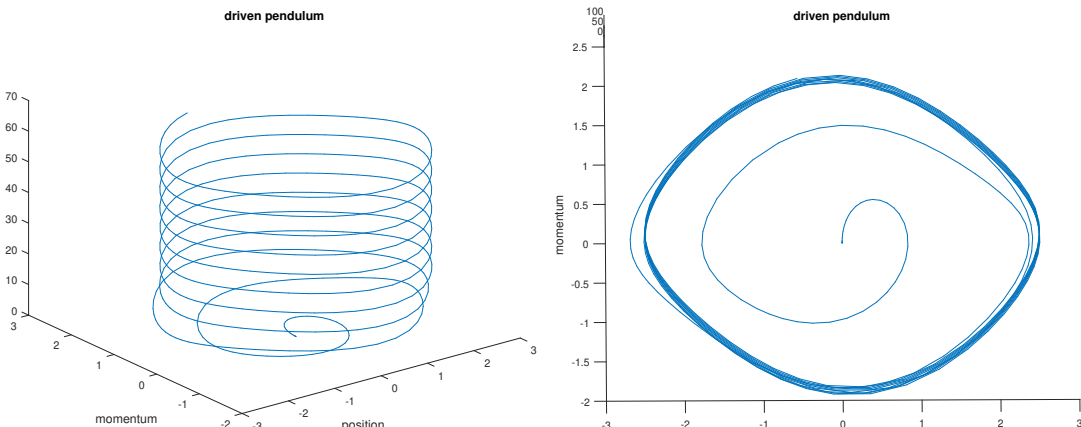
We find that while the SHO and pendulum behave differently—the SHO is behaving in the same way as before, as we expect from its linearity, and the pendulum is rotating rather than oscillating, which the SHO cannot do—our chaotic behaviour is gone.

9.4 Driven damped pendulum

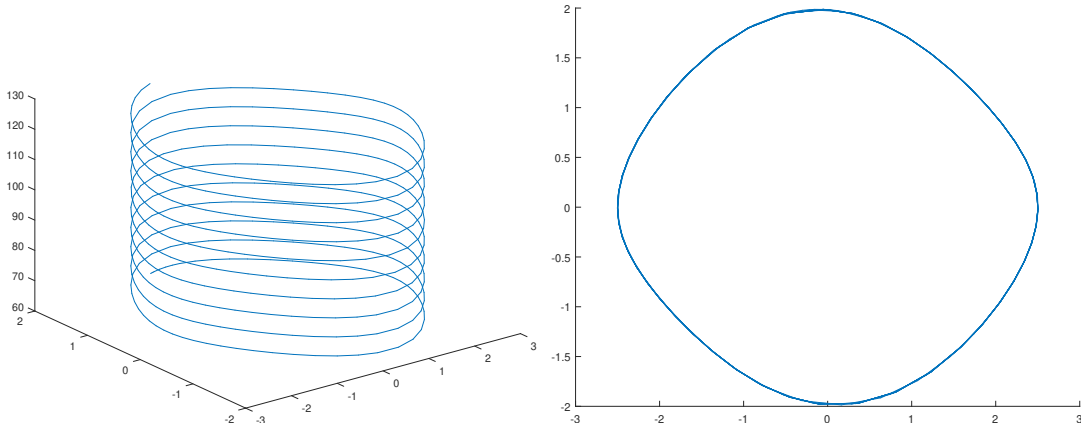
If we introduce a damping term, the equation of motion becomes

$$\ddot{\phi} = -d\dot{\phi} - \kappa \sin \phi + \epsilon \cos \tau. \quad (9.4.19)$$

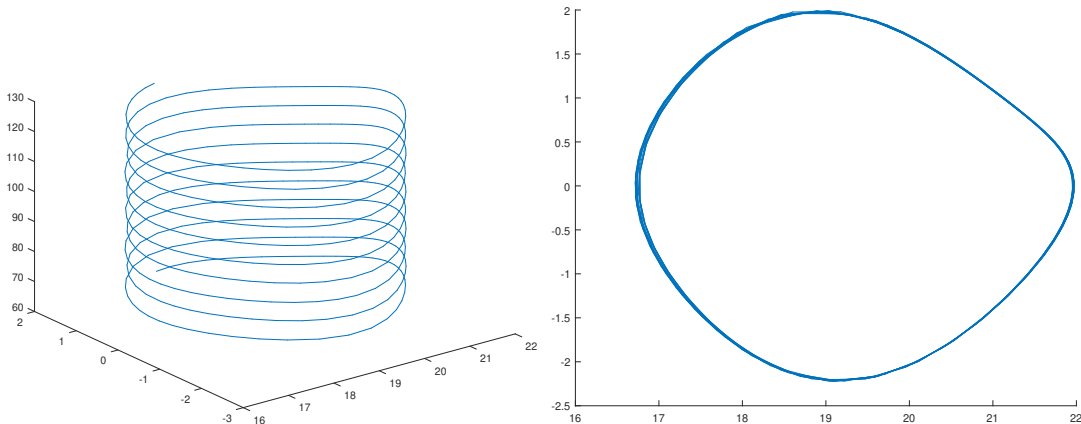
Choosing $\omega_D = (2/3)\omega_0$ as before, and $d = 1/2$, we can use a strong driving force, $\epsilon = 0.9$, and fail to obtain chaos:



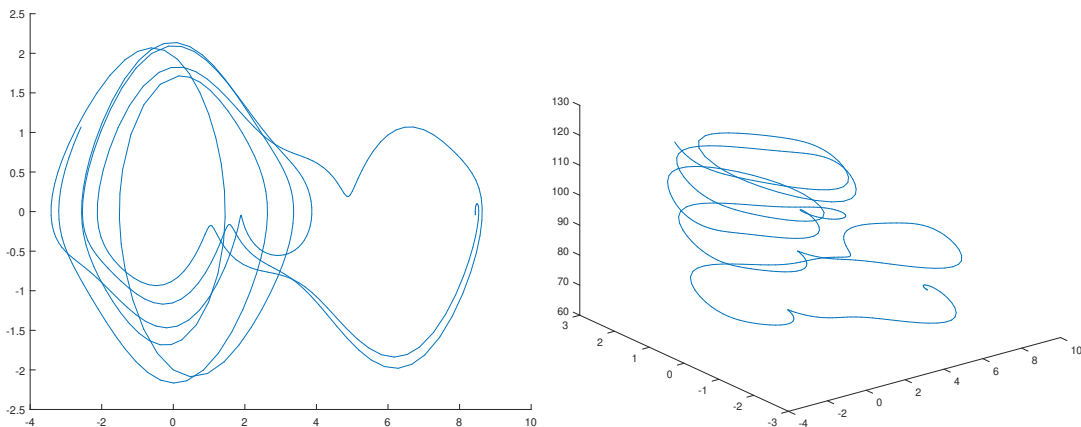
We can obtain a neater trajectory by calculating the path for 10 periods so that the pendulum has reached its steady-state behaviour, and then plotting a further 10 periods:



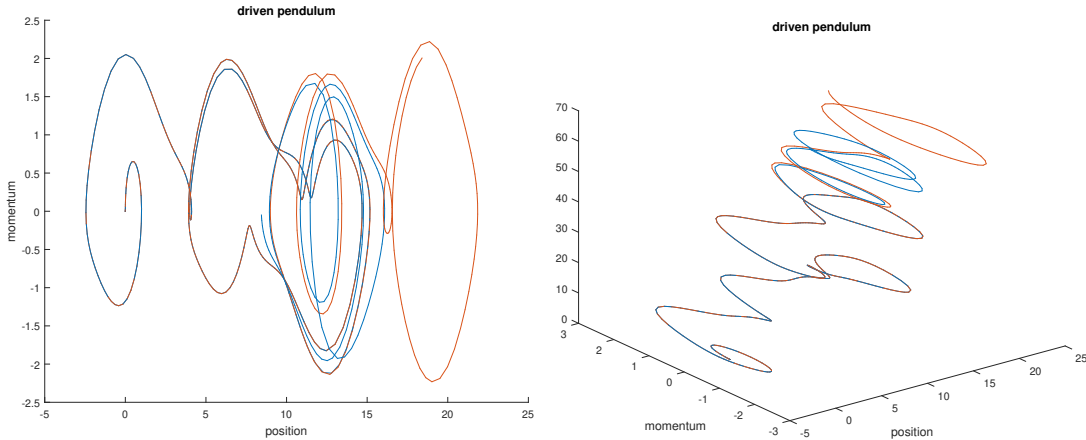
If we increase the driving force a little, to $\epsilon = 1.06303$, we see that the motion is no longer periodic with period T (it might be periodic with period $2T$, period doubling as we might see close to the onset of chaos, very similarly to the bifurcation pattern of the logistic map):



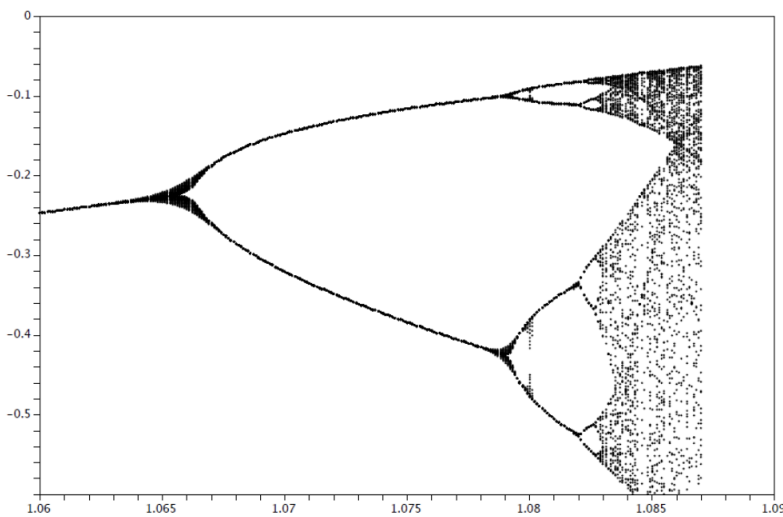
With a small further increase of the driving force, to $\epsilon = 1.07$, we have chaos:



It is useful to check that we have sensitivity to initial conditions, so we can compare two trajectories that initially begin close together:



It is indeed clear that the trajectories diverge. Interesting the transition to chaos can be seen (we don't discuss in detail but it is inspiring to see it) to possess a bifurcation structure absolutely analogue to the logistic map, see the following figure which describe a bifurcation pattern for the damped driven pendulum.



9.5 Recurrence plots and Poincaré sections

As we saw in the previous sections, the phase portraits for non-conservative Hamiltonian systems such as described by equation (9.2.16) can get extremely messy, as the trajectories are no longer curves with constant energy. This is clearly visible in Figure 9.1. While it was possible to plot 3D paths in our 3D phase space, these are not always easy to interpret.

Instead, it can be very useful to plot points in phase space that represent the system at a discrete moment in time. This is called a *recurrence plot*. Rather than projecting the entire 3D path onto our 2D (q, p) space, we collapse a stack of discrete "slices" of the 3D path onto our 2D space. Each of these slices will only contribute a single point to our recurrence plot. Generally, we choose times separated by some $\Delta\tau$. If there is some natural period T in the system, such as the period of the force driving a pendulum, it is conventional, and very useful, to choose $\Delta\tau = T$.

Recurrence plots of this type are often called a Poincaré section. While this is common, it is technically incorrect. A *Poincaré section* is a slice through a fixed position in *phase space* (we will see examples in the next chapter), whereas the recurrence plot is a slice through a fixed position in *time*. Unlike our time-slices in a

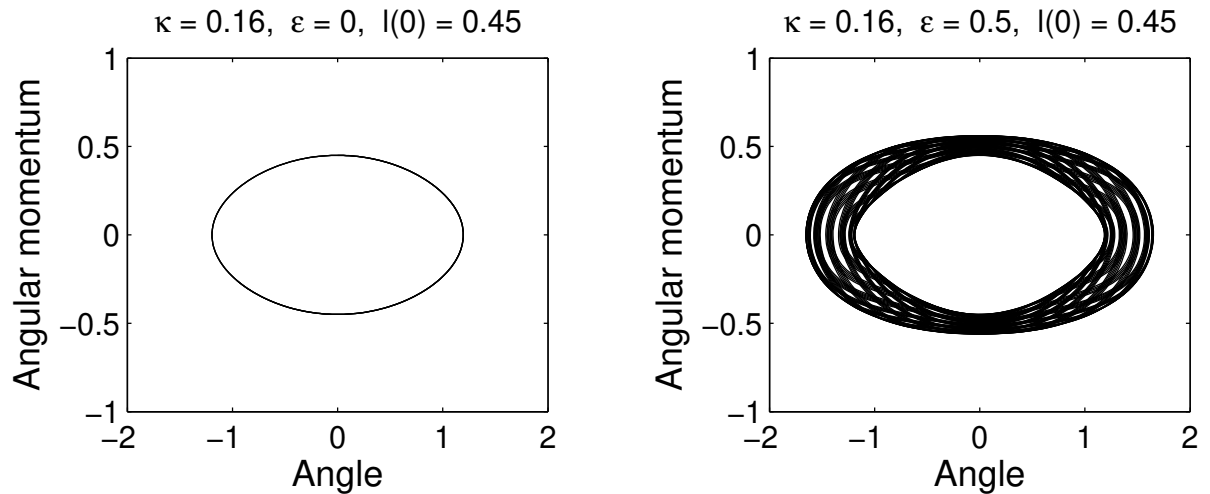


Figure 9.1: Phase portrait for a single trajectory of the pendulum: undriven (left) and driven (right).

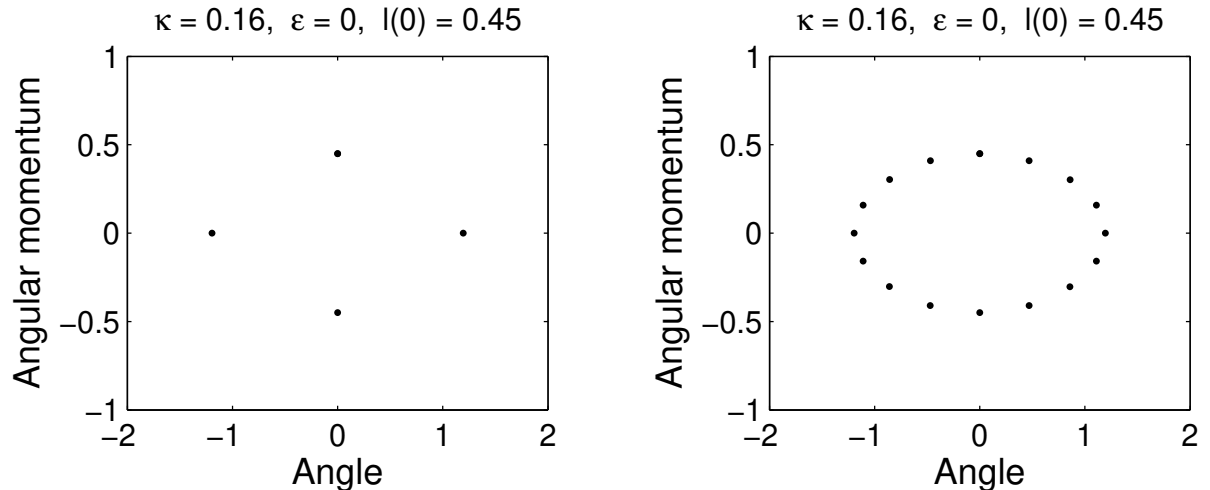


Figure 9.2: Example of recurrence plots: left $\Delta\tau = T/4$, right $\Delta\tau = T/16$.

recurrence plot, which each only contribute a single point, the Poincaré section—a single slice through phase space—contributes many points (usually).

However, Poincaré sections are closely related to recurrence plots. Consider how we might generate a Poincaré section in practice. As we calculate a path through the, e.g., 4-dimensional phase space of a 2-degree of freedom system, we can take a snapshot in time as the trajectory passes through some given value of one coordinate, say $\theta_2 = 0$, moving in a particular direction, say $p_{\theta_2} \geq 0$. This gives us a single point in our (θ_1, p_{θ_1}) sub-space. As we collapse a series of such snapshots in time into a single plot, we build up our Poincaré section. Thus, a Poincaré section can be considered to be a recurrence plot with the time-slices not necessarily uniformly spaced.

The trajectory on the left in Fig. 9.1 had a period $T = 2\pi/\omega(H)$. If we choose $\Delta\tau = T/4$ then only four points will appear. Likewise, if we choose $\Delta\tau = T/16$ then only sixteen points will appear. This is illustrated in Fig. 9.2

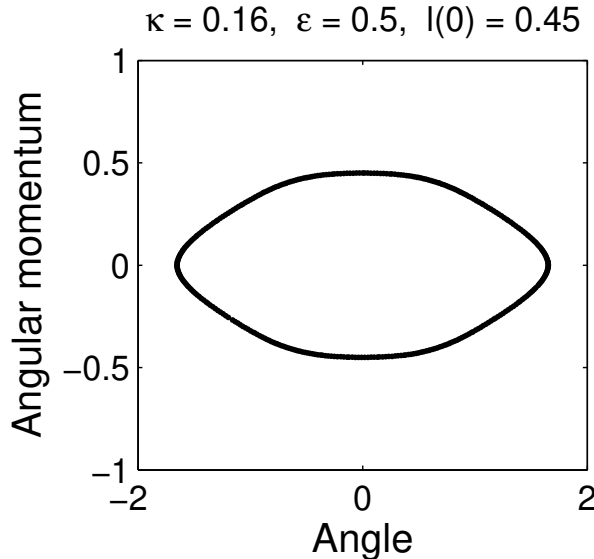


Figure 9.3: Recurrence plots for the same parameters as the trajectory on the right of Fig. 9.1, sampled at the driving frequency ω_D for 350 driving periods. This is a sufficient number of points to pretty much fill in the entire curve.

In general, if $\Delta\tau = \frac{m}{n}T$, where m, n are positive integers, then there will be at most n possible distinct points in phase space. However, if $\Delta\tau = \alpha T$, where α is any *irrational* number, then in the limit that $\tau \rightarrow \infty$ an infinite number of points will build up giving a solid line.

The recurrence plot can be viewed as subjecting the continuous trajectory in phase space to a *strobe* of frequency $\Omega = 2\pi/\Delta\tau$. We have

$$\frac{\Delta\tau}{T} = \frac{2\pi/\Omega}{2\pi/\omega(H)} = \frac{\omega(H)}{\Omega}. \quad (9.5.20)$$

If this is irrational, an infinite number of points will appear. Otherwise, there will be a finite number of points.

Recurrence plots are a very useful concept in the analysis of complicated systems, and we use it for the driven pendulum. It is a graphical representation of the mapping of the point (q_n, p_n) at time $\tau = n\Delta\tau$ to the point (q_{n+1}, p_{n+1}) , where we have $q_n = q(n\Delta\tau)$, $n = 0, 1, 2, \dots$, etc. This can also be written

$$(q_{n+1}, p_{n+1}) = T(q_n, p_n) \quad (9.5.21)$$

for an appropriate operator T , in a similar manner to the 1D maps that we looked at earlier. However, in this situation it is very hard or impossible to find a closed expression for T . Even in simplified cases, the study of 2D maps has shed remarkable clarity in the understanding of chaotic behaviour. We will not study this subject, but the connection with recurrence plots clearly indicates its usefulness.

In recurrence plots for driven systems we typically sample the system once every driving period, i.e. $\Omega = \omega_D$.

9.6 Irrational Recurrence Plots

We take the parameters $\ell(0) = 2/3$, $\kappa = 0.16$, and show what happens as the strength of the driving ϵ is increased. For these parameters we have $\omega_D/\omega(H) = 3.15853287332306$ which is close to being irrational (MATLAB shows that $10420/3299 = 3.15853288875417$ gets the first seven decimal places correct). Hence, the recurrence plot forms a closed curve for $\epsilon = 0$, as is shown in Fig. 9.4.

Note that the curves *remain closed* as ϵ increases. However, this suddenly breaks down above a certain ϵ and the motion becomes chaotic.

This is an important concept in dynamics: if $\omega(H)/\omega_D$ is irrational then for a sufficiently small perturbations ϵ the phase space trajectory remains a closed curve but is distorted. This is especially interesting when the frequency varies with energy and then different orbits can have rational or irrational ratios. The irrational ones play a very important role, they are the most stable orbits as indicated by the KAM theorem (one of the major results of classical dynamics of the 20th century).

KAM theorem (Kolmogorov, Arnold and Moser): “For sufficiently irrational surfaces and sufficiently weak perturbations, the surfaces of constant action are preserved under the perturbation and are not destroyed.”

This theorem, which we stated in a simplified and paraphrased way, has a quite broad scope: it does not refer to specific trajectories or time scales. It defines a type of global stability. The theorem holds for systems that are defined as perturbations of integrable hamiltonian systems. We will come back to the theorem in the next chapter.

9.7 Recurrence plots with rational frequencies

Here we take the initial parameters $\ell(0) = 0.58517059$, $\kappa = 0.16$ which have been chosen such that $\omega_D/\omega(H) = 3$. Hence for the undriven system with $\epsilon = 0$ we get three points only, as is shown in Fig. 9.5.

However, as soon as $\epsilon > 0$ the points become an island chain. This is certainly not a mere distortion. This is an example of a resonance, and is a typical feature of such systems. They play a crucial role in the transition to chaotic dynamics. Within the islands there still exist what are known as fixed points. However, eventually these break up as well when ϵ continues to get larger.

9.8 Transition to chaos

Finally we finish this section by giving an example of how a global recurrence plot changes as we increase the driving frequency. Look in detail at Figure 9.6. These recurrence plots were generated by solving Hamilton’s equations numerically for 500 driving periods, with a range of initial conditions with $\phi(0) = 0$ and $\ell(0)$ equally spaced from -3 to 3, with $\omega_D = 0.8\omega_0$, $\kappa = 1.5625$.

The unperturbed recurrence plot ($\epsilon = 0$) looks very similar to our previous phase portrait for the pendulum. An interesting and useful difference is that orbits with commensurable frequencies with the driving force have finite points while for incommensurable orbits we see almost continuous lines. As ϵ is increased, chaotic layers first appear near the separatrices. This is a typical behaviour for such systems. Separatrices are the most fragile orbits under pertur-

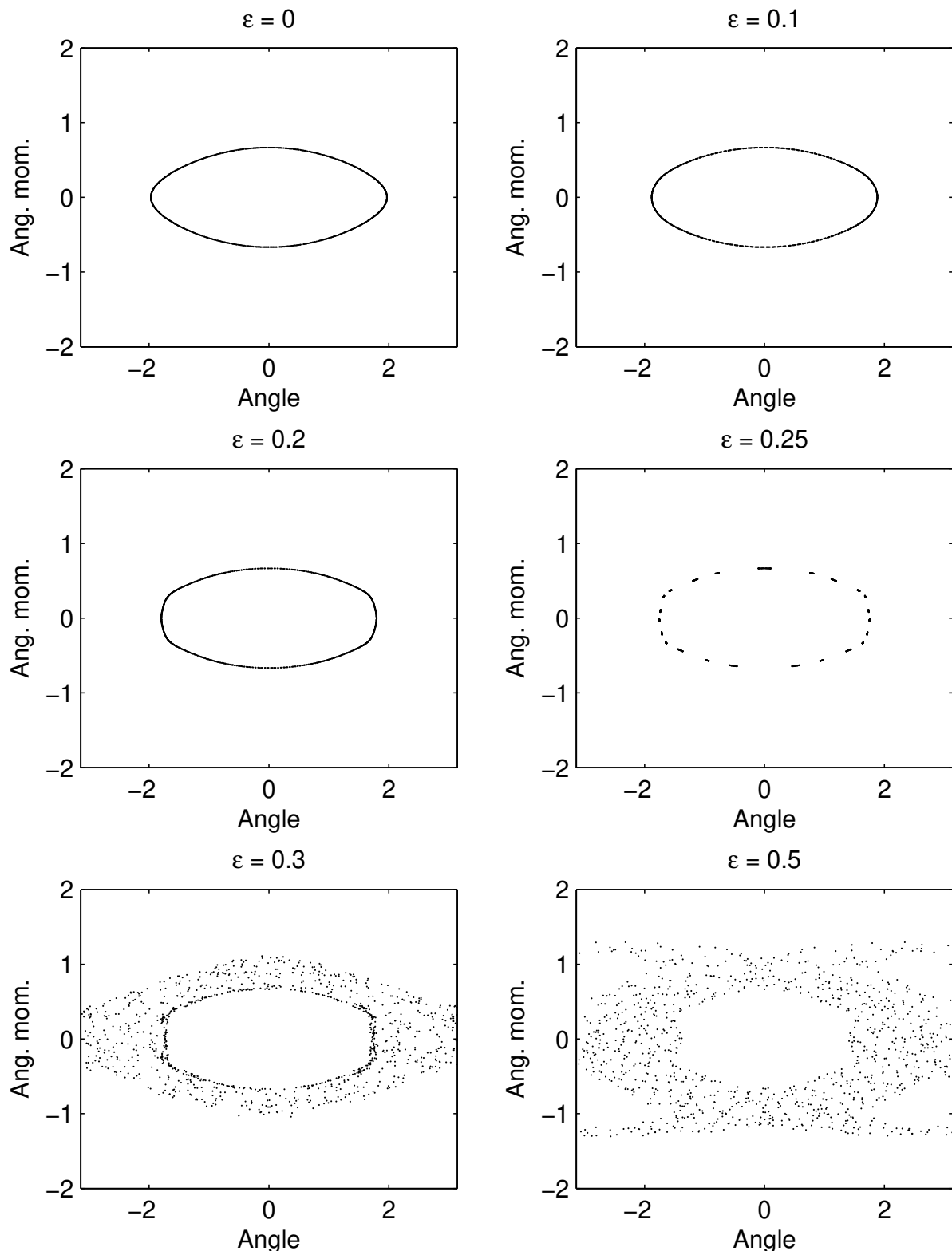


Figure 9.4: Recurrence plot for $\ell(0) = 2/3, \phi(0) = 0, \kappa = 0.16$ and a range of drive strengths ϵ as indicated.

bations. An important feature is that new islands of stability appear associated to resonances. As ϵ increases, the area of the chaotic region grows and secondary islands appear. From the figure it is also interesting to see the KAM theorem at work, some of the curves that first get destroyed are commensurable with the driving force, as it is indicated by the fact that they are described by a finite number of points in the recurrence plots.

9.9 Non-sinusoidal driving forces

We can study similar systems driven by non-sinusoidal driving forces. For the non-linear case, this will typically force us to resort to numerical solution. For the linear case (the driven SHO), it can be useful to express the force as a sum of components as

$$F(t) = \sum_n F_n(t) \quad (9.9.22)$$

If the driving force is periodic, the $F_n(t)$ are a Fourier series.

For the driven damped SHO, we have

$$m\ddot{x} + c\dot{x} + kx = F(t). \quad (9.9.23)$$

If we can solve the motion subject to driving by the individual $F_n(t)$ terms, we can obtain solutions $x_n(t)$ such that

$$m\ddot{x}_n + c\dot{x}_n + kx_n = F_n(t) \quad (9.9.24)$$

and our solution for driving by $F(t)$ is the superposition

$$x(t) = \sum_n x_n(t). \quad (9.9.25)$$

9.9.1 The restricted 3-body problem

One example of an interesting system with non-sinusoidal driving force is the restricted three body problem. We have three bodies moving about each other subject to gravitational attraction. Note that the two body problem is integrable but not the three body one. If the mass of one of the three bodies is much greater than those of the others, then we can assume that body is at rest. If the other two bodies are in initially circular orbits about the body at rest, they will perturb each other, due to their mutual gravitational force.

If one of the bodies has a mass much smaller than the other two, then its perturbation of the motion of the middle-mass body will be much smaller than the middle-mass body's perturbation of its motion. Therefore, the motion of the least massive body can be treated as a non-sinusoidally driven oscillator.

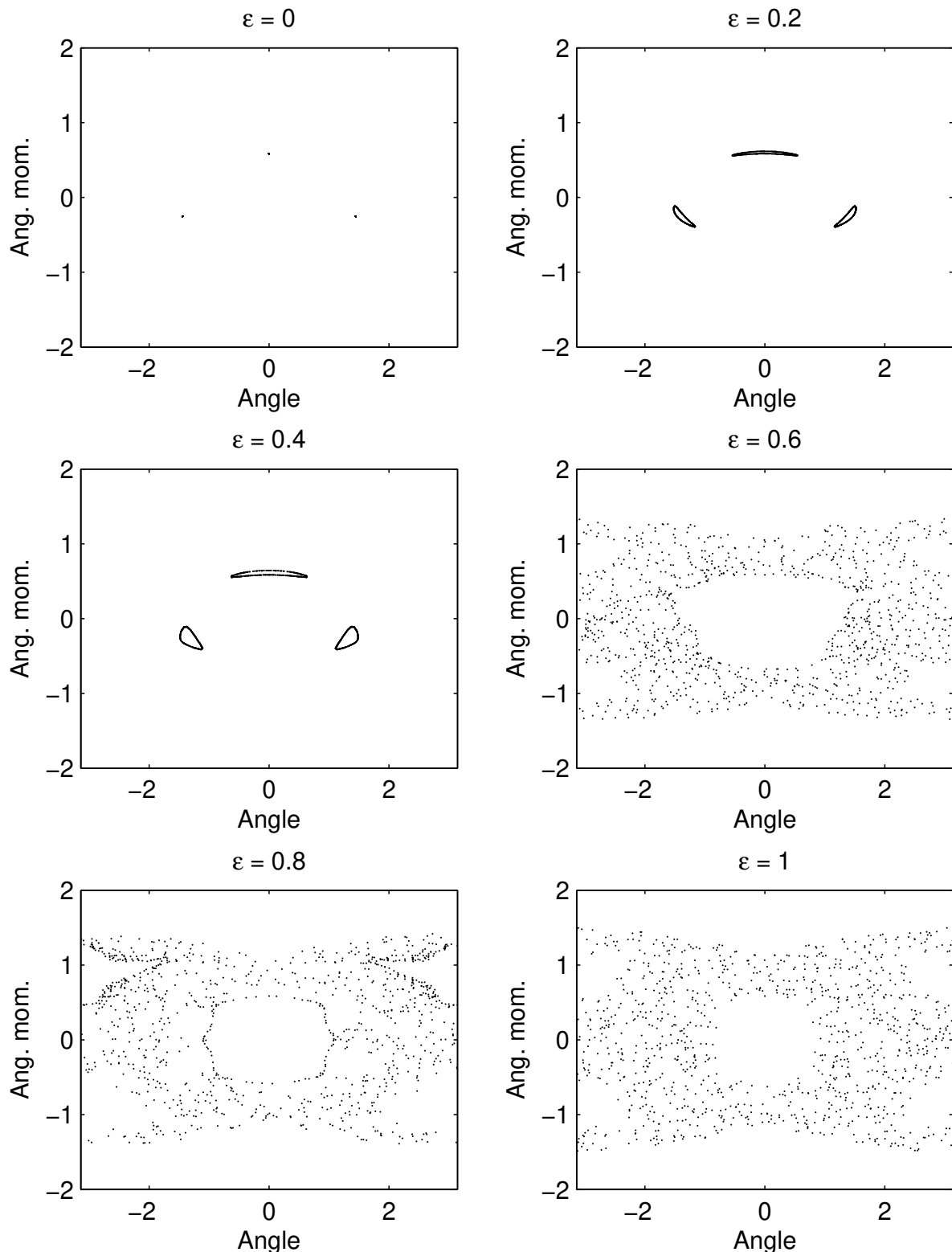


Figure 9.5: Recurrence plot for $\ell(0) = 0.58517059, \phi(0) = 0, \kappa = 0.16$ and a range of drive strengths ϵ as indicated.

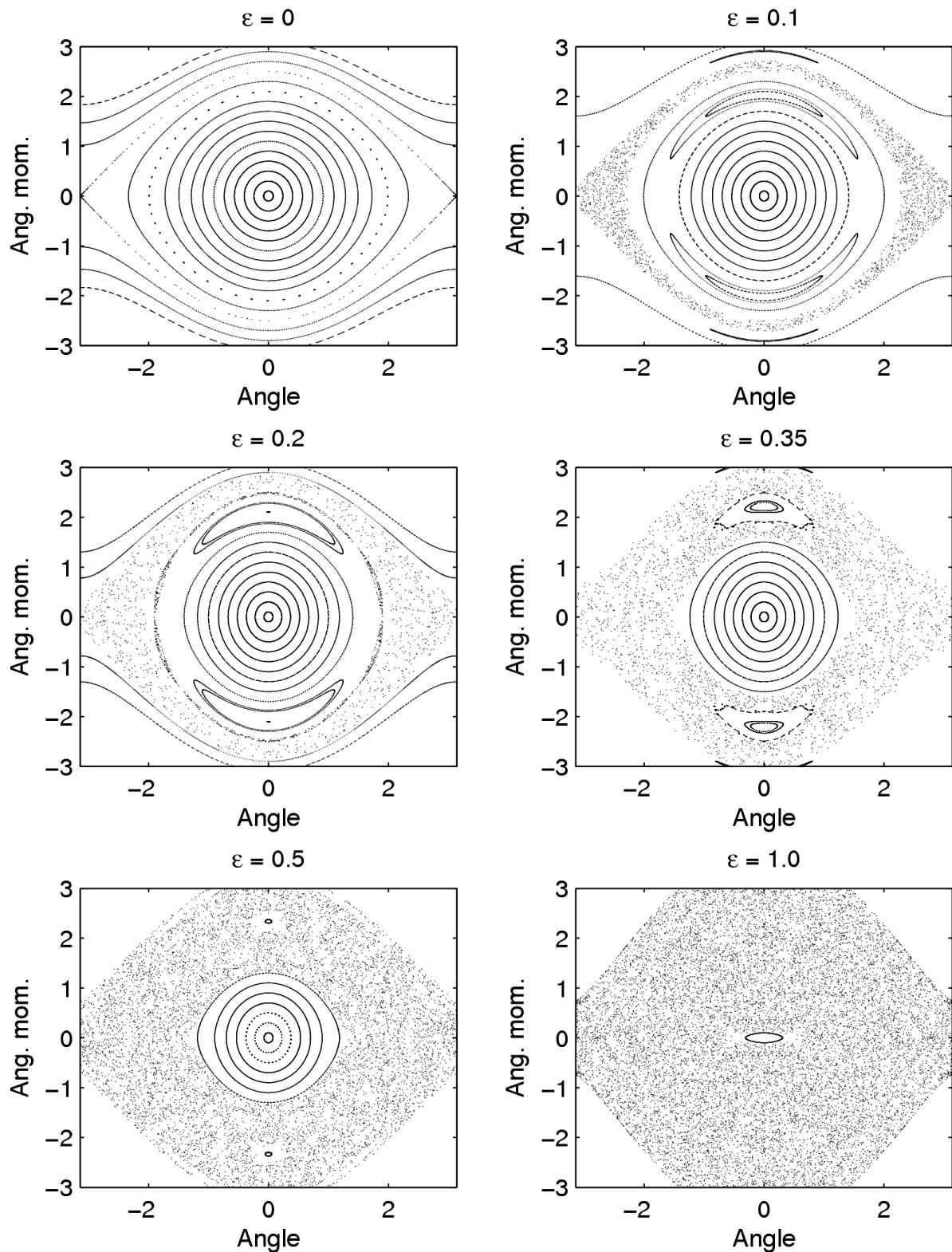


Figure 9.6: Recurrence plots for $\omega_D = 0.8\omega_0$, $\kappa = 1.5625$. The islands that appear on the top and bottom contain period-one fixed points. The chaos layer increases as ϵ is increased, and will eventually engulf the entire phase space.

CHAPTER 10

The double pendulum

An example of a conservative Hamiltonian system that exhibits chaotic dynamics is the double pendulum. This is shown in figure 10.1. The two pivot points are assumed to be frictionless, and the two masses are free to rotate in the vertical plane with gravity acting downwards.

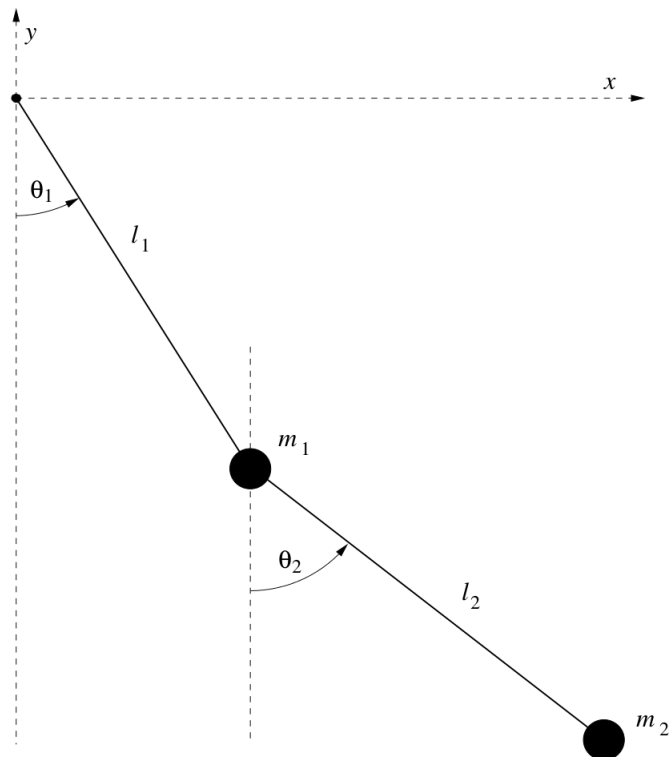


Figure 10.1: Double pendulum. Mass m_1 hangs at a distance l_1 from a central pivot, at an angle θ_1 from vertical. Mass m_2 hangs at a distance l_2 from mass m_1 , at an angle θ_2 from vertical.

Using the notation in Figure 10.1, we can write down the Cartesian coordinates of the two masses in terms of the angles θ_1 and θ_2 , which give holonomic constraints and reduces the dimensionality of the problem from four

(x_1, x_2, y_1, y_2) to two (θ_1, θ_2) :

$$\begin{aligned} x_1 &= l_1 \sin \theta_1, \\ x_2 &= l_1 \sin \theta_1 + l_2 \sin \theta_2, \\ y_1 &= -l_1 \cos \theta_1, \\ y_2 &= -l_1 \cos \theta_1 - l_2 \cos \theta_2. \end{aligned} \quad (10.0.1)$$

We can easily write down the Lagrangian $\mathcal{L} = T - V$ in Cartesian coordinates, from the kinetic energy T and potential energy V ,

$$T = \frac{m_1}{2}(\dot{x}_1^2 + \dot{y}_1^2) + \frac{m_2}{2}(\dot{x}_2^2 + \dot{y}_2^2), \quad (10.0.2)$$

$$V = m_1 g y_1 + m_2 g y_2. \quad (10.0.3)$$

This gives, in angular coordinates,

$$\begin{aligned} \mathcal{L} &= \frac{m_1 + m_2}{2} l_1^2 \dot{\theta}_1^2 + \frac{m_2}{2} l_2^2 \dot{\theta}_2^2 + m_2 l_1 l_2 \dot{\theta}_1 \dot{\theta}_2 \cos(\theta_1 - \theta_2) \\ &\quad + (m_1 + m_2) g l_1 \cos \theta_1 + m_2 g l_2 \cos \theta_2. \end{aligned} \quad (10.0.4)$$

The Euler–Lagrange equations for the coordinates θ_1 and θ_2 are

$$\frac{d}{dt} \left(\frac{\partial \mathcal{L}}{\partial \dot{\theta}_n} \right) = \frac{\partial \mathcal{L}}{\partial \theta_n}. \quad (10.0.5)$$

Hence the two equations of motion are

$$(m_1 + m_2) l_1^2 \ddot{\theta}_1 + m_2 l_1 l_2 \cos(\theta_1 - \theta_2) \ddot{\theta}_2 = -m_2 l_1 l_2 \sin(\theta_1 - \theta_2) \dot{\theta}_2^2 - (m_1 + m_2) g l_1 \sin \theta_1 \quad (10.0.6)$$

for θ_1 , and

$$m_2 l_2^2 \ddot{\theta}_2 + m_2 l_1 l_2 \cos(\theta_1 - \theta_2) \ddot{\theta}_1 = m_2 l_1 l_2 \sin(\theta_1 - \theta_2) \dot{\theta}_1^2 - m_2 g l_2 \sin \theta_2 \quad (10.0.7)$$

for θ_2 .

10.1 Small oscillations

From the equations of motion, we can see immediately that the fixed points of the motion (with $\ddot{\theta}_i = 0$ and $\dot{\theta}_i = 0$) occur at $\sin \theta_1 = \sin \theta_2 = 0$. Hence there are fixed points at $\theta_i = 0, \pm\pi$. From what we know about the single pendulum, we expect that the fixed point at $\theta_i = 0$ will be stable (elliptic). We can proceed to prove this.

We Taylor-expand our equations of motion to first order about $\theta_i = 0$. This gives two coupled equations,

$$(m_1 + m_2) l_1^2 \ddot{\theta}_1 + m_2 l_1 l_2 \ddot{\theta}_2 = -(m_1 + m_2) g l_1 \theta_1 \quad (10.1.8)$$

$$m_2 l_2^2 \ddot{\theta}_2 + m_2 l_1 l_2 \ddot{\theta}_1 = -m_2 g l_2 \theta_2. \quad (10.1.9)$$

We may express this in matrix form as

$$M \begin{pmatrix} \ddot{\theta}_1 \\ \ddot{\theta}_2 \end{pmatrix} = -K \begin{pmatrix} \theta_1 \\ \theta_2 \end{pmatrix}, \quad (10.1.10)$$

where

$$M = \begin{pmatrix} (m_1 + m_2)l_1^2 & m_2 l_1 l_2 \\ m_2 l_1 l_2 & m_2 l_2^2 \end{pmatrix} \quad (10.1.11)$$

and

$$K = \begin{pmatrix} (m_1 + m_2)gl_1 & 0 \\ 0 & m_2 gl_2 \end{pmatrix}. \quad (10.1.12)$$

We wish to find a new set of coordinates for which the matrices are diagonal. Then the matrix equation has the form of a simple harmonic oscillator. We seek solutions

$$\begin{pmatrix} \theta_1 \\ \theta_2 \end{pmatrix} = \begin{pmatrix} A_1 \\ A_2 \end{pmatrix} \cos(\omega t + \varphi) = A \cos(\omega t + \varphi). \quad (10.1.13)$$

We may then express the equations of motion in matrix form as

$$(-\omega^2 M + K)A = 0. \quad (10.1.14)$$

This is satisfied when

$$\det(K - \omega^2 M) = 0 \quad (10.1.15)$$

and leads to an equation quartic in the frequency ω ,

$$m_1 l_1 l_2 \omega^4 - (m_1 + m_2)g(l_1 + l_2)\omega^2 + (m_1 + m_2)g^2 = 0. \quad (10.1.16)$$

Simplifying to the case when $l_1 = l_2 = l$ and $m_1 = m_2 = m$, we obtain the frequencies

$$\omega_{1,2}^2 = \frac{g}{l}(2 \pm \sqrt{2}). \quad (10.1.17)$$

These frequencies correspond to the so-called *normal modes*. Substituting these frequencies back into the matrix equation, the eigenvectors corresponding to the normal modes may be found. The low-frequency mode corresponds to the two masses moving in phase, and the high-frequency mode has the two masses moving out of phase. Every linearised solution will be a linear combination of the two normal modes. The stability of the $\theta_i = 0$ fixed point simply arise from the elliptic fixed nature of the two decoupled normal modes. Similar analysis can be performed for the other fixed points where it is not too difficult to rigorously prove that the other configurations are all unstable.

10.2 Hamilton's Equations

To derive the Hamiltonian from the Lagrangian, we use

$$H = \sum_i \dot{q}_i p_i - \mathcal{L} \quad (10.2.18)$$

where q_i is the generalized coordinate, and the corresponding generalized momentum p_i is

$$p_i = \frac{\partial \mathcal{L}}{\partial \dot{q}_i}. \quad (10.2.19)$$

Hence we can find our generalized momenta for the double-pendulum,

$$p_{\theta_1} = \frac{\partial \mathcal{L}}{\partial \dot{\theta}_1} = (m_1 + m_2)l_1^2 \dot{\theta}_1 + m_2 l_1 l_2 \dot{\theta}_2 \cos(\theta_1 - \theta_2), \quad (10.2.20)$$

$$p_{\theta_2} = \frac{\partial \mathcal{L}}{\partial \dot{\theta}_2} = m_2 l_2^2 \dot{\theta}_2 + m_2 l_1 l_2 \dot{\theta}_1 \cos(\theta_1 - \theta_2). \quad (10.2.21)$$

We need to express the velocities as a function of the momenta,

$$\dot{\theta}_1 = \frac{l_2 p_{\theta_1} - l_1 p_{\theta_2} \cos(\theta_1 - \theta_2)}{l_1^2 l_2 [m_1 + m_2 \sin^2(\theta_1 - \theta_2)]}, \quad (10.2.22)$$

$$\dot{\theta}_2 = \frac{l_1 (m_1 + m_2) p_{\theta_2} - l_2 m_2 p_{\theta_1} \cos(\theta_1 - \theta_2)}{l_1 l_2^2 m_2 [m_1 + m_2 \sin^2(\theta_1 - \theta_2)]}. \quad (10.2.23)$$

Hence the Hamiltonian is

$$\begin{aligned} H &= \dot{\theta}_1 p_{\theta_1} + \dot{\theta}_2 p_{\theta_2} - \mathcal{L} \\ &= \frac{m_2 l_2^2 p_{\theta_1}^2 + (m_1 + m_2) l_1^2 p_{\theta_2}^2 - 2m_2 l_1 l_2 p_{\theta_1} p_{\theta_2} \cos(\theta_1 - \theta_2)}{2l_1^2 l_2^2 m_2 [m_1 + m_2 \sin^2(\theta_1 - \theta_2)]} \end{aligned} \quad (10.2.24)$$

$$-(m_1 + m_2) g l_1 \cos \theta_1 - m_2 g l_2 \cos \theta_2. \quad (10.2.25)$$

We can now write down Hamilton's equations of motion for this system,

$$\dot{p}_{\theta_1} = -\frac{\partial H}{\partial \theta_1} = \frac{\partial T}{\partial \theta_1} - (m_1 + m_2) g l_1 \sin \theta_1 \quad (10.2.26)$$

$$\dot{p}_{\theta_2} = -\frac{\partial H}{\partial \theta_2} = \frac{\partial T}{\partial \theta_2} - m_2 g l_2 \sin \theta_2 \quad (10.2.27)$$

where T is the kinetic energy part of the Hamiltonian. Note that this term depends on the generalized coordinates only through $\cos(\theta_1 - \theta_2)$. Hence we have

$$\begin{aligned} \frac{\partial T}{\partial \theta_1} &= -\frac{\partial T}{\partial \theta_2} \\ &= \frac{\sin(2\theta_1 - 2\theta_2) [m_2 l_2^2 p_{\theta_1}^2 + (m_1 + m_2) l_1^2 p_{\theta_2}^2 - 2m_2 l_1 l_2 p_{\theta_1} p_{\theta_2} \cos(\theta_1 - \theta_2)]}{l_1 + l_2 [m_1 + m_2 \sin^2(\theta_1 - \theta_2)]}. \end{aligned} \quad (10.2.28)$$

10.3 Poincaré sections

This is as far as we can get for the full equations—except for trivial rearrangements they do not simplify any further. Hence we need to use numerical solutions to investigate further. Because the phase space is 4-dimensional, it is hard to visualize. Instead, it is useful to look at what is known as a *Poincaré section*, which is a two-dimensional slice through the phase space where the trajectory passes through some given value of one coordinate, say $\theta_2 = 0$, moving in a particular direction, say $p_{\theta_2} \geq 0$. We have already mentioned Poincaré sections in the previous chapter and here they will play an important role. Due to energy conservation, the trajectories of the double pendulum lie on a 3-dimensional hypersurface in the four dimensional phase space. We then project down to two dimensions taking an appropriate Poincaré section. Once more, because the total energy is conserved, one coordinate is redundant since we can express it as a function of the other 3 coordinates plus the total energy. So we do not need to plot p_{θ_2} .

There are several simulators for solving the double pendulum available on the internet; a particularly good one is from the Open Source Physics site:
<http://www.opensourcephysics.org/items/detail.cfm?ID=9384>

10.3.1 Low energy

A Poincaré section for low energy ($E = 1\text{J}$, in SI units, with $l_1 = l_2 = 1\text{m}$, $m_1 = m_2 = 1\text{kg}$) appears in Figure 10.2. We can see curves through phase space that correspond to tori through phase space. In fact the angle coordinates describe a two dimensional torus and in the low-energy limit the system is equivalent to two independent simple harmonic oscillators whose dynamics is integrable. Fixed the two action variables of the SHO, the dynamics lies on a 2D torus equivalent to the orbits portrayed in Figure 4.5. In Figure 10.2 the ratio of the frequencies of the normal modes is irrational—the curves fill the surface of a torus, which projects onto a closed curve in $(\theta_1, \dot{\theta}_1)$ space. We can see the locations of the two normal modes, where θ_1 and $\dot{\theta}_1$ are locked together (either in phase or opposite phase).

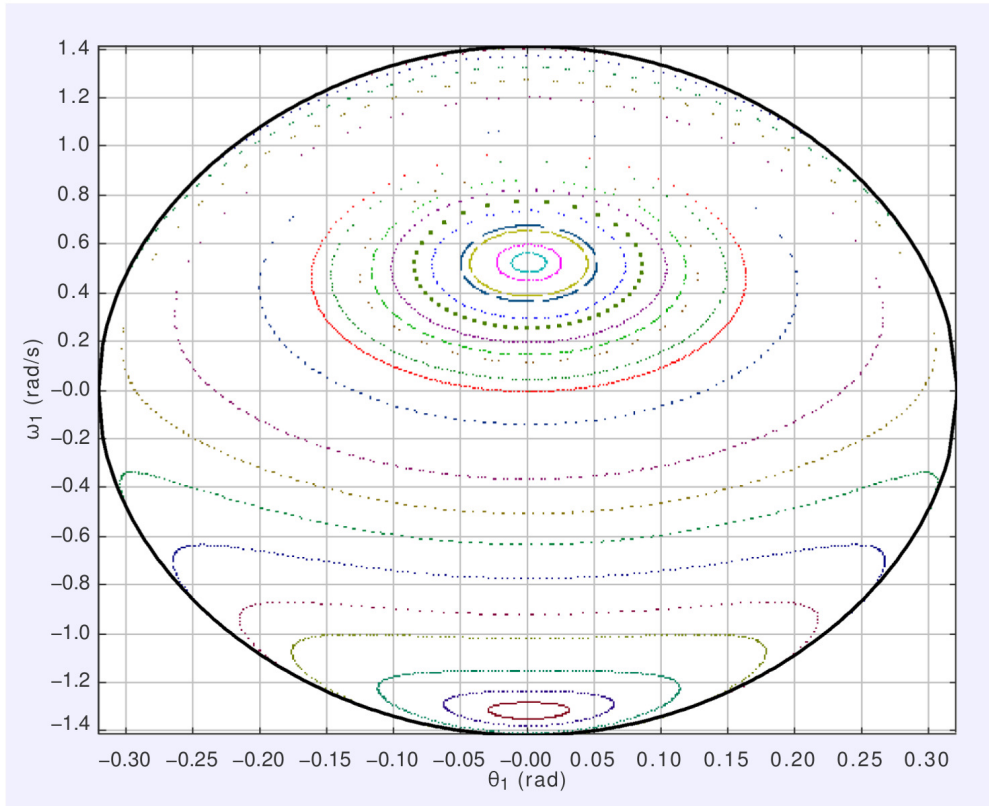


Figure 10.2: Poincaré section for the double pendulum at low energy.

10.3.2 Mid-range energy

As the energy is increased ($E = 8\text{J}$), we can see that the Poincaré section has broken into many different pieces. Most of the orbits are still periodic, but the behavior has become a lot more complicated. Some orbits appear to have no periodic structure, but fill out a region of phase space. Islands of stability appear in place of resonant (rational) orbits in a fashion completely analogue to the driven pendulum. The role of the driving amplitude ϵ is played here by the total energy of the system. For low-energy the system is integrable and described by two SHO. With higher-energy non-linearities kick in and the system can be considered as a deformation of the SHO.

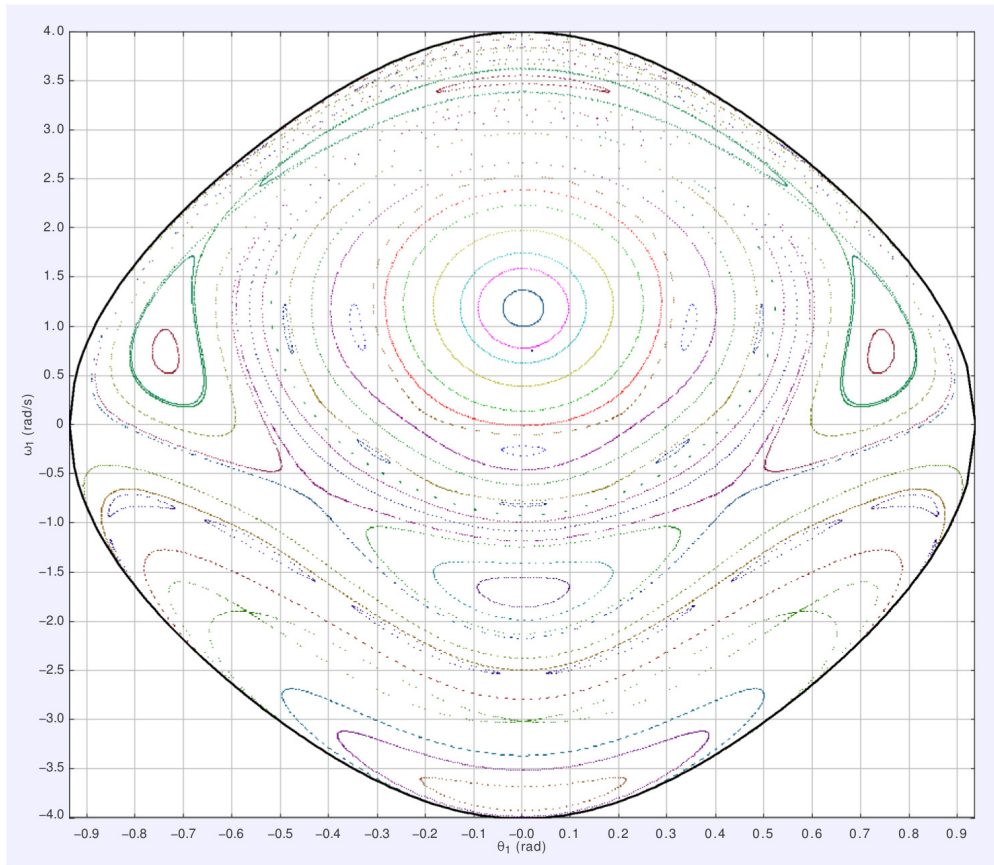


Figure 10.3: Poincaré section for the double pendulum at energy $E = 8\text{J}$. The orbits are mostly periodic, but with a complicated structure.

10.3.3 Higher energy

If the energy is increased even more, say to $E = 15\text{J}$, then we see almost no periodic structure. Almost all trajectories are chaotic. But there are still several regions of the phase space where periodic orbits may be found. For very large energy, $E = 500\text{J}$, in the regime of rotations, the orbits are again mostly periodic, but still some regions of chaos can be found.

10.4 KAM Theorem

The behaviour of the double pendulum is quite complex. As the energy is increased, the invariant tori in phase space tend to break up, either into discrete segments, or new tori emerge.

The reason for this behaviour can be explained by considering what happens when we perturb an orbit by a non-linear perturbation to the Hamiltonian,

$$H = H_0(I_n) + \epsilon H_1(I_n, \Theta_n). \quad (10.4.29)$$

Here $H_0(I_n)$ is the hamiltonian of an integrable system, for instance the pair of two SHO, where (Θ_n, I_n) are the set of action-angle variables of the integrable hamiltonian H_0 which for convenience we have expressed directly as a function of the action variables only (do not confuse Θ_n with the θ_i of the double pendulum since the latter are angles but not the ones of the action-angle of the double

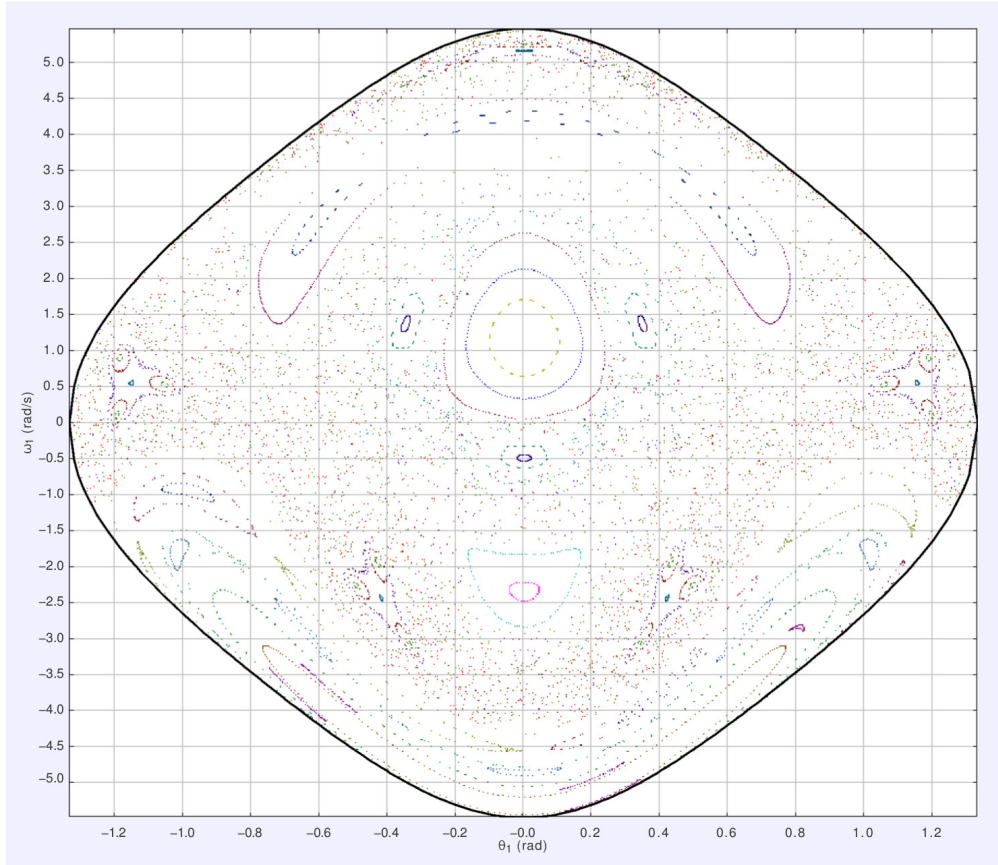


Figure 10.4: Poincaré section for the double pendulum at higher energy, $E = 15\text{J}$. Almost all orbits are chaotic.

harmonic oscillator). Suppose we represent one iteration of the Poincaré section by an operator T ,

$$T(\theta_n, p_n^\theta) \rightarrow (\theta_n, p_n^\theta). \quad (10.4.30)$$

After s iterations, we can get periodic behaviour where $\theta_{n+s} = \theta_n$, and with rational winding numbers the tori will be broken into discrete segments. For irrational winding numbers, then we get closed islands of stability.

As the tori break up into pieces, we get many hyperbolic (unstable) fixed points emerging. Perturbations will tend to mix nearby stable and unstable trajectories, causing the perturbed system to be unstable.

The general behaviour of Hamiltonian systems with non-linear perturbations can be summarized by the KAM Theorem (named for Kolmogorov–Arnold–Moser) which we mentioned already in the previous chapter. This theorem (paraphrased...) implies that

- Most tori remain for a small perturbation.
- The set of remaining tori occupy a finite region of phase space.
- The tori that break first have rational winding numbers.
- The last to break are the ‘most irrational’.

What do we mean by ‘most irrational’? For any irrational number s , there is a rational approximation,

$$\left| s - \frac{p}{q} \right| < \frac{1}{q}, \quad (10.4.31)$$

which improves as q increases. For irrational numbers this upper bound in the approximation can typically be improved to some $1/Kq^n$ factors. The idea of

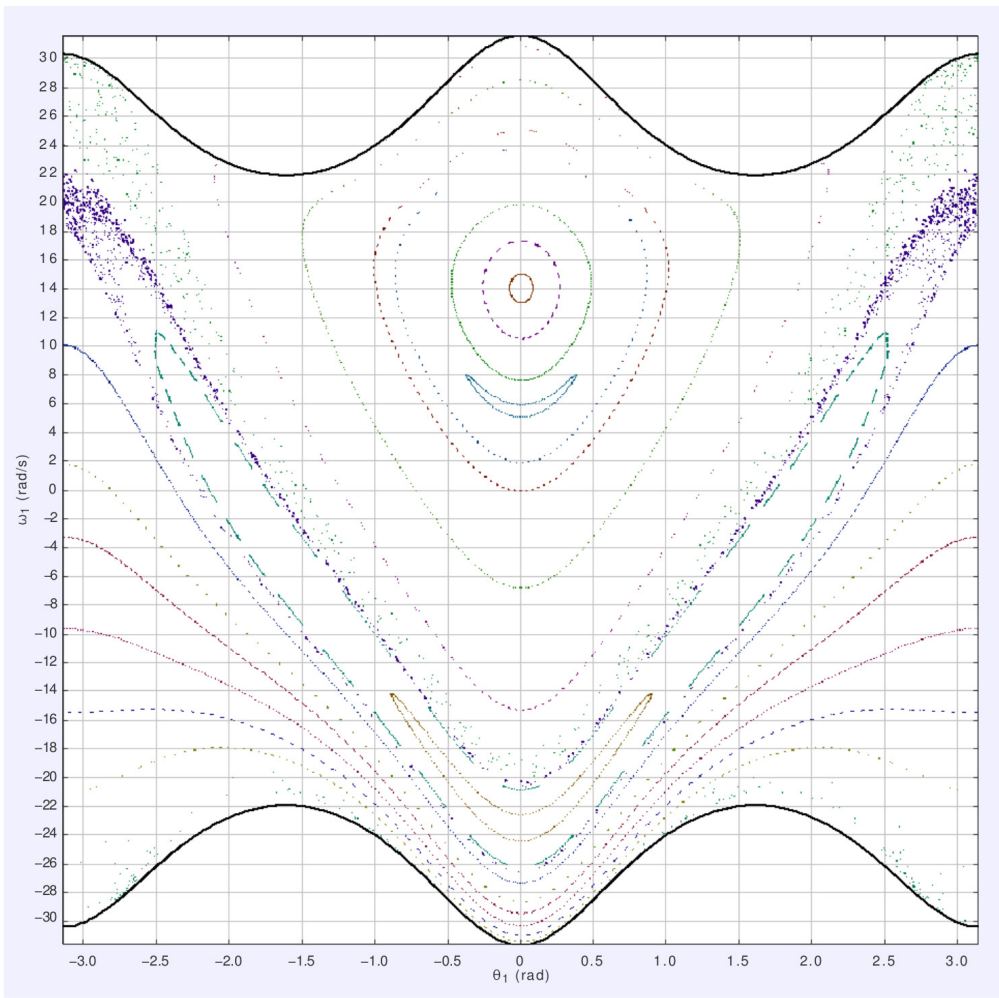


Figure 10.5: Poincaré section for the double pendulum at very high energy, $E = 500\text{J}$. Almost all orbits are periodic again, but there are some regions of chaos.

irrational approximation can be represented by the continued fraction expansion,

$$s = a_0 + \frac{1}{a_1 + \frac{1}{a_2 + \frac{1}{a_3 + \dots}}} \quad (10.4.32)$$

Truncating this expression after n steps gives a rational approximation to our number, with accuracy

$$\left| s - \frac{p_n}{q_n} \right| < \frac{1}{q_n q_n - 1}. \quad (10.4.33)$$

The slowest convergence of this series is if all $a_n = 1$. This is

$$\varphi = 1 + \frac{1}{1 + \frac{1}{1 + \frac{1}{1 + \dots}}} \quad (10.4.34)$$

This is $\varphi = (1 + \sqrt{5})/2$, the golden mean. This is the ‘most irrational’ number and proves to be bounded by rational approximations as

$$\left| \varphi - \frac{p}{q} \right| < \frac{1}{q^2 \sqrt{5}}$$

which is the worst an irrational number can be approximated. Roughly speaking, the irrational numbers that cannot be approximated better by rationals with better factors than a $1/kq^2$ factors ($k \geq \sqrt{5}$ is a constant), are said to satisfy a Diophantine condition and are the "most irrationals" real numbers. It's a remarkable fact that these numbers play a fundamental role in the convergence of perturbations of hamiltonian systems and arise in a lot of different chaotic systems.

The KAM theorem implies that tori described by quasi-periodic orbits with a winding number equal to the golden mean are the most stable to perturbations, and will survive for longest while tori with 'less irrational' winding numbers (including periodic/rational orbits) are unstable to chaos. A hierarchy of scales (as a fractal) then arises due to this hierarchy of very irrational, vs rational numbers in all the possible values of ratios of frequencies. Though it is not evident from the previous figures, phenomena like the appearance of quasi-periodic motions and bifurcation cascades characterise the transitions to chaos also for this system where chaos and order fight and coexist in the same dynamical system.

CHAPTER 11

Other chaotic systems

In the previous lectures, we have seen two necessary ingredients for chaos in dynamical systems:

1. Non-linear equations of motion.
2. More than one degree of freedom.

Time-dependence, in the form of a time-dependent potential or time-dependent driving force, can provide an additional degree of freedom. Such systems are not conservative. Conservative systems with additional degrees of freedom include the N -body problem, coupled oscillators, etc. While the addition of one degree of freedom (giving us a three or four dimensional system) still allows us to examine trajectories in phase space using tools such as recurrence plots and Poincaré sections, this becomes much more difficult if we add further degrees of freedom. So it is useful to see some ways in which we can study, or at least identify, chaotic behaviour in systems with many degrees of freedom.

11.1 Non-linear coupled oscillators

One such system is N coupled non-linear oscillators. We can model each oscillator as a non-linear spring:

$$F_n = - \sum_{i=1} k_n^i x_n^i. \quad (11.1.1)$$

For simplicity, we can choose to have only terms with odd i non-zero (to give a symmetric potential) and to only have a small number of non-zero terms. For example, we can choose

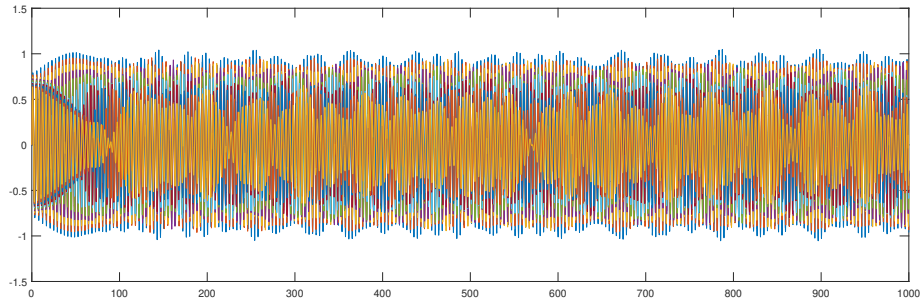
$$F_n = - \sum_{i=1,3,5} k_n^i x_n^i. \quad (11.1.2)$$

Coupling between the oscillators can be assumed to be linear, described by

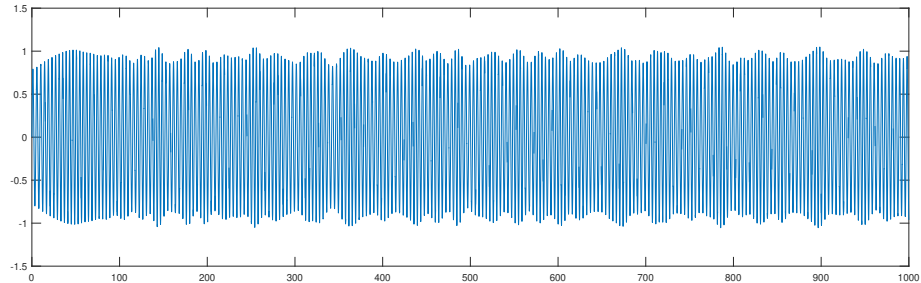
$$F_{nm} = c_{nm}(x_m - x_n) \quad (11.1.3)$$

where $n \neq m$. Many systems can be described where the oscillators are only coupled to their nearest neighbours, so that $c_{nm} \neq 0$ only for $m = n \pm 1$. In other systems, all oscillators couple to all other oscillators.

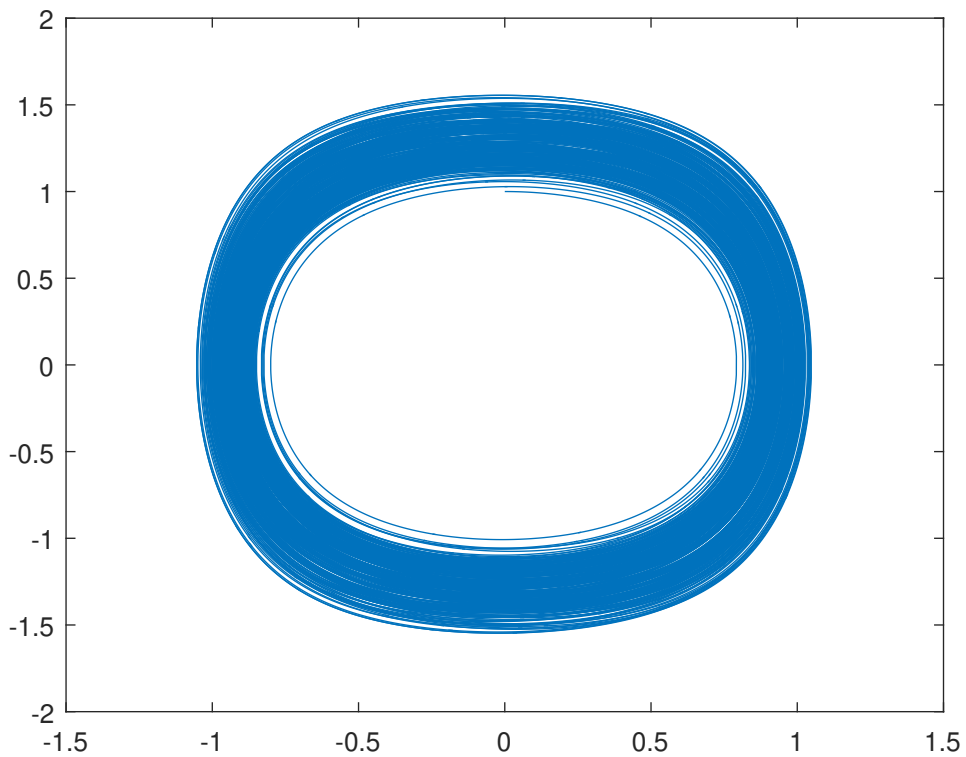
If we consider a system of 10 oscillators, and plot the positions of all of them as a function of time:



we obtain a difficult-to-read plot. Perhaps this will be easier to read if we only plot the motion of a single oscillator?



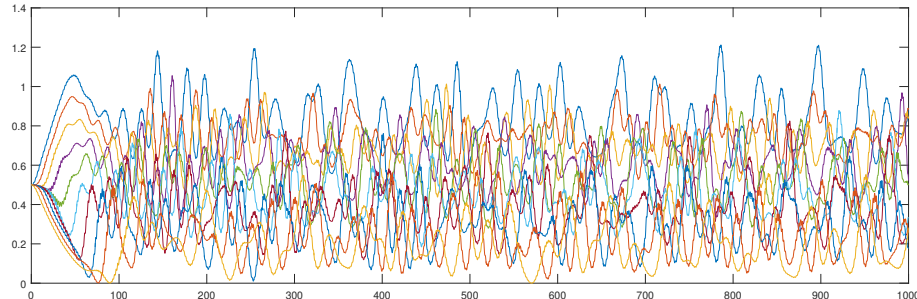
Alas not! We obtain a simpler picture if we plot the motion of a single oscillator in its 2D subspace of the phase space:



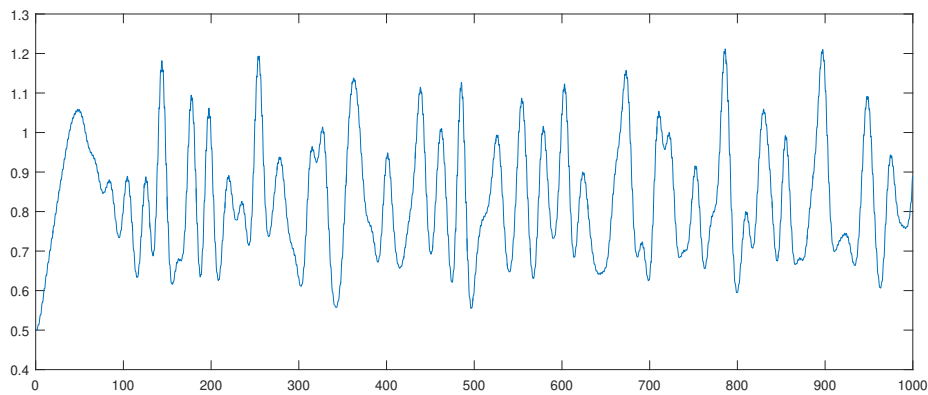
but this projection of the 21D trajectory for the entire system only contains a small fraction of the total information, and doesn't provide us with an easy-to-read plot.

One difficulty with these plots is that the oscillatory motion of the oscillator(s) makes these plots very busy and crowded. Since this system is conservative, we can eliminate this oscillatory motion from the plots by plotting the energy instead; the energy of each individual oscillator can be readily calculated as $T +$

V. For the 10 oscillators, we obtain



which is easier to read than our plots for the position, and if we only show a single oscillator, we obtain:

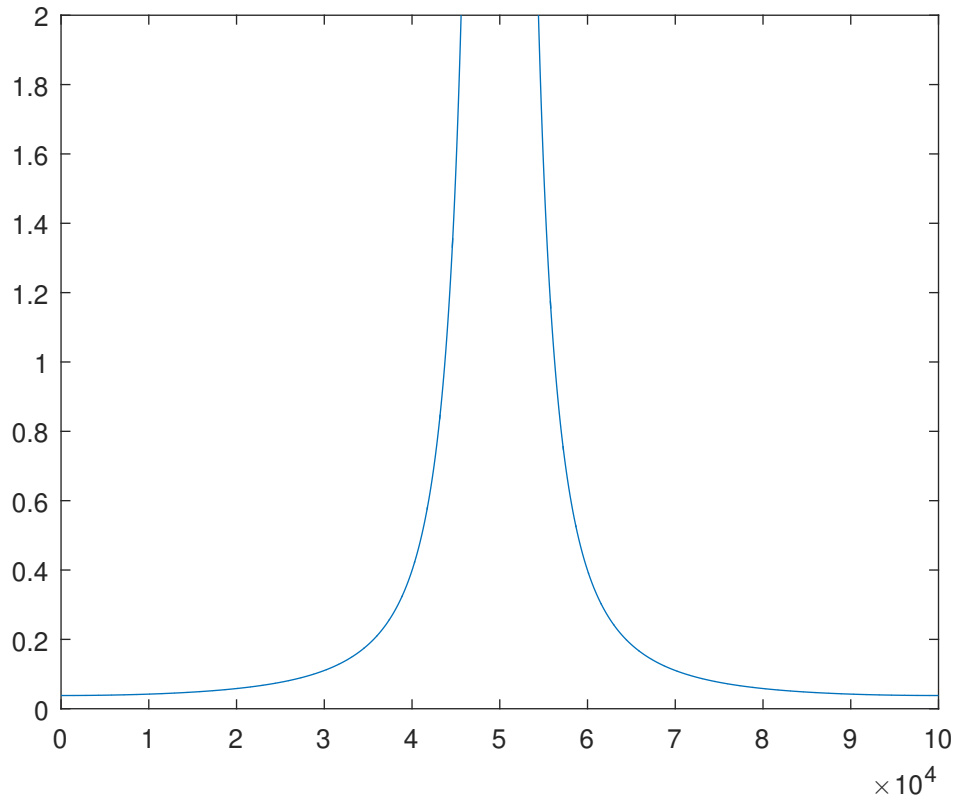


We have now reduced our initial plots to something that looks understandable. We still haven't shown that the system is undergoing chaotic motion. We will shortly look at the divergence of trajectories in phase space (Lyapunov exponents). First, we will see if the amount of energy in our oscillator above varies periodically (not chaotic) or aperiodically (chaotic).

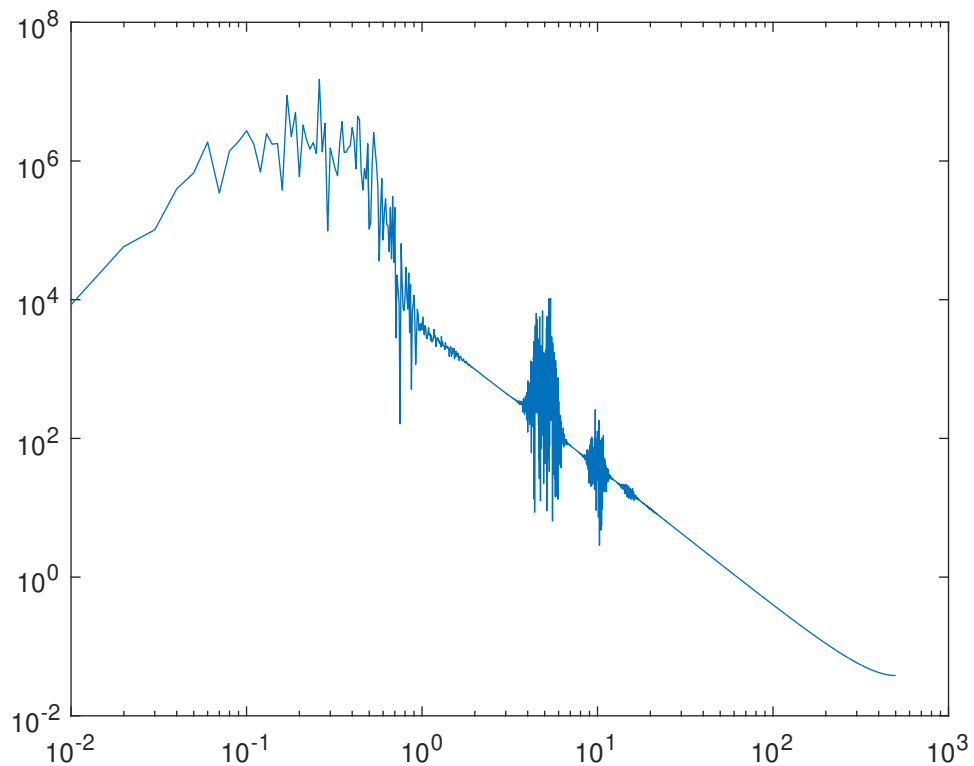
11.1.1 Aperiodic motion

Noting that chaotic motion is *aperiodic* (which is why we can recognise it in recurrence plots), we can computationally investigate the frequency spectrum of the energy in one of our oscillators above. This is most simply done by taking the fast Fourier transform (FFT) of the energy as a function of time. Since our numerical solution of the equations of motion gives us the positions and momenta (and therefore the energy) at a discrete set of points in time, FFT is a convenient algorithm.¹ This can be conveniently performed in Matlab using the functions `fft` and `fftshift`. Since the spectrum is complex, we can take the squared magnitude and plot it:

¹The FFT of a signal in time is only the Fourier transform of the signal if and only if the signal is discrete (i.e., not a continuous function of time) and periodic (giving a discrete and periodic spectrum, as assumed by FFT).



Here, we have centred the spectrum on zero (and not adjusted the scale on the x -axis!). We have a very large DC peak in the centre (note that the energy fluctuated about a value of approximately 0.8, so we should expect a large DC component). Since the magnitude of the spectrum varies a lot over the frequency range, we can plot the positive-frequency half of the spectrum (i.e., the right-hand half) as a log-log plot:

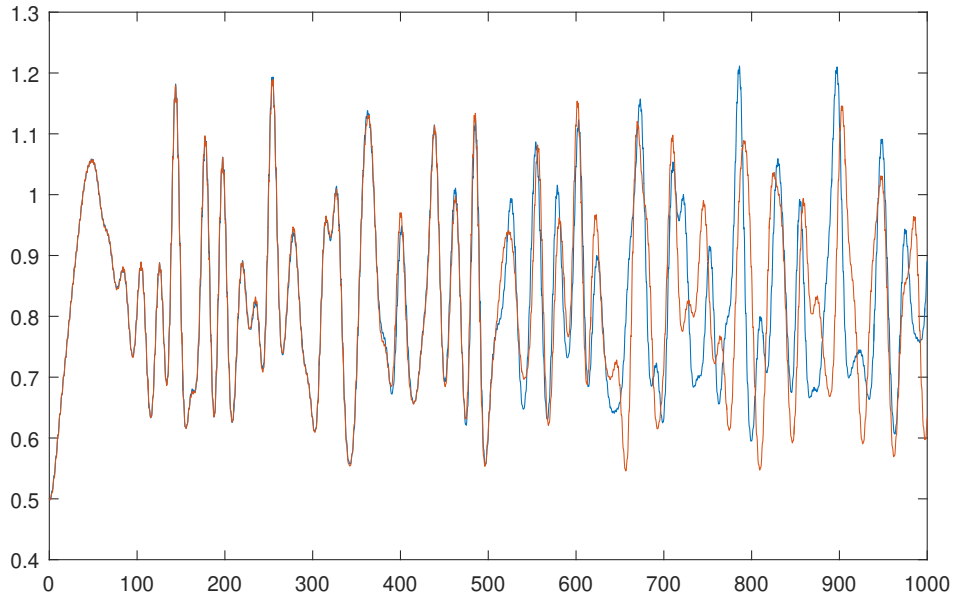


Notably, the spectrum closely resembles the spectrum of a random walk (e.g., Brownian motion), which is characterised by a $1/f^2$ spectral density.

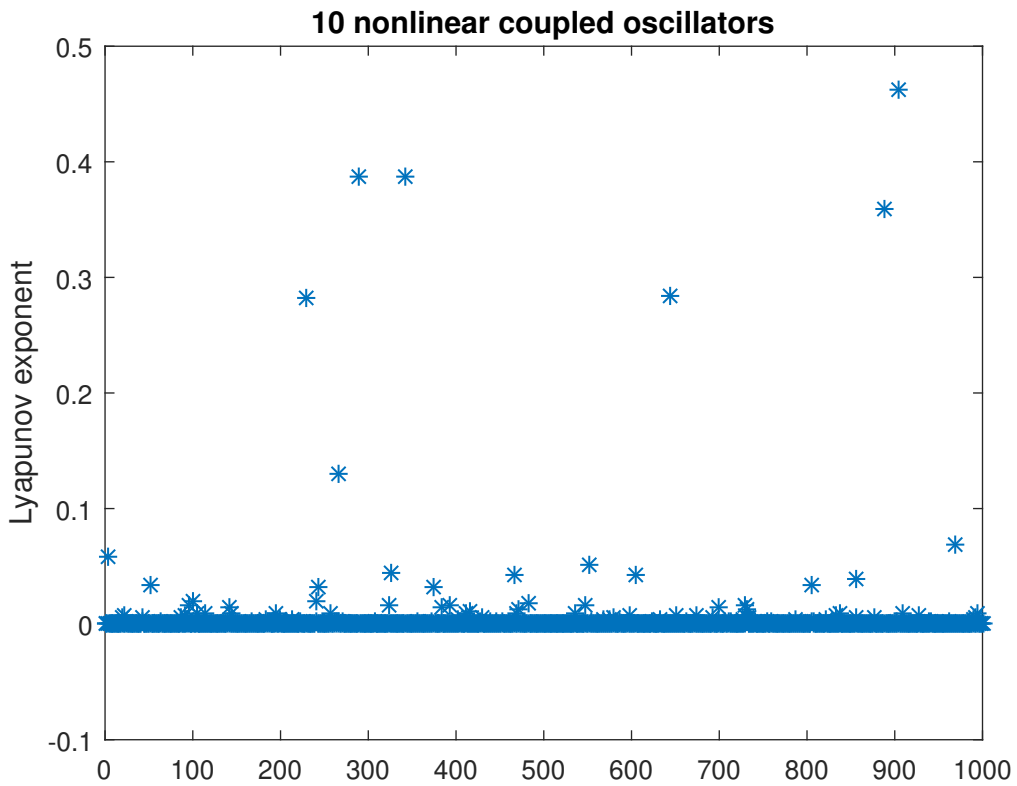
11.2 Lyapunov exponents

Finally, we can investigate the sensitivity to initial conditions. Since we expect the rate of divergence of nearby trajectories in phase space (i.e., the Lyapunov exponent) to depend on where in the phase space the trajectories are, we need to explore the behaviour for a variety of initial conditions. Since the phase space is high-dimensional (20D for 10 oscillators), and systematic exploration would scale exponentially (as $O(\exp(N))$), we use a Monte Carlo approach: we choose a random set of initial conditions to give us one trajectory, with a small variation to give us a second trajectory to compare with the first, and repeat until we have a reasonable idea of the behaviour.

If we compare two initially-close trajectories over sufficient time, we can see that they diverge:

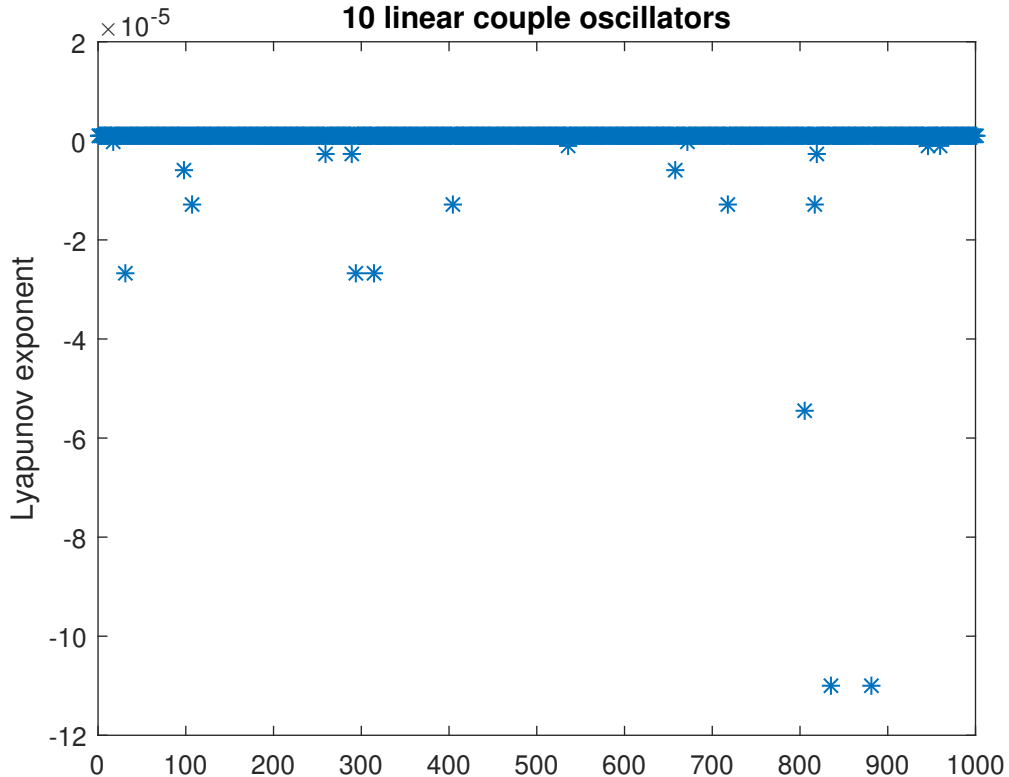


We do not need to calculate the trajectories for a long time in order to estimate the Lyapunov exponents; this only requires calculation for a few time steps. For a randomly chosen set of 1000 initial conditions, we obtain



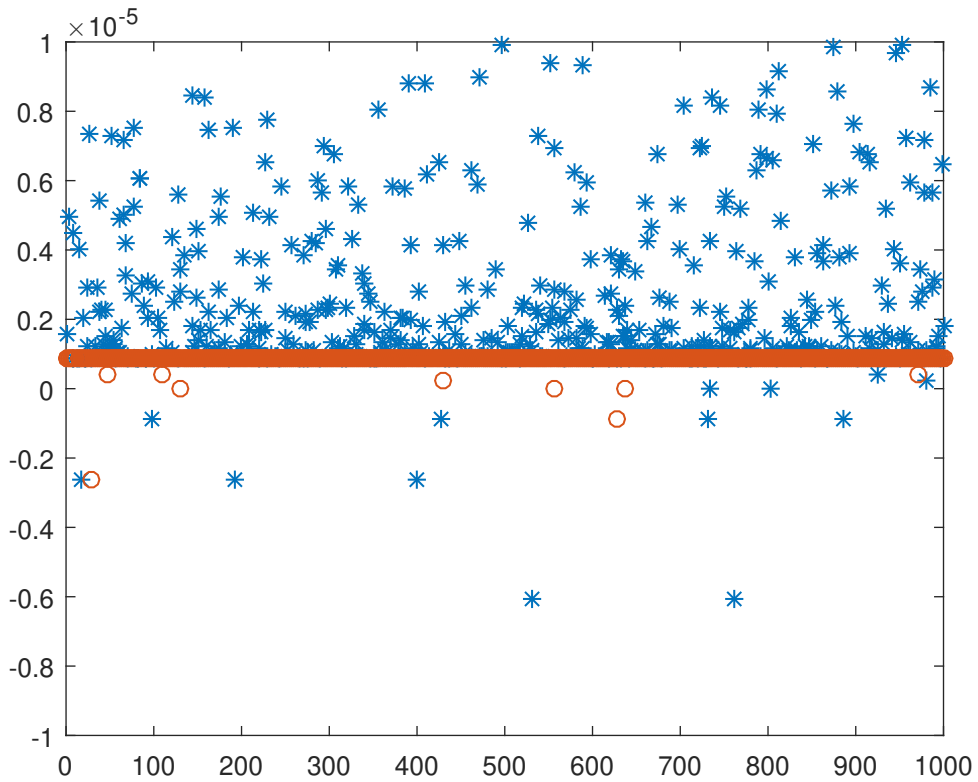
and see that we have positive Lyapunov exponents, as expected.

Noting that these values will have some numerical error, we can obtain an estimate of our error by calculating Lyapunov exponents for a similar system of coupled linear oscillators. For this system, which is not chaotic, we obtain the following Lyapunov exponents:



The maximum value (and the value of most of the random trials) is a little under

10^{-6} . Comparing the values obtained for the non-linear and linear cases, we see that the positive values of the Lyapunov exponent for the non-linear case are typically much larger than this estimated error, and can be assumed to be genuine positive values (i.e., the difference between our positive values and zero is much larger than our estimate of the numerical error):



11.3 Turbulence

Classical fluid flow is described by the Navier–Stokes equations. These are non-linear, and as PDEs, there are infinite degrees of freedom. Thus, we have the possibility of chaotic fluid flow.

Turbulence is characterised by vortices across a large range of size scales (it's self-similar, i.e., fractal). The largest scale of vortices is determined by the size of features influencing the flow (e.g., a vortex can't be wider than a pipe in which the flow is taking place), and the smallest scale is determined by the distance over which viscosity comes to dominate the flow.

If we look at the onset of turbulence in a flow, such as in the transition from laminar flow to turbulence which we can see in many convective plumes (such as above a candle flame), we see the flow forming vortices. The first vortices to form are large-scale. This is an example of bifurcation—at this part of the flow, we have two distinct states, clockwise and anti-clockwise vortices. As we look further along the flow, we see the formation of smaller and smaller vortices, and each scale of vortex gives us a new bifurcation. In the ideal case of a continuous inviscid fluid, we will form vortices at all smaller size scales, giving us an excellent example of chaos.

In practice, viscosity will limit how small the vortices can be (and if we had an inviscid fluid, the size would still be limited by the atomic structure of the fluid).

Turbulence is often considered to be a *random* process, rather than a chaotic process. The difference is that while chaotic dynamics are sensitive to initial conditions, they are deterministic. In general, for a fluid mechanics problem, we don't know the initial conditions. In particular, we don't know the thermal fluctuations in the fluid in detail, but only in a statistical sense (this will be the same whether we consider a continuous fluid or an atomic fluid). So it can be convenient to model turbulence as a random process. However, in the classical limit, we have no source of true randomness.

Further reading:

- <http://www.meridian-int-res.com/Aeronautics/Chaos.pdf>
- http://www.currentscience.ac.in/Downloads/article_id_056_13_0629_0645_0.pdf
- <http://www.annualreviews.org/doi/abs/10.1146/annurev.fluid.32.1.1>

11.4 Lasers

Variation in the power of a single mode laser provides us with an example of chaos. The system is described by the Maxwell–Bloch equations, which are equivalent to the Lorenz system.

A good introductory treatment is available at http://www.scholarpedia.org/article/Chaos_in_lasers and I will not reproduce that here in the notes.

Further reading:

- <http://www.nature.com/nphoton/journal/v9/n3/full/nphoton.2014.326.html>

11.5 Cardiac rhythms

Heart rate is not constant but varies considerably, even in the absence of physical or mental stress. A power spectrum of heart rate reveals at least two frequency ranges in which there is significant power, a low frequency range of 0.04–0.15 Hz and a high frequency range of 0.15–0.4 Hz. Beside these more or less periodic components, the heart rate spectrum also shows a broad, noise-like variability over a large frequency span. It seems that this irregular variability, which accounts for the largest proportion of heart rate variability, is due to non-linearities in the control network.

In healthy adults, non-linear dynamics in the heart rate seems to represent the normal situation. These are obscured under pathological circumstances, e.g., such as when the cardiovascular–respiratory interplay is impaired, which can also be observed in patients after heart transplantation. In line with the view that the healthy state is characterised by a certain degree of chaos, it has been found that abnormalities in autonomic system functions diminish cardiac chaos. This was recently demonstrated for congestive heart failure, where an increase in non-chaotic heart rate fluctuations was observed, which alternate with chaotic short-term variations.

They discovered unstable periodic orbits (UPO) in rate-rate (RR) time series. Periodic orbits reflect the deterministic dynamics of the underlying system, but the UPOs are unstable, which means that they have a positive Lyapunov exponent and are therefore typical for chaotic systems.

Chaos in cardiac rhythms, and its importance, remains controversial.

Further reading:

- <http://cardiovascres.oxfordjournals.org/content/40/2/257>
- <https://www.physionet.org/challenge/chaos/>
- <http://www.lptl.jussieu.fr/user/lesne/Chaos-biology.pdf>